PATHWAY TO ALLOSTERY:

DIFFERENTIAL ROUTES FOR ALLOSTERIC COMMUNICATION

IN PHOSPHOFRUCTOKINASE FROM *ESCHERICHIA COLI*

A Dissertation

by

NILUBOL MONIQUE PARICHARTTANAKUL

Submitted to the Office of Graduate Studies of
Texas A&M University
in partial fulfillment of the requirements for the degree of

DOCTOR OF PHILOSOPHY

December 2004

Major Subject: Biochemistry

PATHWAY TO ALLOSTERY:

DIFFERENTIAL ROUTES FOR ALLOSTERIC COMMUNICATION

IN PHOSPHOFRUCTOKINASE FROM *ESCHERICHIA COLI*

A Dissertation

by

NILUBOL MONIQUE PARICHARTTANAKUL

Submitted to the Office of Graduate Studies of
Texas A&M University
in partial fulfillment of the requirements for the degree of

DOCTOR OF PHILOSOPHY

Approved as to style and content by:

_____	_____
Gregory D. Reinhart (Chair of Committee)	J. Martin Scholtz (Member)
_____	_____
Dorothy E. Shippen (Member)	Donald W. Pettigrew (Member)

_____
Gregory D. Reinhart
(Head of Department)

December 2004

Major Subject: Biochemistry

ABSTRACT

Pathway to Allostery: Differential Routes for Allosteric Communication in Phosphofructokinase from *Escherichia coli*.

(December 2004)

Nilubol Monique Paricharttanakul, B.S., Texas A&M University

Chair of Advisory Committee: Dr. Gregory D. Reinhart

Phosphofructokinase from *Escherichia coli* (EcPFK) is allosterically regulated by MgADP and phospho(enol)pyruvate (PEP). Both molecules compete for binding to the same allosteric site, however, MgADP activates and PEP inhibits the binding of fructose-6-phosphate (F6P) to the active site. The mode by which this enzyme can differentiate between the two ligands and cause the appropriate response is important for the understanding of the basis of allosteric regulation.

We studied the interactions between an active site and an allosteric site (heterotropic interactions) within the protein, and found that each of the four unique heterotropic interactions is unique and the magnitudes of the coupling free energies for MgADP activation sum up to 100% that of wildtype EcPFK without homotropic cooperativity in F6P binding. We took on the kinetic and structural characterization of phosphofructokinase from *Lactobacillus bulgaricus* (LbPFK) to reveal an enzyme that exhibits allosteric properties in spite of previous kinetic studies performed by Le Bras et al. (1991). We have identified residues in EcPFK (Asp59, Gly184 and Asp273), which

are important for the allosteric responses to both MgADP and PEP. Interestingly, Lys214 is only important in PEP inhibition and not MgADP activation. We can also differentially disrupt the MgADP heterotropic interactions with the introduction of G184C within the protein. These results suggest that there are different pathways for allosteric communication within the enzyme: different paths for MgADP activation and PEP inhibition, and different paths for each heterotropic interaction with Gly184 being important for the 33Å MgADP heterotropic interaction.

DEDICATION

I would like to dedicate this work to my family, without them I would not be here today. Daddy dearest, you have been my inspiration with your sacrifices and hard work to get where you are. Your guidance and love have meant the world to me. Dear Mommy, you have instilled in me patience and perseverance. With your love and encouragement, you have motivated me to succeed in my pursuits. I appreciate all that both of you have done for me. I strive not to ever disappoint you. To my big brother, P'Nut, I value your love, understanding and support through good times and bad times. I could not have asked for a better brother. I am proud of all of you, and grateful for all that we have. You have taken good care of me and I thank you. Finally, to my baby, Scarlett, who has kept me sane throughout graduate school, with her unconditional love and doggie kisses. I love all of you very much.

ACKNOWLEDGMENTS

I would like to take this opportunity to thank all the people who had been instrumental to my education. I thank all my teachers at Gandhi Memorial International School, Indonesia and Ruamrudee International School, Thailand, and my professors at Texas A&M University for providing me with an exceptional quality of education. Thank you for having high standards in performance and behavior, and for showing me that science can be fun.

A special thanks goes to past and present Reinhart lab members: Dr. Michelle Lovingshimer, Dr. Aron Fenton, Dr. Jason Johnson, Dr. Mauricio Lasagna, Dr. Ally Ortigosa, Dr. Jason Quinlan, Ann Menefee, Libby Badgett, Cui Juan Tie, Lin Fan, Scarlett Blair and Andrew Bigley. They make going to work interesting and having lunch so much fun. To my dear classmates for getting us through the hard times in the first year: Leonardo Marino, Scott Pinkerton and Aglaia Chandler, I thank you. I would like to thank Dr. Sheng Ye from the Sacchettini lab for solving the crystal structure of phosphofructokinase from *L. bulgaricus* and assisting me with the writing of the structure part of my dissertation. I also thank my committee members, Dr. Donald Pettigrew, Dr. Dorothy Shippen and Dr. Martin Scholtz, for their guidance and support at Texas A&M University.

Without the love and support of my family and friends, graduate school would have been miserable. I would like to thank my family especially Ku Srinual, Ku Nit, Ah Ying and Ah Tiew for their encouragement and words of wisdom. To my friends, Chao

Hsien Hwang, Carla Theimer, Sarah Bache, Yu Kang Ku, Lawrence Lee and Henry Tan, for being there for me. And to the Rileys and the Lovingshimers for making me feel like part of their family.

Finally, I would like to express my deepest thanks to Dr. Greg Reinhart for being a great teacher and mentor. Thank you for giving me a great graduate experience and education. You have always amazed me with your knowledge and English. I hope that one day I can be a bit of what you are. Thank you for your understanding and patience. And a heartfelt thanks for making me feel like a member of the Reinhart family with your fatherly care and advice, and for including me in your family functions.

NOMENCLATURE

Abbreviations

A	Generally denotes substrate or single letter code for alanine
ADP	Adenosine 5'-diphosphate
Ala	Alanine
AMP	Adenosine-5'-monophosphate
Arg	Arginine
Asp	Aspartate
ATP	Adenosine 5'-triphosphate
BCA	Bicinchoninic Acid
BsPFK	Phosphofructokinase from *Bacillus stearothermophilus*
C	Single letter code for cysteine
D	Single letter code for aspartate
DTT	Dithiothreitol
E	Generally denotes enzyme or single letter code for glutamate
EcPFK	Phosphofructokinase from *Escherichia coli*
EDTA	Ethylenediamine tetraacetic acid
EPPS	N-(2-hydroxy-ethyl)piperazine-N'-(3-propanesulfonic acid)
F	Single letter code for phenylalanine
F6P	Fructose-6-phosphate
FBP	Fructose-1,6-bisphosphate

G	Single letter code for glycine
GDP	Guanosine 5'-diphosphate
Glu	Glutamate
Gly	Glycine
H	Single letter code for histidine
His	Histidine
I	Single letter code for isoleucine
K	Single letter code for lysine
KSCN	Potassium thiocyanate
L	Single letter code for leucine
LB	Luria Bertani broth
LbPFK	Phosphofructokinase from *Lactobacillus bulgaricus*
Leu	Leucine
Lys	Lysine
M	Single letter code for methionine
MES	2-(N-morpholino)ethanesulfonic acid
Met	Methionine
MOPS	3-[N-Morpholino]propanesulfonic acid
N	Single letter code for asparagine
NAD^+	Nicotinamide adenine dinucleotide (oxidized form)
NADH	Nicotinamide adenine dinucleotide (reduced form)
P	Generally denotes product or single letter code for proline

PAGE	Polyacrylamide gel electrophoresis
PEP	Phospho(enol)pyruvate
PFK	Phosphofructokinase
PGA	Phosphoglycolate
Phe	Phenylalanine
Q	Single letter code for glutamine
R	Single letter code for arginine
S	Single letter code for serine
SDS	Sodium dodecyl sulfate
Ser	Serine
T	Single letter code for threonine
Tris	Tris[hydroxymethyl]aminomethane
TtPFK	Phosphofructokinase from *Thermus Thermophilus*
UTP	Uridine 5'-triphosphate
V	Single letter code for valine
W	Single letter code for tryptophan
X	Generally denotes activator
Y	Generally denotes inhibitor or single letter code for tyrosine

Mathemathical Terms

K_{ia}^{o}	Thermodynamic dissociation constant for A in the absence of effector
K_{ia}	Thermodynamic dissociation constant for A in the saturating presence of effector
K_{ix}^{o}	Thermodynamic dissociation constant for X in the absence of substrate
K_{ix}	Thermodynamic dissociation constant for X in the saturating presence of substrate
K_{iy}^{o}	Thermodynamic dissociation constant for Y in the absence of substrate
K_{iy}	Thermodynamic dissociation constant for Y in the saturating presence of effector
τ	Torsion angle
°C	Degree Celsius
Å	Angstroms
F	Structure factor
I	Intensity
$K_{0.5}$	Concentration of substrate to produce half-maximal activity
k_{cat}	Turnover number of the enzyme
kDa	Kilodalton
K_i	Inhibition constant
K_m	Michaelis constant
mg	Milligram
mL	Milliliter
mM	Millimolar

n_H	Hill number
nm	Nanometer
Q_{ax}	Coupling constant for the interaction between A and X
Q_{ay}	Coupling constant for the interaction between A and Y
R	Gas constant
R_{free}	Free R-factor
rmsd	Root mean square deviation
R_{sym}	Error in measured intensities of equivalent reflections
T	Temperature
U	Units
v	Initial velocity
V	Maximal velocity in the saturating presence of effector
V_{max}	Maximal velocity
V^o	Maximal velocity in the absence of effector
W_{ax}	Coupling constant for the interaction between A and X which alters the maximal velocity
ΔG_{ax}	Coupling free energy for the interaction between A and X
ΔG_{ay}	Coupling free energy for the interaction between A and Y
μL	Microliter

TABLE OF CONTENTS

Page

CHAPTER Page

LIST OF TABLES

LIST OF FIGURES

FIGURE Page

FIGURE Page

CHAPTER I

INTRODUCTION

The study at the molecular level of chemical processes in living organisms is the science of biochemistry. In living organisms, the four major complex biomolecules found in cells and tissues are proteins, nucleic acids, polysaccharides and lipids. All these complex biomolecules are made up of small molecules that combine in repeating units of each other. Amino acids are the building blocks of proteins. Deoxyribonucleic acids (DNA) and ribonucleic acids (RNA) contain deoxyribonucleotides and ribonucleotides, respectively. Sugars form polysaccharides, and lipids are made up of fatty acids. The study of these complex biomolecules, the determination of their structures and the investigations into their function is what biochemistry is all about.

Proteins are the most abundant biomolecules in many organisms, e.g., humans (Murray et al, 1996) and *Escherichia coli* (Voet and Voet, 1995). They play many major cellular and structural functions. One of their important roles is as enzymes that mediate the many biochemical reactions required for proper function of the cell. Enzymes catalyze specific biochemical reactions or types of reactions without being consumed in the process. This specificity allows for the rates of biological processes to be regulated by changes in the levels or catalytic efficiency of specific enzymes. For example, the

---

This dissertation follows the style and format of *Biophysical Journal*.

hydroxylation of phenylalanine to tyrosine is catalyzed by phenylalanine hydroxylase. In infants with phenylketonuria, a heritable disorder that results in signs of mental retardation, the levels of liver phenylalanine hydroxylase average approximately 25% of normal levels, and the hydroxylase is insensitive to regulation by phenylalanine (Murray et al., 1996). Phenylalanine hydroxylase is very specific for phenylalanine as its substrate. It can hydroxylate tryptophan to a small extent, but not tyrosine (Daubner et al, 2000). Due to the abundance of enzymes in the cell and their medical importance, many scientists have devoted themselves and their resources to the study of enzymes and how they work.

Cells control the balance necessary for correct function in response to changing environmental factors and nutritional levels by regulating the level of enzymes or the activity of enzymes. The right balance between the rate of enzyme synthesis from amino acids and the rate of enzyme degradation determines the quantity of an enzyme available in the cell. On the other hand, the catalytic efficiency of enzymes can be altered as a result of changing levels of substrates and metabolites in the cell. Enzyme activity can also be modulated by conformational changes caused by covalent modifications, protein-protein interactions and allosteric regulation. One such enzyme that exhibits two of the above-mentioned types of regulation is glycogen phosphorylase. This enzyme can be covalently modified by the phosphorylation at Ser14 by phosphorylase kinase resulting in glycogen degradation and the dephosphorylation by phosphoprotein phosphatase. Glycogen phosphorylase is also subject to allosteric regulation. It is allosterically activated by AMP and inhibited by ATP and glucose-6-phosphate (Voet and Voet,

1995). An example of regulation by protein-protein interactions is phosphoprotein phosphatase which is inhibited by its binding to phosphoprotein phosphatase inhibitor (Voet and Voet, 1995).

One of the ways enzymes are subject to stringent control in the cell is through allosteric regulation. Allosteric regulation is triggered by ligands known as effectors that bind to specific sites remote from the substrate-binding site on an enzyme and cause the enzyme to be activated or inhibited. The effects on the specific activity of the enzyme (V-type) and/or the binding of substrate (K-type) to the enzyme are two types of allosteric effects that are possible. K-type effects are most common (Reinhart, 2004).

Homotropic effects are observed when two ligands are identical and can result in cooperativity in ligand binding. Positive cooperativity is represented by sigmoidal binding profiles and occurs when the binding of the first ligand increases the binding affinity for the second. When there is no cooperativity i.e., no influence in the binding affinity of the first ligand to the subsequent ligand, the binding profiles are hyperbolic. Negative cooperativity is observed when the subsequent binding affinity decreases and can be seen by a shallow slope in the binding profiles (Reinhart, 2004).

When the ligands are different from one another, the allosteric effect is described to be heterotropic. The binding of an allosteric ligand can cause the binding of substrate to increase (K-type activation) or decrease (K-type inhibition), and vice versa. The cooperative responses generated by the binding of heterotropic ligands are known as heterotropic cooperativity and can be found in two classes: heterotropically induced homotropic cooperativity and subsaturating heterotropic cooperativity. The first class

arises when the binding of the effector changes the coupling between substrate binding sites, and can be negative or positive depending on how the effector changes the coupling between the active sites. The latter occurs at intermediate concentrations of the effector and is positive regardless of the nature of the heterotropic interaction (Reinhart, 1988).

Models for Allosteric Regulation

Traditionally, there are two models used to describe allosteric response, the concerted (MWC) and sequential (KNF) models. Both models claim that there are two functional conformational states, the T-state or "taut" state and the R-state or relaxed state. The T-state is the inhibited state of the protein and results when the inhibitor is bound to the enzyme. The R-state is the active form of the enzyme to which the substrate and activator can bind. These two models presume that the enzyme can adopt either the R-state or the T-state conformation.

The concerted model (Monod et al., 1965) states that for an oligomeric protein, all subunits are functionally identical. The two conformational states that the protein can adopt are in equilibrium with one another (Figure 1-1A) even in the absence of bound ligand. The binding of substrate to its binding site shifts the equilibrium of the oligomer to the R-state in a concerted manner and exhibits positive cooperativity. When an activator binds to the enzyme, the equilibrium is shifted towards the R-state facilitating substrate binding. Cooperativity is not observed for substrate binding in the presence of activator because the enzyme is already in the R-state. However, when inhibitor binds to

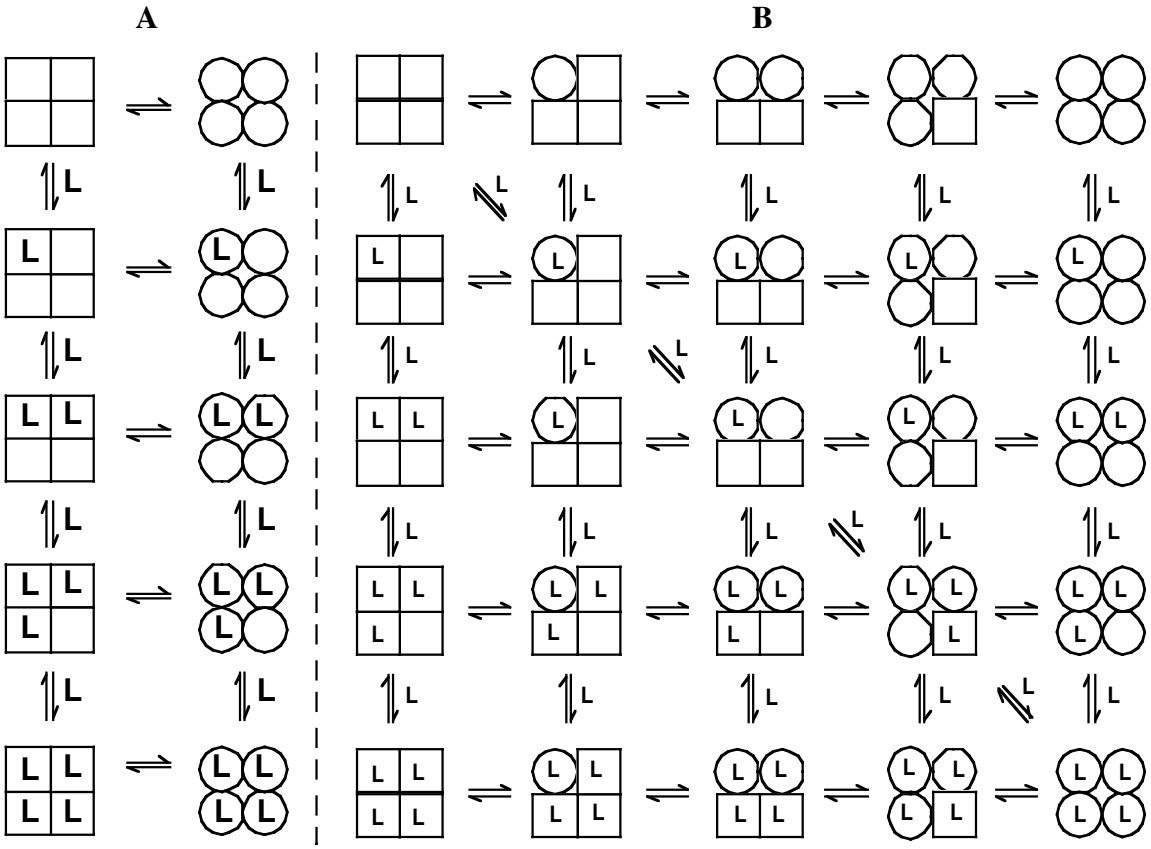

FIGURE 1-1: Schematic diagram of the MWC concerted model and the KNF sequential model for allosteric regulation of a tetrameric protein. L represents any ligand. (A) In the concerted model, all the subunits are postulated to be in one conformation, either all □ (high affinity or active) or ○ (low affinity or inactive). Depending on the equilibrium between □ and ○ forms, the binding of one or more ligands will pull the equilibrium to the R-state (left) or to the T-state (right). In the presence of substrate or activator, the equilibrium is shifted to the left, and to the right with inhibitor. (B) The sequential model allows for each individual subunit to be in either the □ or ○ form. Each subunit can undergo the conformational change individually. The binding of ligand causes an induced fit in the subunit it binds to and in neighboring subunits. The complete transition from one state to the other requires the binding of ligand to all sites. (Adapted from Lehninger et al., 1993)

the enzyme, the equilibrium is shifted more towards the T-state, decreasing the sites available for substrate binding, thereby increasing the cooperativity of substrate binding. Only positive cooperativity is allowed in the MWC model. The sequential model (Koshland et al., 1966) assumes an induced fit scenario in which binding of a ligand to one subunit of the enzyme induces a conformational change in that subunit (Figure 1-1B). The influence that this conformational change has on neighboring subunits can be positive or negative depending on the identity of the ligand. Conformational changes occur sequentially for binding to the remaining subunits and are proportional to the number of ligands bound. The complete conversion from one state to another is observed only when all sites are filled.

These oversimplified models do not accurately depict the nature of all allosteric enzymes. Thermodynamic linkage (Wyman, 1964; Weber, 1972, 1975) serves as a more complete analysis for the investigation of allosterism. This linked function approach describes ligand binding in free energy terms without assuming the nature of structural changes incurred by ligand binding. The basic principle of thermodynamic linkage is that the influence the substrate (A) has on the binding of effector (X) to the enzyme (E) must equal that of X on the binding of A to E as shown in Figure 1-2. There are four ligation states that the enzyme can adopt: E, EA or XE or XEA. Each ligation state is unique and can have different properties. This is in contrast to the two-state models which do not allow for the existence of the ternary complex because the T-state or the R-state of the enzyme could only bind one type of ligand, either A or X, but not both.

Dissociation constants for each binding event can be written (Reinhart, 1983):

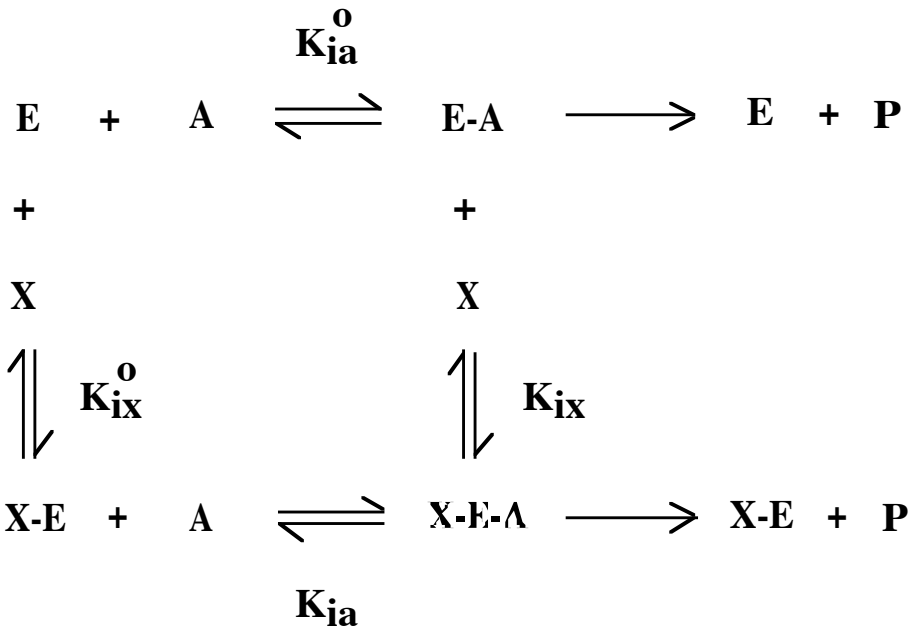

FIGURE 1-2: The simplest scheme depicting a single substrate and a single allosteric effector. E, A, X and P represents enzyme, substrate, effector and product, respectively. The respective dissociation constants are denoted by K's and are described in the text (Reinhart, 1983).

$$K_{ia}^{o} = \frac{[E][A]}{[EA]} \qquad [1\text{-}1]$$

$$K_{ia} = \frac{[XE][A]}{[XEA]} \qquad [1\text{-}2]$$

$$K_{ix}^{o} = \frac{[E][X]}{[XE]} \qquad [1\text{-}3]$$

$$K_{ix} = \frac{[EA][X]}{[XEA]} \qquad [1\text{-}4]$$

$$Q_{ax} = \frac{K_{ia}^{o}}{K_{ia}} = \frac{K_{ix}^{o}}{K_{ix}} \qquad [1\text{-}5]$$

where K_{ia}^{o} and K_{ia} are the dissociation constants of A when there is no X present and when there is saturating X, respectively. K_{ix}^{o} and K_{ix} are the dissociation constants of X in the absence and in the saturating presence of A, respectively. The magnitude of the interaction between A and X can be quantified by the coupling constant Q_{ax}, the influence A has on the binding of X and vice versa. Q_{ax} also represents the thermodynamic equilibrium constant for the following disproportionation equilibrium (Reinhart, 1989):

$$X\text{-}E + E\text{-}A \Leftrightarrow X\text{-}E\text{-}A + E \qquad [1\text{-}6]$$

$$Q_{ax} = \frac{[XE][EA]}{[XEA][E]} \qquad [1\text{-}7]$$

X acts as an activator when $Q_{ax} > 1$ and is an inhibitor when $Q_{ax} < 1$. When $Q_{ax} = 1$, A and X do not influence each other's binding. The magnitude of the interaction between ligands can be described in free energy terms by the equation (Reinhart, 1983, 1985, 1988, 1989):

$$\Delta G_{ax} = -RT \ln Q_{ax} \qquad [1\text{-}8]$$

where ΔG_{ax} is the free energy of interaction or coupling free energy (Weber, 1972, 1975; Reinhart, 1983, 1988). When $\Delta G_{ax} < 0$, X acts as an activator and when $\Delta G_{ax} > 0$, X acts as an inhibitor.

The rate equation for this mechanism, shown in Figure 1-2, can be written if the substrate is assumed to achieve rapid equilibrium during steady-state (Reinhart, 1983):

$$v = \frac{V^{\circ}(K_{ix}^{o}[A] + Q_{ax}W_{ax}[A][X])}{K_{ia}^{o}K_{ix}^{o} + K_{ix}^{o}[A] + K_{ia}^{o}[X] + Q_{ax}[A][X]} \qquad [1\text{-}9]$$

where v is the initial velocity, V° and V are the maximal activity in the absence of X and the saturating presence of X, respectively and W is the ratio of V over V°. When maximal activity is affected by the allosteric ligand, W will not be equal to 1.

Experimentally the coupling constant, Q_{ax}, can be obtained by determining the apparent dissociation constants for the substrate A as a function of effector concentration and can be graphically depicted for X being an inhibitor or an activator (Figure 1-3). The apparent dissociation constant for substrate, $K_{0.5}$ is the concentration at which the velocity is at half maximum and is described by the Hill equation (Hill, 1910):

$$\frac{v}{E_T} = \frac{k_{cat}[A]^{n_H}}{K_{0.5}{}^{n_H} + [A]^{n_H}} \qquad [1\text{-}9]$$

where v is the rate of the reaction, E_T is total enzyme active sites, k_{cat} is the turnover number and n_H is the Hill number that depicts cooperativity in substrate binding. When $n_H > 1$, positive cooperativity is observed, and when $n_H < 1$, negative cooperativity is observed. When $n_H = 1$, $K_{0.5}$ is equivalent to the Michaelis constant K_m. Assuming that the rapid-equilibrium is valid, the dependence of the apparent dissociation constants on

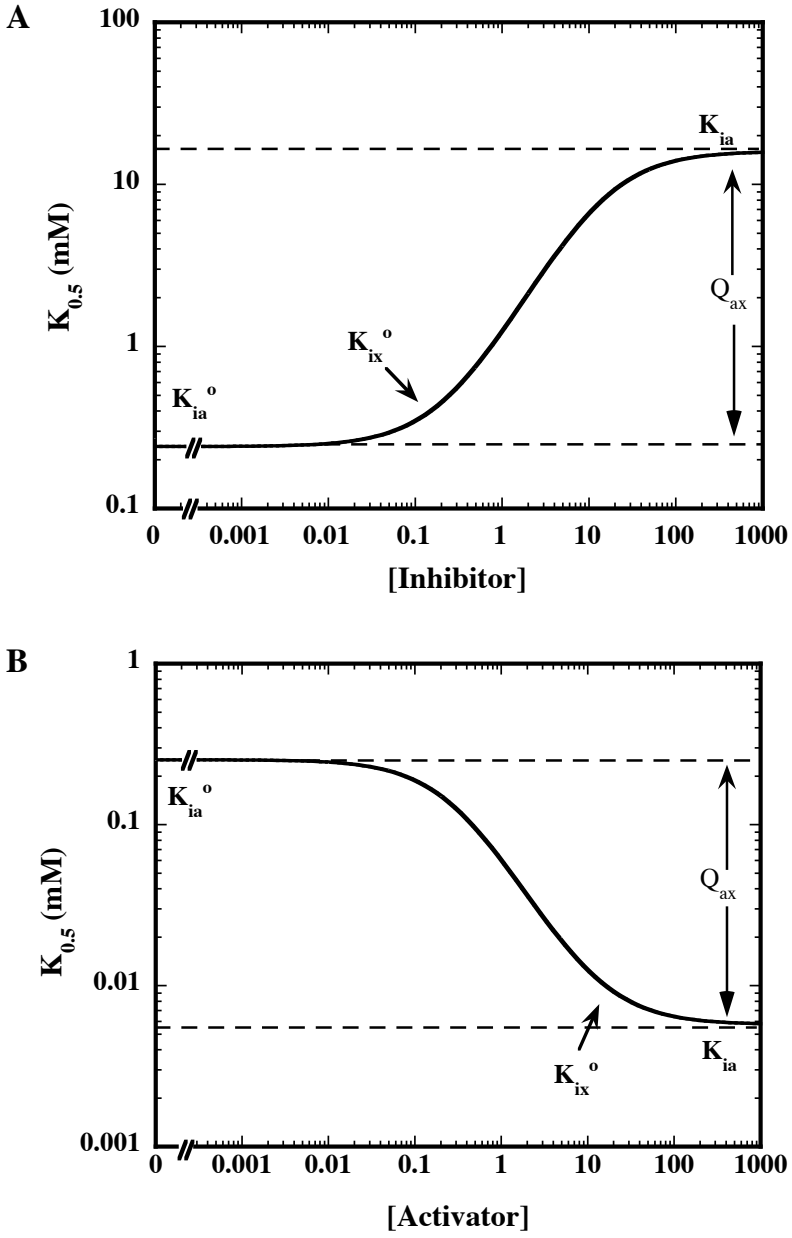

FIGURE 1-3: Graphical representation for the determination of the coupling constant Q_{ax}. The apparent dissociation constant for substrate $K_{0.5}$ increases as a function of inhibitor (A) and decreases as a function of activator (B) when the rapid-equilibrium assumption is valid. Q_{ax} is the difference between the two plateaus that are defined by K_{ia}^{o} and K_{ia} . The dissociation constants for the two effectors K_{ix}^{o} are labeled on the graphs.

effector concentration can be described by the following equation (Reinhart, 1983, 1985, 1988, 1989, 2004):

$$K_{0.5} = K_{ia}^{o}\left[\frac{K_{ix}^{o} + [X]}{K_{ix}^{o} + Q_{ax}[X]}\right] \qquad [1\text{-}10]$$

Phosphofructokinases

Phosphofructokinase (PFK) plays a key regulatory role in glucose metabolism. PFK catalyzes the first committed step in glycolysis as shown in Figure 1-4 with the phosphorylation of fructose-6-phosphate (F6P) by MgATP leading to the formation of fructose-1,6-bisphosphate and MgADP. The importance of this enzyme demands for the presence of a system of checks and balances of enzymatic activity in order to respond to changing levels of substrates or products in the cell. It is therefore crucial that in many organisms, PFKs are subject to allosteric regulation by numerous metabolites.

Eukaryotic PFKs are usually homotetrameric enzymes with twice the size of prokaryotic PFKs, proposed to be evolutionarily derived from gene duplication of prokaryotic homologs (Poorman et al, 1984), and can form higher order polymeric states (Uyeda, 1979). They are allosterically regulated by a large number of effectors. AMP, cyclic AMP, MgADP, inorganic phosphate, fructose-6-phosphate and fructose-1,6-bisphosphate are allosteric activators. Inhibitors include citrate, phosphocreatine, 3-phosphoglycerate, 2-phosphoglycerate, 2,3-bisphosphoglycerate, phospho(enol)pyruvate (PEP), MgATP and UTP (Uyeda, 1979).

Bacterial PFKs are homotetramers with subunit molecular weights of 34 kDa and

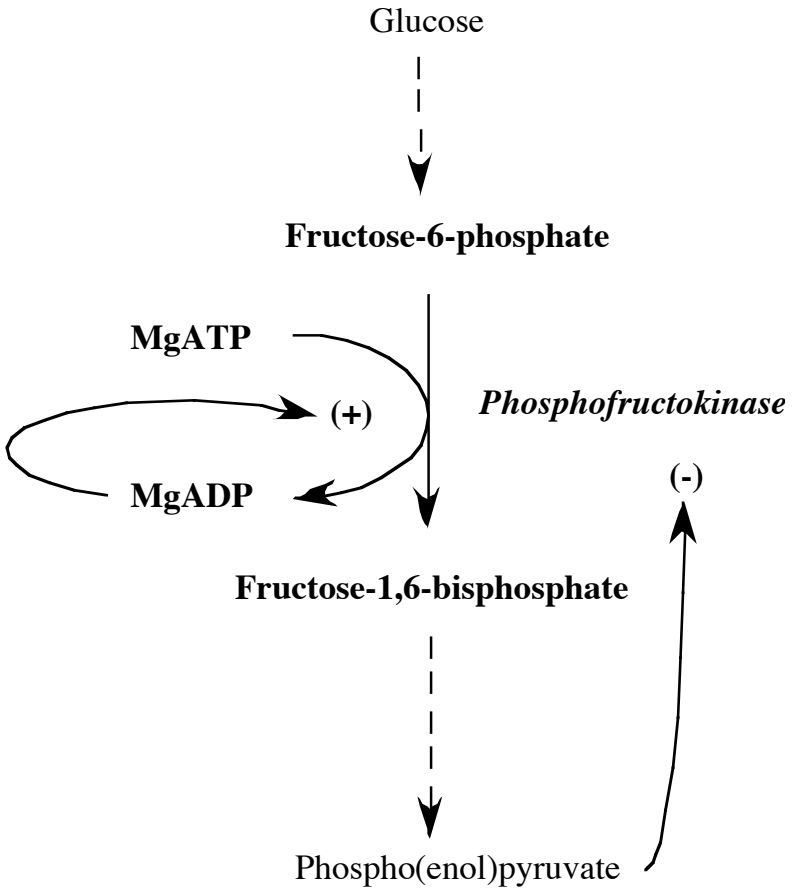

FIGURE 1-4: The reaction phosphofructokinase catalyzes. MgADP activates and PEP inhibits bacterial PFKs.

are allosterically activated by MgADP and MgGDP, and inhibited by PEP (Blangy et al, 1968; Uyeda, 1979; Tlapak-Simmons and Reinhart, 1998; Johnson and Reinhart, 1994, 1997). Two extensively characterized bacterial PFKs are from *Escherichia coli* (EcPFK) and *Bacillus stearothermophilus* (BsPFK). A K-type allosteric effect is observed in the presence of MgADP or PEP in both enzymes (Blangy et al, 1968; Tlapak-Simmons and Reinhart, 1998). MgADP and PEP compete for binding to the same allosteric site, and once bound, MgADP increases the binding affinity for substrate, F6P, whereas PEP decreases F6P binding. How these enzymes distinguish between the two molecules and how these molecules induce their respective responses in the enzymes are questions that still need to be addressed.

EcPFK and BsPFK exhibit many similar characteristics. They show 73% similarity and 54% identity in amino acid sequence. The crystal structures of both enzymes have been solved and their structures are very similar based on the α-carbon superimposition of the two structures (Evans et al, 1981; Shirakihara and Evans, 1988). Figure 1-5 shows the tetrameric structure of EcPFK. Both PFKs are homotetramers with four active sites and four allosteric sites that form at subunit interfaces. Each site is composed of two half sites from each monomer to complete that site to which substrate or effector binds. PFK is a dimer of dimers with the active site interface being weaker than the allosteric site interface and can be stabilized by F6P. PEP however, stabilizes the allosteric site interface. The dissociation of the tetramer into dimers occurs with the loss of activity, and further dissociation into monomers occurs in the presence of denaturants: guadinidium chloride, potassium thiocyanate (KSCN) and urea following

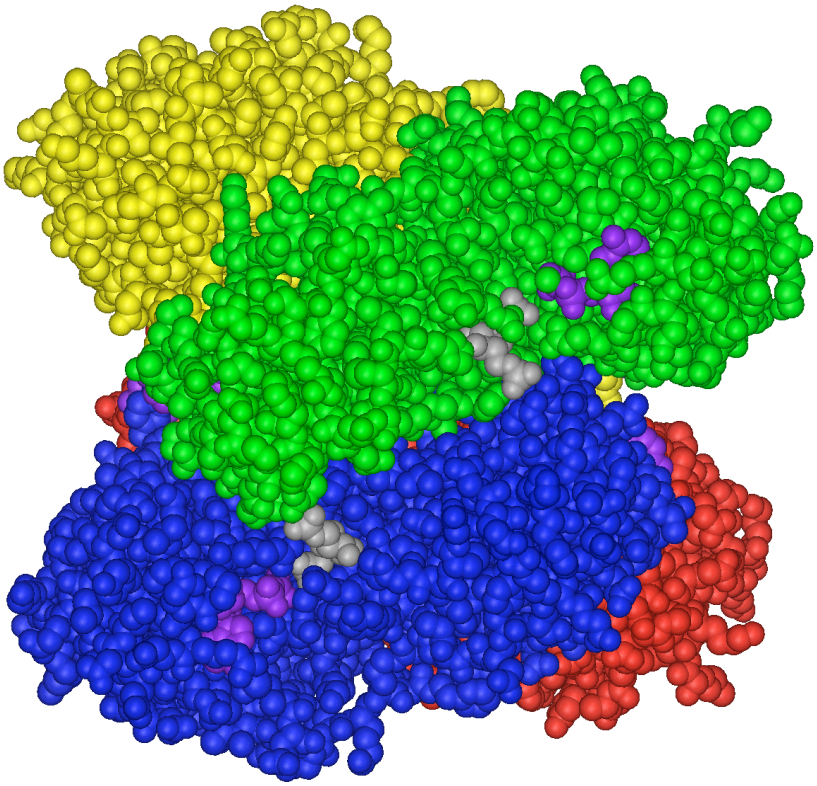

FIGURE 1-5: Crystal structure of EcPFK homotetramer (Shirakihara and Evans, 1988). The four subunits are represented in blue, green, red and yellow. MgADP binds to the four active sites and allosteric sites and is shown in purple, whereas the product fructose-1,6-bisphosphate binds only to the active sites and is in grey.

circular dichroism and fluorescence measurements performed on EcPFK (Teschner et al., 1990; Le Bras et al, 1989; Deville-Bonne et al, 1989). Because there are four active sites and four allosteric sites that are capable of communicating with one another, there are twenty-eight possible pair-wise interactions between binding sites in EcPFK and BsPFK. This makes the understanding of allosteric communication within the protein complex. Of the twenty-eight, twelve interactions are homotropic or between like-binding sites (Figure 1-6A) and sixteen are heterotropic or between an active site and an allosteric site (Figure 1-6B). However, there are only ten unique interactions, six homotropic (Figure 1-6C) and four heterotropic (Figure 1-6D), due to the symmetries present within the protein. This multiplicity of interactions must be simplified to study only the four unique heterotropic interactions in order to understand exactly how allosteric information is transmitted between one active site and one allosteric site.

The differences between EcPFK and BsPFK lie in their kinetic and allosteric properties. EcPFK is more active than BsPFK by almost two-fold (Valdez et al, 1989). In the absence of effectors, positive cooperativity is observed for the binding of F6P to EcPFK with a Hill number of 3.8 (Blangy et al, 1968) that is dependent on the presence of ATP (Johnson and Reinhart, 1992), but no such cooperativity is observed for BsPFK (Valdez et al, 1989). PEP does not influence the positive cooperativity in F6P binding in EcPFK, however, subsaturating heterotropically induced homotropic cooperativity is observed for BsPFK in which positive cooperativity in F6P binding is observed only at intermediate concentrations of PEP (Reinhart, 1988, Kimmel and Reinhart, 2001). MgADP does not affect F6P binding to the same extent between the two enzymes. In

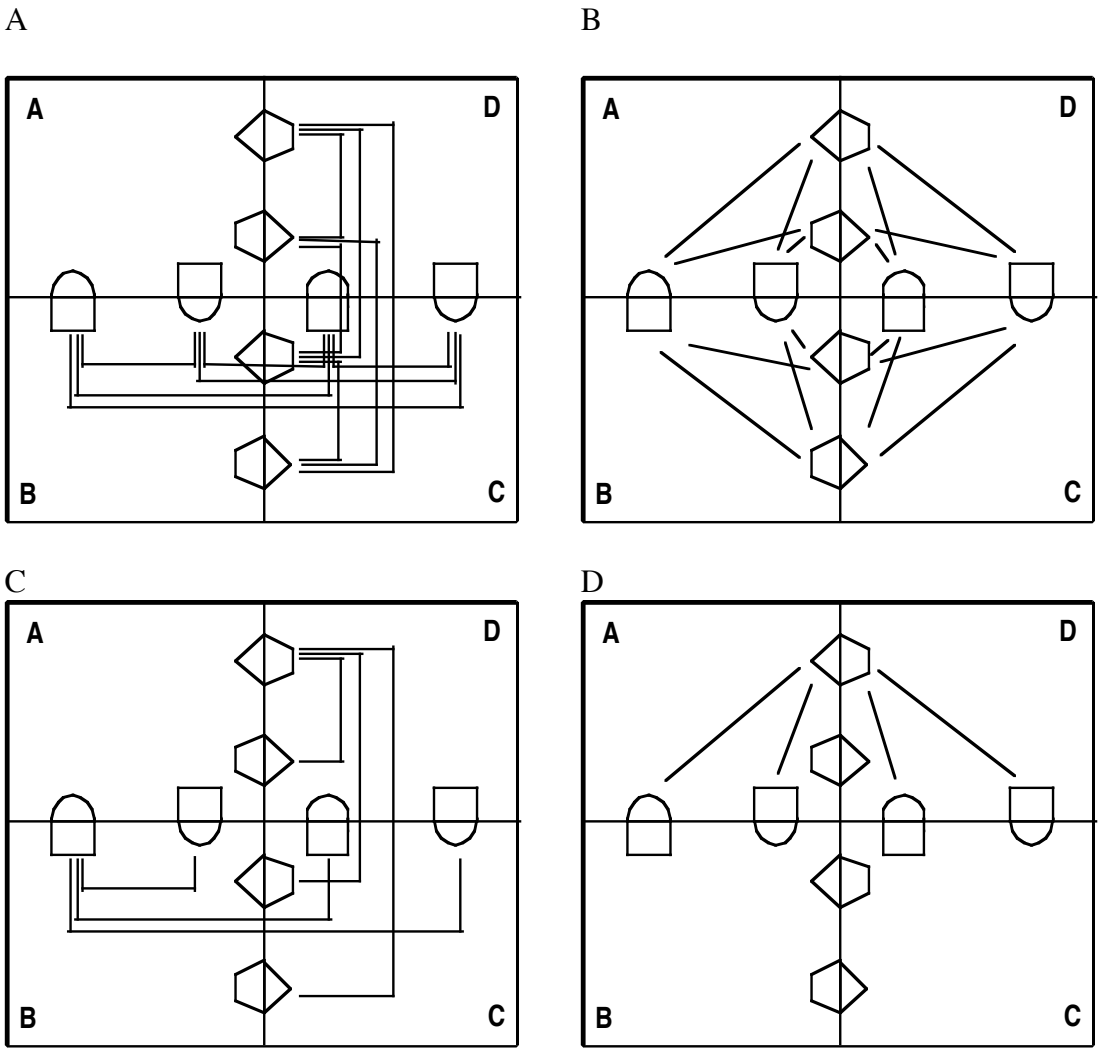

FIGURE 1-6: Two-dimensional representation of the PFK tetramer. The active site interface lies vertically and the allosteric site interface lies horizontally. The complexity of interactions found within the enzyme is comprised of (A) multiple homotropic interactions (B) multiple heterotropic interactions (C) unique homotropic interactions and (D) unique heterotropic interactions.

BsPFK, MgADP activation is barely noticeable at room temperature as compared to EcPFK. At higher temperatures, the magnitude of activation in BsPFK increases. No activation was observed at 16°C, however at temperatures below 16°C, MgADP becomes an inhibitor. This temperature-induced crossover of allosteric response by MgADP (Braxton et al, 1994) is not observed in EcPFK. Figure 1-7 shows the differences in the allosteric responses to PEP and MgADP between the two enzymes at 25°C and pH 8.0. The extent of PEP inhibition is greater and MgADP activation is smaller for BsPFK than EcPFK. The allosteric properties in BsPFK are dependent on pH, unlike those in EcPFK (Deville-Bonne et al, 1991; Tlapak-Simmons and Reinhart, 1998).

The crystal structures of BsPFK with substrate bound (so-called R-state) and that with a PEP analog, phosphoglycolate, bound (so-called T-state) have revealed two conformations of the active site (Evans and Hudson, 1979; Schirmer and Evans, 1990). In the presence of phosphoglycolate, there is a 7° rotation along one axis and the position of residues Glu161 and Arg162 in the active site switch between the two structures. For many years, this switch was proposed to be the mechanism for allosteric inhibition by PEP in BsPFK. The favorable interactions between Glu161 and Arg243, and Glu161 and Arg252 are proposed to close the active site from F6P binding and therefore lock the structure in the T-state (Schirmer and Evans, 1990). However, thermodynamic, kinetic and mutagenic studies have proven the mechanism incorrect (Kimmel and Reinhart, 2000). No such mechanism was proposed for EcPFK.

Extensive mutational analyses of both enzymes have been performed by many

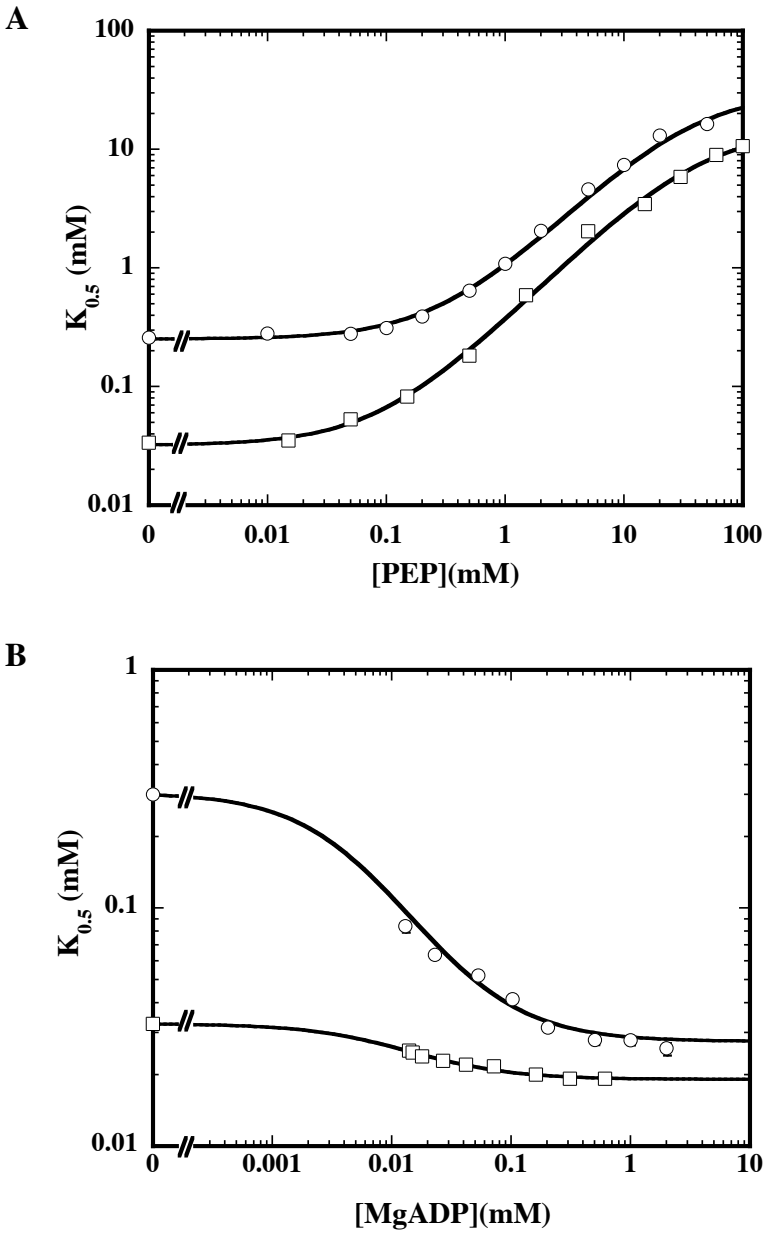

FIGURE 1-7: Allosteric properties of EcPFK and BsPFK at pH 8.0 and 25°C. The circles are data for EcPFK, the squares are data that pertains to for BsPFK (Tlapak-Simmons and Reinhart, 1998). Errors are plotted on the points. Data was fit to equation 1-10. Both EcPFK and BsPFK are inhibited by PEP (A) and activated by MgADP (B) to different extents.

groups to probe for residues important for binding of substrates and effectors (Valdez et al, 1988, 1989, Lau and Fersht, 1989, Berger and Evans, 1992, Wang and Kemp, 1999, Fenton et al., 2003). Traditionally, MgGDP was used instead of MgADP, because MgGDP is presumed not to bind to the active site, and therefore specific for binding in the allosteric site (Blangy et al., 1968, Auzat et al, 1997). Tables 1-1 and 1-2 summarize the kinetic characterization of mutations in the active site and the allosteric site, respectively in EcPFK. However, not much work has been done to study the role internal residues play in enabling allosteric communication (Serre et al, 1990, Auzat et al, 1994, Pham et al., 2001). A summary of the mutations characterized which are not in the binding sites in EcPFK can be seen in Table 1-3. All but one were in the subunit interface. Therefore, our goal in this dissertation is to increase our understanding of the basis for allosteric regulation in EcPFK by simplifying the complex allosteric communications in EcPFK and shedding light on the path or residue(s) important for allostery.

Non-allosteric Phosphofructokinases

Even though phosphofructokinases have been isolated and studied from many different organisms, they show certain similarities in size and homotetrameric structure. However, phosphofructokinases that are not allosterically regulated have been reported in bacteria and eukaryotes over the years. Phosphofructokinases from *Dictylostelium discoideum* (Baumann and Wright, 1968), *Arthrobacter cystallopoietes* (Ferdinandus and Clark, 1969), *Lactobacillus casei*, *Lactobacillus plantarum* (Doelle, 1972), *Desulfurococcus amylolyticus* (Hansen and Schönheit, 2000) and *Aeropyrum pernix*

TABLE 1-1: Kinetic characterization of active site mutations as compared to wildtype EcPFK.

Mutation	Effect	References
D127S	k_{cat} 18,000-fold less	Hellinga and Evans, 1987
R171S	k_{cat} 3-fold less	
R171S/D127S	k_{cat} 62,000-fold less	
R162S	F6P binding 165-fold weaker	Berger and Evans, 1990
R243S	F6P binding 50-fold weaker	
R72S	F6P binding 3-fold weaker, k_{cat} 34fold less	
D103A	k_{cat} 28-fold less, ATP binding 2-fold tighter	Berger and Evans, 1992
T125A	k_{cat} 900-fold less, F6P binding 320-fold weaker, ATP binding 2-fold tighter	
D127E	k_{cat} 134-fold less, F6P binding 325-fold weaker, ATP binding 10-fold tighter	
D127Y	k_{cat} 960-fold less, ATP binding 3-fold tighter	
D129S	k_{cat} 960-fold less, F6P binding 12-fold weaker, ATP binding, 2-fold tighter	
E222S	$k_{cat,}$ F6P and ATP binding no change	
D127S	k_{cat} 2150-fold less	Laine et al., 1992
D129S	k_{cat} 940-fold less, F6P binding 13-fold weaker	
I126A	k_{cat} 2-fold less, F6P binding 620-fold weaker, ATP binding 2-fold tighter	Zheng and Kemp, 1992
R72H	k_{cat} 370-fold less, F6P binding 2-fold weaker	
T125S	k_{cat} 3-fold less, F6P binding 4-fold weaker, ATP binding 3-fold tighter	Auzat et al., 1994
D127S	k_{cat} 220,000fold less	Zheng and Kemp, 1994b
D127A	F6P binding 2-fold weaker, k_{cat} 44,000fold less	
D127S/D129N/R252Q	F6P binding 4-fold weaker, k_{cat} 15,000-fold less	
R72H	k_{cat} 560-fold less	
R171H	k_{cat} 2-fold less, F6P binding 3-fold weaker, ATP binding 2-fold weaker	
R72H/R171H	k_{cat} 1,200-fold less, F6P binding 3-fold weaker, ATP binding 4-fold weaker	

TABLE 1-1 (Continued).

Mutation	Effect	References
I256A	F6P binding 380-fold weaker, k_{cat} 3-fold less	Zheng and Kemp, 1994a
I256S	F6P binding 300-fold weaker, k_{cat} 4-fold less	
N128A	F6P binding 180-fold weaker, ATP binding 2-fold weaker, k_{cat} 3-fold greater	
N128S	F6P binding 390-fold weaker, k_{cat} 3-fold greater	
R252Q	F6P binding 1,560-fold weaker, ATP binding 3-fold tighter, k_{cat} 22-fold less	
Q161E	F6P binding 6-fold weaker	Auzat et al., 1995
Q161R	F6P binding 3-fold weaker	
Q161A	F6P binding 3-fold weaker	
R252Q	F6P binding 1590-fold weaker, k_{cat} 45-fold less, ATP binding 3-fold tighter	Zheng and Kemp, 1995
D127S/R252Q	k_{cat} 2,100-fold less	
R171E	k_{cat} 18-fold less, F6P binding 3-fold weaker	Fenton et al., 2003
R72E	k_{cat} 200-fold less, F6P binding 3-fold tighter	
T125A	k_{cat} 4,200-fold less, F6P binding 2-fold weaker	

TABLE 1-2: Kinetic characterization of allosteric site mutations as compared to wildtype EcPFK.

Mutation	Effect	References
Y55F	GDP binding slightly weaker	Lau et al., 1987
Y55G	GDP binding 6-fold weaker	
E187A	F6P binding >2-fold weaker	Lau and Fersht, 1987
E187A + 10 mM PEP	F6P binding <2-fold weaker	
R21A	GDP binding >250-fold weaker, PEP binding 130-fold weaker	Lau and Fersht, 1989
R25A	GDP binding 30-fold weaker, PEP binding 170-fold weaker	
R54A	GDP binding 140-fold weaker, PEP binding 36-fold weaker	
D59A	GDP binding 32-fold weaker, PEP binding 46-fold weaker	
R154A	GDP binding 110-fold weaker, PEP binding 46-fold weaker	
K213A	GDP binding >250-fold weaker, PEP binding 46-fold weaker	
E187A	GDP causes inhibition, PEP causes activation	
E187N	GDP causes inhibition, PEP binding 2-fold weaker	
Y319deletion	GDP binding 41-fold weaker, PEP binding 40-fold weaker	
K213A	ADP binding 13-fold weaker, PEP binding 40-fold weaker Fluorescence insensitive to ADP or PEP	Berger and Evans, 1991
E187A	No allosteric effect by ADP, No ADP inhibition	Pham and Reinhart, 2001

TABLE 1-3: Kinetic characterization of other mutations as compared to wildtype EcPFK.

Mutation	**Effect**	**Location**	**References**
Limited proteolysis by subtilisin	Hill number reduced from 4 to 2, not sensitive to ADP or PEP F6P stabilizes dissociation	C-terminal 40-50 residues removed	Le Bras and Garel, 1982, 1985
L178W	Loss of heterotropic interactions	Helix 7 (between active and allosteric sites)	Serre et al., 1990
Y279Ochre stop W311Amber stop	Not active PEP binding 30-fold weaker, GDP binding 25-fold weaker	Final 41 residues removed Final 9 residues removed	Serre and Garel, 1990
R63S L153V T156G + insert S S159N H160N V246T	k_{cat} 5-fold less k_{cat} 23-fold less, F6P binding 2-fold weaker No activity, F6P binding >125-fold weaker No activity, F6P binding >1,000fold weaker k_{cat} 4-fold less, F6P binding 19-fold weaker k_{cat} 3-fold less	Helix 6 (subunit interface)	Kundrot and Evans, 1991
E148A E148D R152A R152K E148A/R152A	F6P binding 3-fold weaker F6P binding 3-fold weaker F6P binding 3-fold weaker, Hill number >4 F6P binding 2-fold weaker, Hill number >4 F6P binding 5-fold weaker, Hill number >4	Subunit interface	Auzat et al., 1995
L178V L178W E148L	F6P binding 3-fold weaker k_{cat} 2-fold less, GDP increases k_{cat} to wildtype k_{cat} 2-fold less, ATP binding 2-fold tighter,F6P binding 3-fold weaker	Helix 7 (between active and allosteric site) Helix 6 (subunit interface)	Auzat et al., 1997

(Hansen and Schönheit, 2001) do not exhibit allosteric properties. Isozymes of PFK from *E. coli* (Babul, 1978) and *Thermus thermophilus* (Xu et al, 1991) are also found to be non-allosteric.

Phosphofructokinase from *Lactobacillus delbrueckii* subspecies *bulgaricus* (LbPFK) was reported to be non-responsive to MgGDP or MgADP. Inhibition of activity by PEP was observed at pH 6 but not at pH 8.2 (Le Bras et al, 1991). This organism is a gram-positive, facultative anaerobic bacterium that is important in the food and dairy industry for the fermentation of milk by converting lactose to lactic acid (Delley and Germond, 2002). This lactic acid bacterium does not possess an extensive respiratory chain, tricarboxylic acid or glyoxylate cycle. This bacterium does not use gluconeogenic sources and its carbon sources are only glucose, fructose, lactose and galactose (Le Bras et al, 1991, Burgos-Rubio et al., 2000). The inhibition of LbPFK by PEP observed at low pH could be needed to control intracellular pH during fermentation (Le Bras et al., 1991).

The amino acid sequence of this relatively non-allosteric PFK is 47% identical and 66% similar to that of EcPFK, and 56% identical and 74% similar to that of BsPFK. Knowing that the sequence, structure and function of EcPFK and BsPFK are very similar, we can hypothesize that LbPFK would also have similar structure and function with EcPFK and BsPFK. However, LbPFK exhibits diminished allosteric responses as compared to EcPFK and BsPFK. Understanding the binding and allosteric behavior of LbPFK in response to MgADP and PEP, and comparing the sequence and structure of LbPFK should help in the understanding of the structural basis for allosteric regulation in EcPFK and/or BsPFK.

Chapter Overview

Chapter II discusses the materials, experimental procedures and data analyses used in this dissertation for the kinetic characterization of EcPFK to address how allosteric communication is transmitted within EcFPK.

The focus of Chapter III is the isolation and characterization of two of the four unique heterotropic interactions in EcPFK with respect to their allosteric responses to MgADP as compared to a control created for the wildtype EcPFK without homotropic cooperativity in F6P binding (Fenton and Reinhart, 2002; Fenton et al., 2004). These two combined with the other two heterotropic interactions characterized by my colleague, Dr. Aron Fenton, would allow for a better understanding on how activation is transmitted within the tetramer by measuring the coupling free energies of each heterotropic interaction.

The four unique heterotropic interactions with respect to PEP inhibition had been characterized for BsPFK. The magnitudes of the coupling free energies for each of the unique heterotropic interactions are unique and sum up to the magnitude of the coupling free energy of a control hybrid without homotropic cooperativity in PEP binding (Kimmel and Reinhart, 2001; Ortigosa et al, 2004).

Chapter IV is the study of the structure-function relationship in PFK from *Lactobacillus bulgaricus*. The re-examination into the allosteric properties of this enzyme and the determination of its crystal structure are presented to provide insight into the structural basis for allosteric regulation in EcPFK and BsPFK.

Chapter V describes the kinetic characterization of mutant proteins of EcPFK in which amino acids in EcPFK have been substituted by their corresponding amino acids

from LbPFK to see if we could create proteins with little or no allosteric characteristics and thereby identifying residues that play important roles in allosteric communication. Sequence alignment between three bacterial allosteric PFKs including EcPFK, BsPFK and PFK from *Thermus thermophilus*, and LbPFK has provided twenty-two conserved residues in the three allosteric PFKs but not in LbPFK. These twenty-two residues were substituted for their counterpart from LbPFK, the proteins purified and characterized.

Using the strategy from Chapter III, we can introduce one of the mutations identified from Chapter V, that resulted in diminished allosteric responses to MgADP and PEP, into each of the four unique heterotropic interactions. The effect this mutation has on one or more of the heterotropic interactions in EcPFK with respect to PEP and MgADP is addressed in Chapter VI.

This dissertation aims to define the basis for allosteric regulation in EcPFK by determining which allosteric site is coupled to which active site and by probing the differences between EcPFK and BsPFK, and LbPFK. This work should enlighten us onto the path and/or residues important for the transmission of allosteric information in EcPFK.

CHAPTER II

GENERAL METHODS

Materials and Methods

Materials. All chemical reagents and buffers were analytical grade, purchased from Fisher Scientific or Sigma-Aldrich. The sodium salts of fructose-6-phosphate, phospho(enol)pyruvate, NADH and phosphocreatine, and the potassium salt of ADP were purchased from Sigma. Creatine kinase, the ammonium sulfate suspensions of aldolase, triose phosphate isomerase and glycerol-3-phosphate dehydrogenase, the sodium salt of ATP and dithiothreitol were purchased from Roche Diagnostics. Dye Matrex Blue A resin and Mimetic Blue-1 resin for affinity chromatography were purchased from Amicon and Prometic Biosciences, respectively. Mono Q 10/10, an anion exchange column, was purchased from Pharmacia for use on their Fast Performance Liquid Chromatrography (FPLC) system. DE-52 resin, an anion exchange resin, was obtained from Whatman. BCA protein assay reagents were purchased from Pierce. Glycerol stocks of BMH 71-18 mutS and XL1Blue cells were purchased from Promega and Stratagene, respectively. A glycerol stock of *E. coli* DF1020 cells (cells deleted of PFK-1 and PFK-2 genes, Daldal, 1983) was obtained from Dr. Robert Kemp (Chicago Medical School). DNA oligonucleotides were ordered either from Gene Technologies Laboratory (GTL) at Texas A&M University or Integrated DNA Technologies, Inc (IDT). Plasmid miniprep kit was purchased from Qiagen. DNA

sequencing was performed by GTL on Applied Biosystems 373XL and 377XL DNA sequencers.

Site-directed Mutagenesis. The Altered Sites II *in vitro* mutagenesis system from Promega was primarily used to introduce site-specific substitutions in pGDR16 (Johnson et al, 2001). This plasmid contains *E. coli* PFK-1 gene cloned into pAlter-1 from Promega and is used to express wildtype EcPFK and construct all mutants. The protocol from the Altered Sites system was followed to introduce single or multiple mutations in pGDR16 (Figure 2-1). Single-stranded pGDR16 was produced using R408 helper phage and purified. Oligonucleotides that are complementary to the single-stranded DNA containing the mutation(s) of interest and an oligonucleotide that repairs the ampicillin resistance gene in the plasmid were annealed to the single stranded DNA. The oligonucleotides were extended using T4 DNA polymerase and ligated with T4 DNA ligase. The resulting plasmid was transformed into a mismatch repair minus strain of *E. coli* (BMH 71-18 mut S) and grown on LB plates containing ampicillin. Colonies were inoculated into 5 mL LB-Amp overnight cultures, and the plasmid was purified using Qiagen plasmid miniprep kit. Because of the instability of BMH cells, the purified plasmid was transformed into competent XL1Blue cells. Plasmid was purified out of the XL1Blue cells and sequenced using Sanger dideoxy method using dye-labeled terminators and ABI sequenchers to confirm the sequence of the mutated DNA.

QuikChange Site-directed Mutagenesis system was used to introduce additional mutations in pGDR16 (Figure 2-2). Two oligonucleotides complementary to one another containing the mutation(s) of interest were annealed to the denatured plasmid

1. Clone insert into pALTER-1 vector.

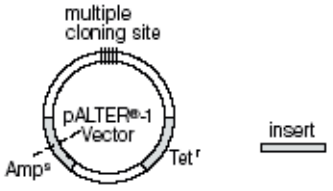

2. Isolate dsDNA.

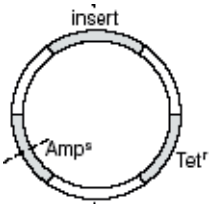

3. Prepare ssDNA and anneal mutagenic oligo(s), Ampicillin Repair oligo and Tetracycline Knockout Oligo.

4. Synthesize mutant strand with T4 DNA Polymerase and T4 DNA Ligase.

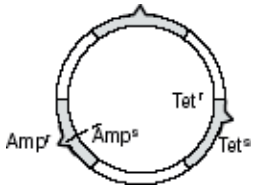

5. Transform competent BMH cells with mutagenesis reaction. Grow overnight with ampicillin selection.

6. Purify plasmid DNA and transform into XL1-Blue cells. Select mutants on ampicillin plates.

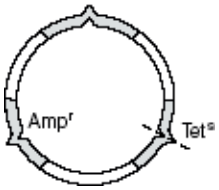

Optional. Perform additional rounds of mutagenesis using selection for Tet repair alternating with Amp repair.

FIGURE 2-1: Altered Sites II *in vitro* mutagenesis protocol from Promega. This figure was adapted from Promega.

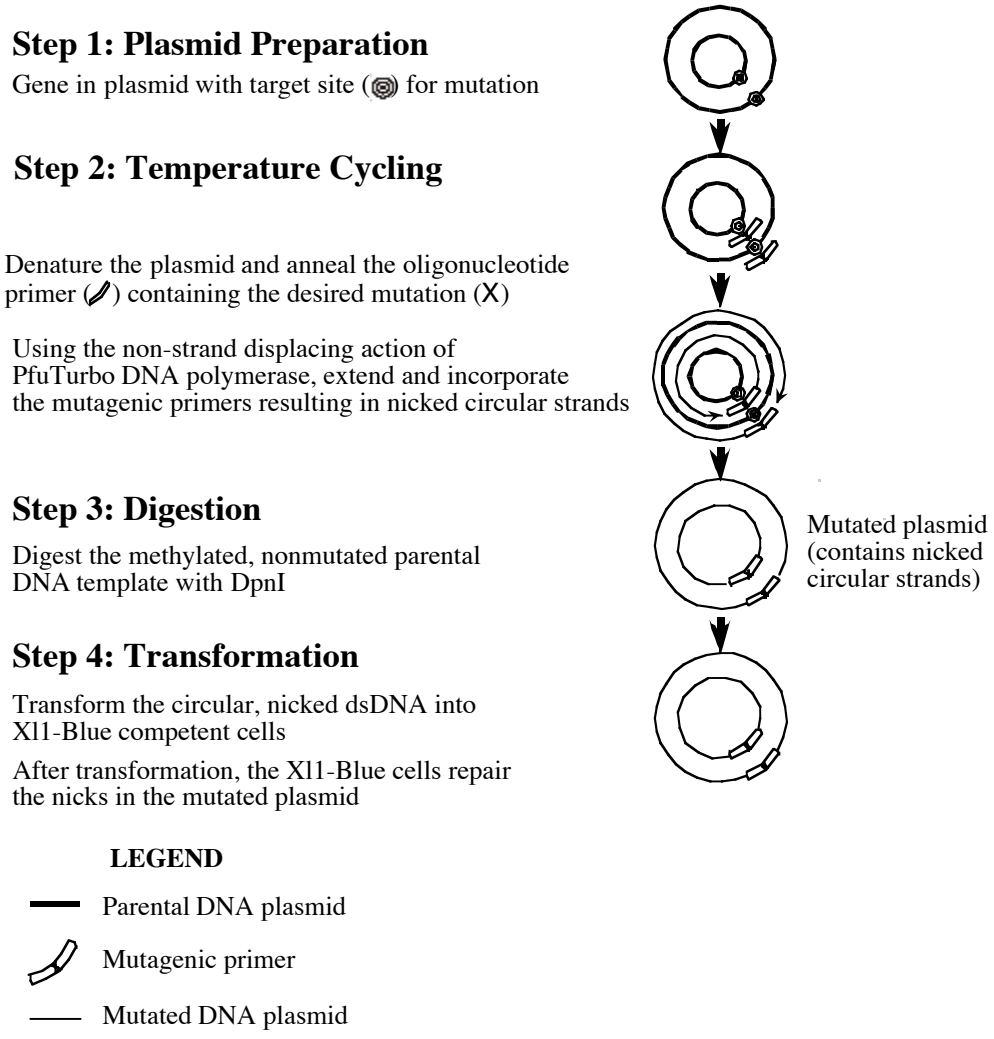

FIGURE 2-2: QuikChange site-directed mutagenesis protocol from Stratagene. This figure was adapted from Stratagene.

and extended during temperature cycling by using PfuTurbo DNA polymerase and treated with DpnI endonuclease that digests the nonmethylated parental DNA template. The newly synthesized DNA was transformed into XL1Blue cells, the plasmid purified and sequenced to verify the sequence of the mutant DNA.

Protein Purification. The purification of wildtype or mutant PFK followed the protocol of Johnson et al. (2001) with modifications. DF1020 cells containing PFK in pALTER1 were grown in 1.5 L LB broth containing 100 μg/ml ampicillin at 37°C for 24 hours. Cells were harvested by centrifugation at 5000 x g using a Beckman Model J-6B centrifuge. Pelleted cells were stored at -20°C until ready for lysis. The frozen cell pellets were resuspended in approximately 30 mL of Buffer A (50 mM Tris-HCl pH 7.5, 5mM $MgCl_2$, 0.1 mM EDTA, 2 mM DTT). Cells were lysed by sonication using a Sonic Dismembrator Model 550 (Fisher Scientific) with 15-second pulses for a total sonication time of 8 minutes. Crude lysate was cleared by centrifugation at 12,000 RPM for 1 hour in a Beckman J2-21 centrifuge with a JA-20 rotor. The supernatant was incubated in the presence of DNase at 37°C for 15 minutes before centrifuging the remaining cell debris away for another hour. The final supernatant containing soluble proteins was applied to a dye-affinity column that has been equilibrated with Buffer A. Two dye-affinity resins have been used and their elution procedures differ. When using Dye Matrex Blue A from Amicon, the column was washed with 100 mL each of Buffer A, Buffer A + 1.5 M NaCl, and Buffer A + 2 mM ATP to elute off any loosely bound proteins. With subsequent re-use of the resin, the affinity the resin has for PFK decreased and PFK was eluted when washed with Buffer A + 2 mM ATP. The remaining PFK was eluted with

Buffer A + 2 mM ATP + 1.5 M NaCl + 10 mM $MgCl_2$. Due to an apparent lower affinity of Mimetic Blue for PFK than the Matrex Blue, when using the Mimetic Blue resin from Prometic Biosciences, the final supernatant was diluted to 100 mL before loading onto the column. The column was then washed with 100 mL of Buffer A before eluting PFK with Buffer A + 1.5 M NaCl and fractions collected. Each fraction was assayed for its absorbance at 280 nm and activity (Figure 2-3). The fractions that have enzymatic activity were pooled, concentrated using Amicon YM-10 concentrators and dialyzed against Buffer A. The purified protein was run on SDS-PAGE (Laemmli, 1970) to check for purity (Figure 2-4). Most of the purified proteins after the Blue column were at least 95% pure. If there were multiple bands on the gel, the protein was passed through anion-exchange chromatography, either a Mono Q column on Pharmacia FPLC or a DE-52 column, and eluted with 0 to 1 M NaCl gradient. Fractions were collected and assayed (Figure 2-5). The fractions containing PFK were pooled, dialyzed against Buffer A and stored at 4°C. A representative purification table is shown Table 2-1.

Enzymatic Activity. Standard activity assays were performed at pH 8.0 and 25°C unless otherwise noted. The production of fructose-1,6-bisphosphate, using a coupled-enzyme system, was monitored by the oxidation of NADH (Figure 2-6). The reaction was started with the addition of 6 μl of PFK to a total volume of 600 μl of an EPPS buffer containing 50 mM EPPS-KOH, 10 mM $MgCl_2$, 10 mM NH_4Cl, 0.1 mM EDTA), 2 mM DTT, 250 μg aldolase, 50 μg glycerol-3-phosphate dehydrogenase, and 5 μg triose phosphate isomerase that was adjusted to pH 8.0. F6P, MgATP and either PEP

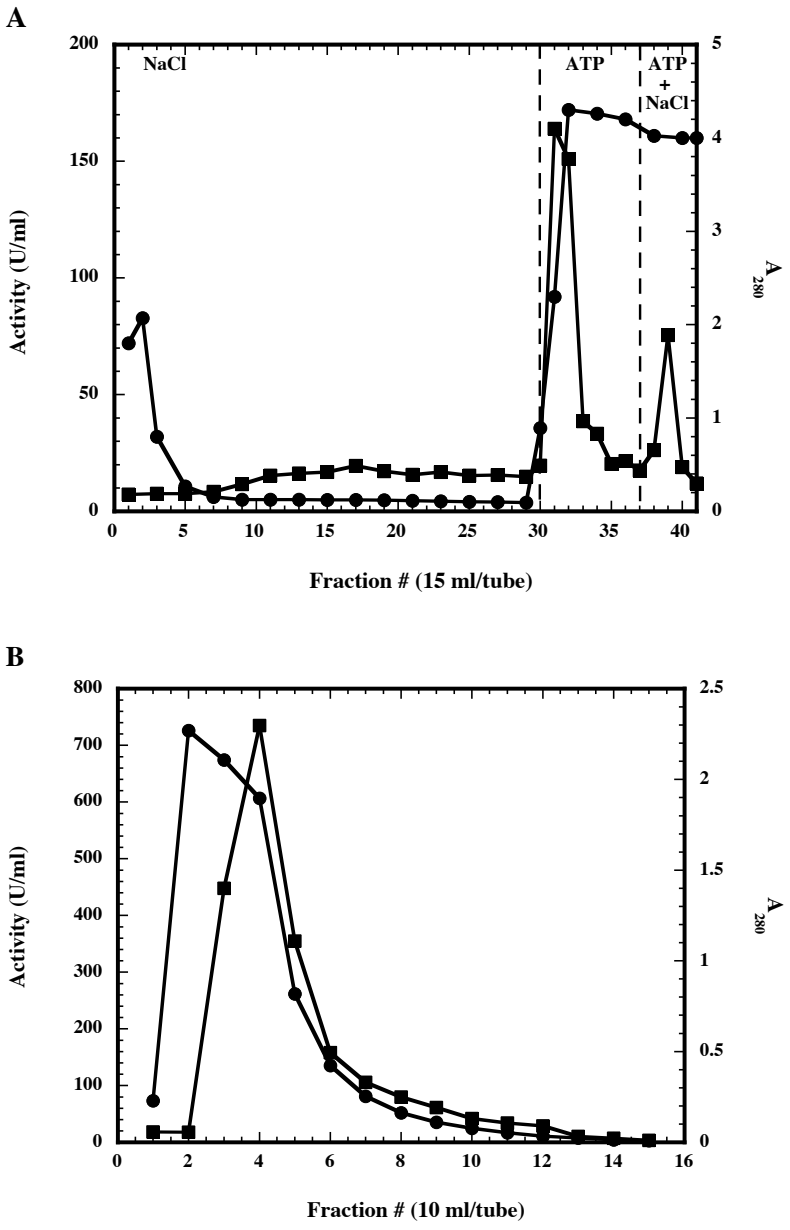

FIGURE 2-3: Elution profile of PFK off Blue dye affinity column. A) Using Amicon Matrex A resin, PFK was eluted off by ATP and ATP+NaCl. B) Using Mimetic Blue resin, PFK was eluted with 1.5M NaCl. Activity and absorbance are represented by ■ and ●, respectively. Fractions containing activity were pooled and dialyzed.

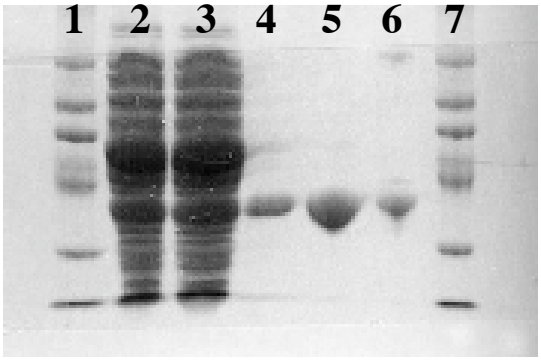

FIGURE 2-4: SDS-PAGE of purified PFK. The first and the seventh lane contains molecular weight ladder. The second lane contains sample after the first centrifugation step. The third lane contains sample before loading onto the Blue A affinity column. The fourth lane contains pooled fractions off the Blue affinity column. The fifth lane contains purified sample off DE-52, an anion-exchange column. The sixth lane is a control PFK sample.

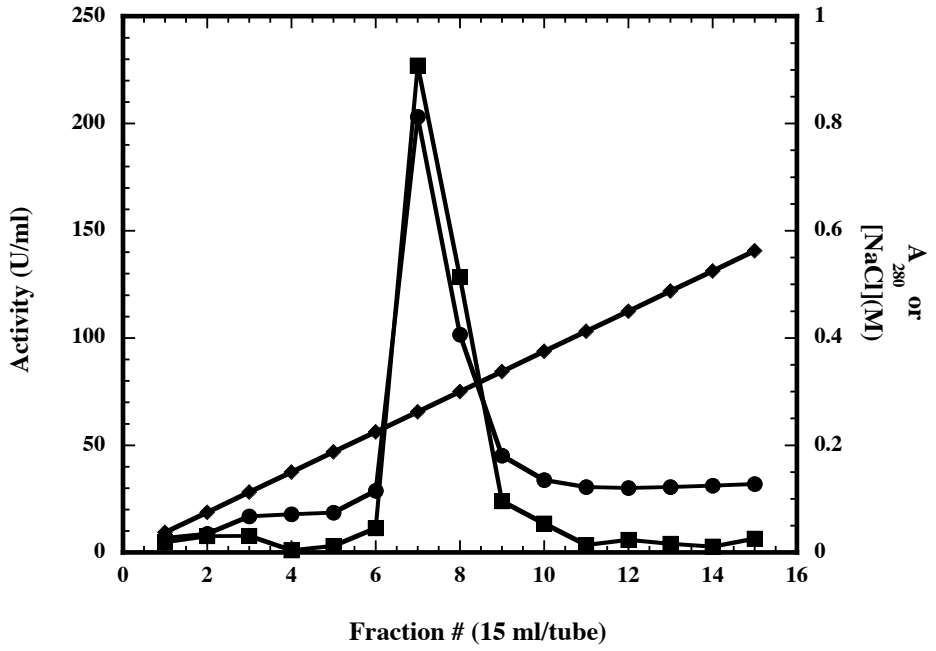

FIGURE 2-5: Elution profile of PFK off an anion-exchange column. PFK was eluted off the DE-52 column with a gradient from 0 to 1 M NaCl. Activity and absorbance are represented by ■ and ● , respectively. NaCl concencentrations are given by ♦. Fractions containing activity were pooled and dialyzed.

TABLE 2-1: A representative purification table for EcPFK.

Steps	Crude	DNase	BlueA	DE-52
Activity (Units/ml)	400	400	120	800
Protein (mg/ml)	10	10	0.7	3.2
Volume (ml)	35.0	34.5	44.5	5.6
Total Activity (Units)	14000	13800	5356	4480
Total Protein (mg)	350	345	32	18
Specific Activity (Units/mg)	40	40	166	250
Fold Purification	-	1.0	4.2	6.3
% yield	100	99	38	32

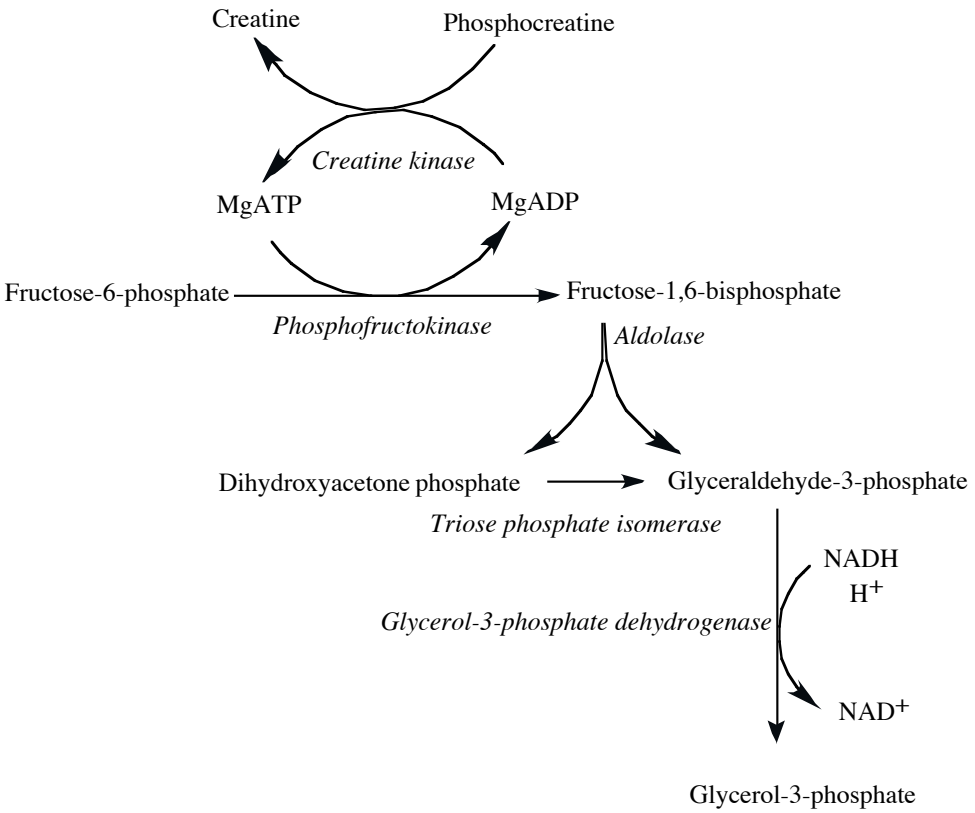

FIGURE 2-6: Coupling enzyme system. Enzymatic activity of PFK is measured by following product formation coupled to NADH oxidation. Enzymes are in italics.

or MgADP concentrations were varied as indicated. For maximal activity, 3 mM ATP and 5 mM F6P were added. For assays at pH 6.0 and 7.0, MES-KOH and MOPS-KOH buffers were used instead of EPPS-KOH, respectively. In the absence of MgADP, 40 μg/ml creatine kinase and 4 mM phosphocreatine were added to convert MgADP contamination from substrate stocks to MgATP (Johnson and Reinhart, 1992). When MgATP is the variable, solutions of equal concentrations of $MgCl_2$ and ATP were added to the cocktail. When MgADP was added, it was added as a solution of equal concentrations of MgADP and MgATP to prevent competition between MgATP and MgADP in the active site (Johnson and Reinhart, 1994). MgADP contamination in the MgATP stock solution was measured enzymatically (Jaworek et al, 1974). The rate of the reaction is measured by the decrease of absorbance at 340 nm as a function of time on a Beckman DU640 spectrophotometer. This absorbance change is converted to activity by the multiplication with a conversion factor that takes into account the extinction coefficient of NADH, the two to one stoichiometry between NAD^+ and fructose-1,6-bisphosphate production, and the dilution of the enzyme. One Unit of enzyme activity is defined as the amount of enzyme needed to produce 1 μmole of fructose-1,6-bisphosphate per minute.

Protein Concentration. Determination of protein concentration was performed using the Bicinchoninic Acid (BCA) Protein Assay from Pierce (Smith et al, 1985) or calculated using the extinction coefficient of PFK of 0.6 mg^{-1} mL^{-1} at 280 nm (Kotlarz and Buc, 1977).

Data Analysis. Data were fit to appropriate equations using the non-linear least squares fitting analysis of Kaleidagraph 3.5 software (Synergy). Enzymatic activity was measured at increasing concentrations of one substrate and at a saturating concentration of the other as indicated. Data were fit to the Hill equation (Hill, 1910)

$$\frac{v}{E_T} = \frac{k_{cat}[A]^{n_H}}{K_{0.5}{}^{n_H} + [A]^{n_H}} \qquad [2\text{-}1]$$

where v is the steady-state rate of turnover, E_T is the total amount of enzyme active sites, k_{cat} is the turnover number, $K_{0.5}$ is the concentration of substrate (A) that gives half-maximal activity and n_H is the Hill coefficient. To study the effect PEP has on the binding of substrate F6P, $K_{0.5}$ values as a function of PEP concentration were determined using equation 2-1 and fit to the following equation (Reinhart et al., 1989):

$$K_{0.5} = K_{ia}^{o}\left[\frac{K_{iy}^{o} + [Y]}{K_{iy}^{o} + Q_{ay}[Y]}\right] \qquad [2\text{-}2]$$

where Y is PEP, $K_{ia}°$ and $K_{iy}°$ are dissociation constants of F6P and PEP in the absence of any other ligands, respectively. Data were weighted to the errors obtained from the fit to equation 2-1. The effect PEP has on the binding of F6P is given by the coupling constant Q_{ay} which has the following relationship (Reinhart, 1983):

$$Q_{ay} = \frac{K_{ia}^{o}}{K_{ia}} = \frac{K_{iy}^{o}}{K_{iy}} \qquad [2\text{-}3]$$

where K_{ia} and K_{iy} are dissociation constants of F6P and PEP in the saturating presence of the other ligand, respectively. The smaller the value of Q_{ay} is, the greater the inhibition. The same experimental approach was taken to study MgADP (X) activation

of F6P binding, with the replacement of X for Y. The value of Q_{ax} is greater than 1 when there is activation. Figure 2-7 shows data for wildtype EcPFK fit to equation 2-2. The dissociation constants in the absence of any other ligands were determined to be 0.30 ± 0.01 mM for F6P, 0.30 ± 0.01 mM for PEP, and 0.048 ± 0.002 mM for MgADP. The coupling constants, Q_{ax} and Q_{ay} are 11.1 ± 0.2 and 0.0083 ± 0.0001, respectively. These data indicate the MgADP activates F6P binding by eleven-fold and PEP inhibits F6P binding by 120-fold.

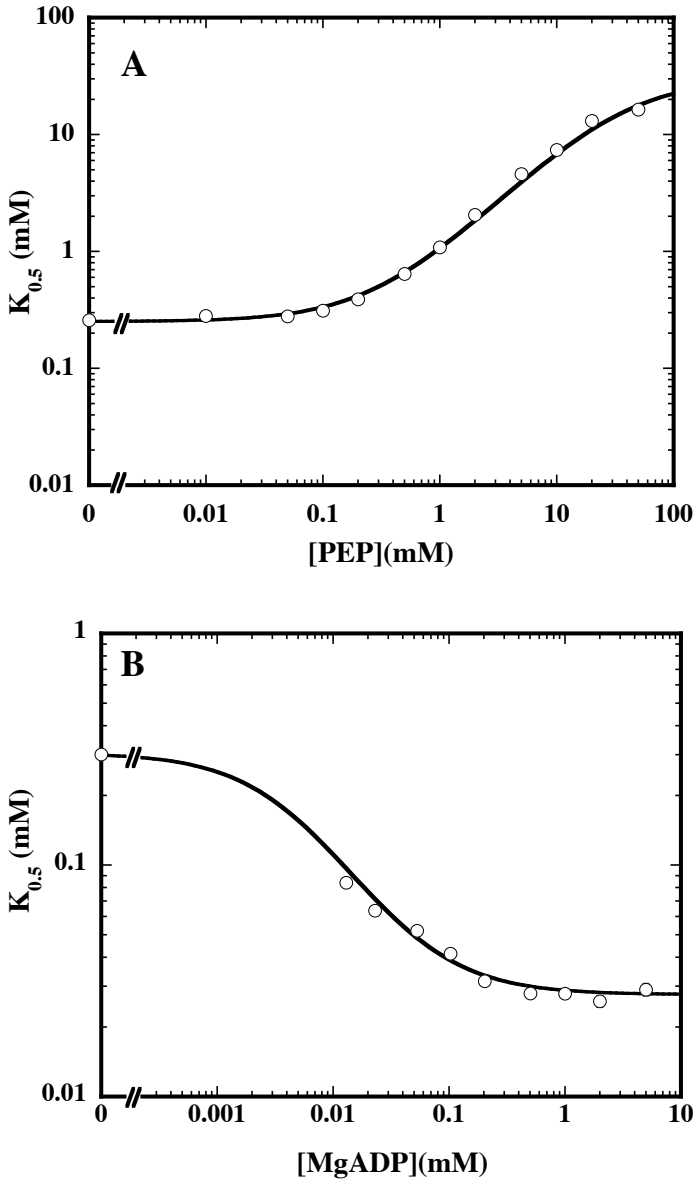

FIGURE 2-7: Allosteric effects on wildtype EcPFK. The extent of PEP inhibition (A) and MgADP activation (B) on F6P binding were determined at pH 8.0 and 25°C. The $K_{0.5}$ for F6P, determined using rates that were fit to equation 2-1, as a function of PEP and MgADP were plotted. Lines represent fits to equation 2-2. Errors are plotted but appear smaller than the data points. MgATP concentration was 3 mM.

CHAPTER III

DISENTANGLING THE WEB OF MgADP ACTIVATION IN PHOSPHOFRUCTOKINASE FROM *ESCHERICHIA COLI*

Introduction

Phosphofructokinase from *E. coli* is subject to allosteric regulation by MgADP and phospho(enol)pyruvate (PEP). These two effectors compete for binding at an allosteric site that is remote from the substrate-binding site. The enzyme can discriminate between the two effectors and once bound, MgADP increases the binding affinity for F6P to the active site whereas PEP decreases the binding affinity of F6P. How this occurs within the enzyme is still an interesting question.

EcPFK is a homotetramer with four active sites and four allosteric sites that form at subunit interfaces. Each site is composed of two half sites from each monomer to complete that site to which substrate or effector binds. Because each binding site can communicate with one another, there are twenty-eight possible pair-wise interactions between binding sites (Figure 3-1A). This allosteric web of potential interactions makes the study of allosteric communication complicated. This web of interactions can be disentangled using mutagenesis and the hybrid tetramer approach (Kimmel and Reinhart, 2001; Fenton and Reinhart, 2002; Ortigosa et al, 2004) to isolate the four unique heterotropic interactions in EcPFK shown in Figure 3-1B. The study of each of the single heterotropic interactions would help in the understanding of how allosteric information is transmitted within the protein.

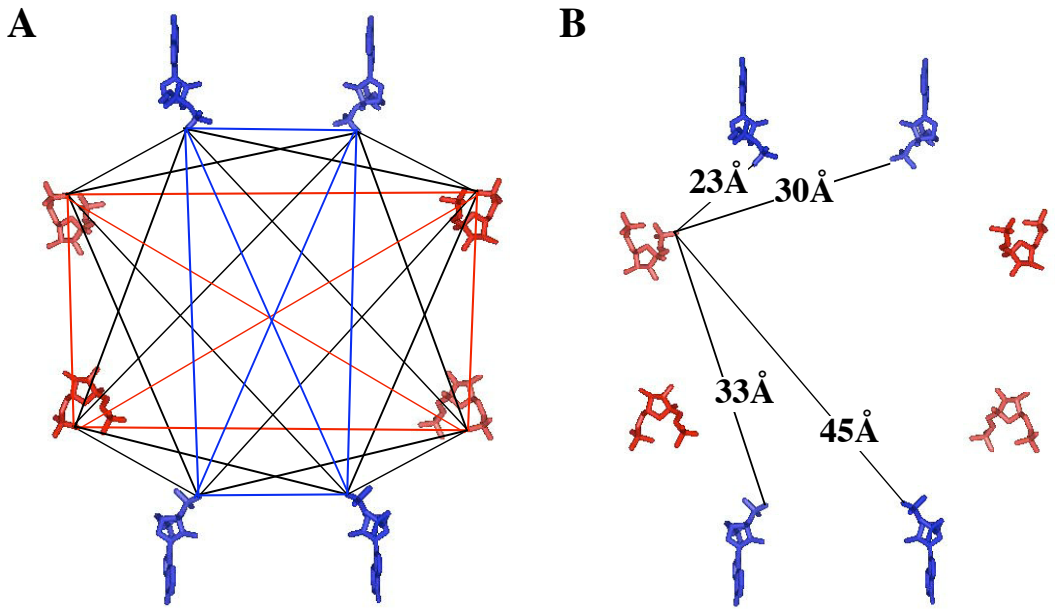

FIGURE 3-1: The potential allosteric interactions found in EcPFK. A) The allosteric web of potential interactions. There are twenty-eight interactions: twelve homotropic interactions shown in the red lines between fructose-1,6-bisphosphate (red) in the active sites and in the blue lines between MgADP (blue) in the allosteric sites, and sixteen heterotropic interactions as shown in the black lines. B) There are only four unique heterotropic interactions, labeled by their spatial distances between sites from the crystal structure determined by Shirakihara and Evans, 1988.

The focus of this chapter is the isolation using the hybrid tetramer approach and characterization of two of the four unique heterotropic interactions with respect to their allosteric responses to MgADP as compared to a control created for the wildtype enzyme that is devoid of homotropic cooperativity in F6P binding (Fenton and Reinhart, 2002). Hybrid tetramers have been created to study the effect PEP has on the four unique heterotropic interactions within PFK from *B. stearothermophilus* (Kimmel and Reinhart, 2001; Ortigosa et al, 2004). Each interaction is unique and their coupling free energies for PEP inhibition sum up to the magnitude of the coupling free energy of a control hybrid without homotropic cooperativity in PEP binding (Ortigosa et al, 2004). Since EcPFK and BsPFK have many similarities in sequence, structure and function, we are interested to ascertain whether the allosteric communication pathways would also be similar between the two enzymes.

Materials and Methods

Materials. All chemical reagents used for protein purification and enzymatic assays were obtained as described in Chapter II. Potassium thiocyanate (KSCN) was purchased from Sigma-Aldrich. The following oligonucleotides were ordered from Gene Technologies Laboratory (GTL) at Texas A&M University and DNA Technologies Integrated (IDT):

K2,3E: CCG-CTT-GTC-AAC-ACA-CCG-ATT-TCC-TCA-ATC-ATG-ACT-ACC-TCT-GAA-GC

R21A: CAG-CGC-AGA-ACG-AAC-AAC-CCC-AGC-AAT-TGC-GGC-GTT-CAT-

GCC-TGG

R154E: CTG-GTG-AGA-AGA-AGA-GGT-GTC-TTC-CAG-ACG-GTC-GAT-CGC-TCC-TAC

K213E: GGT-AAT-CGC-CAC-GAT-CGC-GTG-TTT-TTC-ACC-TTT-CGC-GAT-ACC-CGC

R252E: GGC-ACC-GGA-GAA-CCA-CCT-TCC-TGG-ATG-TGG-CCC-AGC

H249E coding: CTG-TGC-TGG-GCG-AAA-TCC-AGC-GCG-GTG-GTT-CTC-C

H249E noncoding: GGA-GAA-CCA-CCG-CGC-TGG-ATT-TCG-CCC-AGC-ACA-G

Methods. Promega Altered Sites II *in vitro* mutagenesis system was used to perform site-specific substitutions on pGDR16 (Johnson et al., 2001) using the oligonucleotides ordered. Constructs containing single-point mutations (R154E, K213E, R252E and H249E) and constructs for the 30Å mutant (K2,3E, R21A, R252E) and the 33Å mutant (K2,3E, K213E, R252E) were created. Stratagene QuikChange site-directed mutagenesis system was used to replace H252E with H249E in the constructs. Plasmid DNA was isolated using Promega Wizard spin preps. DNA was sequenced across the modified sites to confirm the desired mutations. The mutated plasmids were transformed into DF1020 cells (Daldal, 1983). Protein purification using the Amicon Dye Matrex Blue A resin and kinetic assays were performed at pH 8.0 and 8.5°C as described in Chapter II.

Hybrid Tetramer Formation. The strategy shown in Figure 3-2 was used to create hybrid tetramers. The 30Å or the 33Å mutant (7 mg) was incubated with wildtype EcPFK (3 mg) for 1.5 hours at 25°C with 0.4 M KSCN. The denaturant was

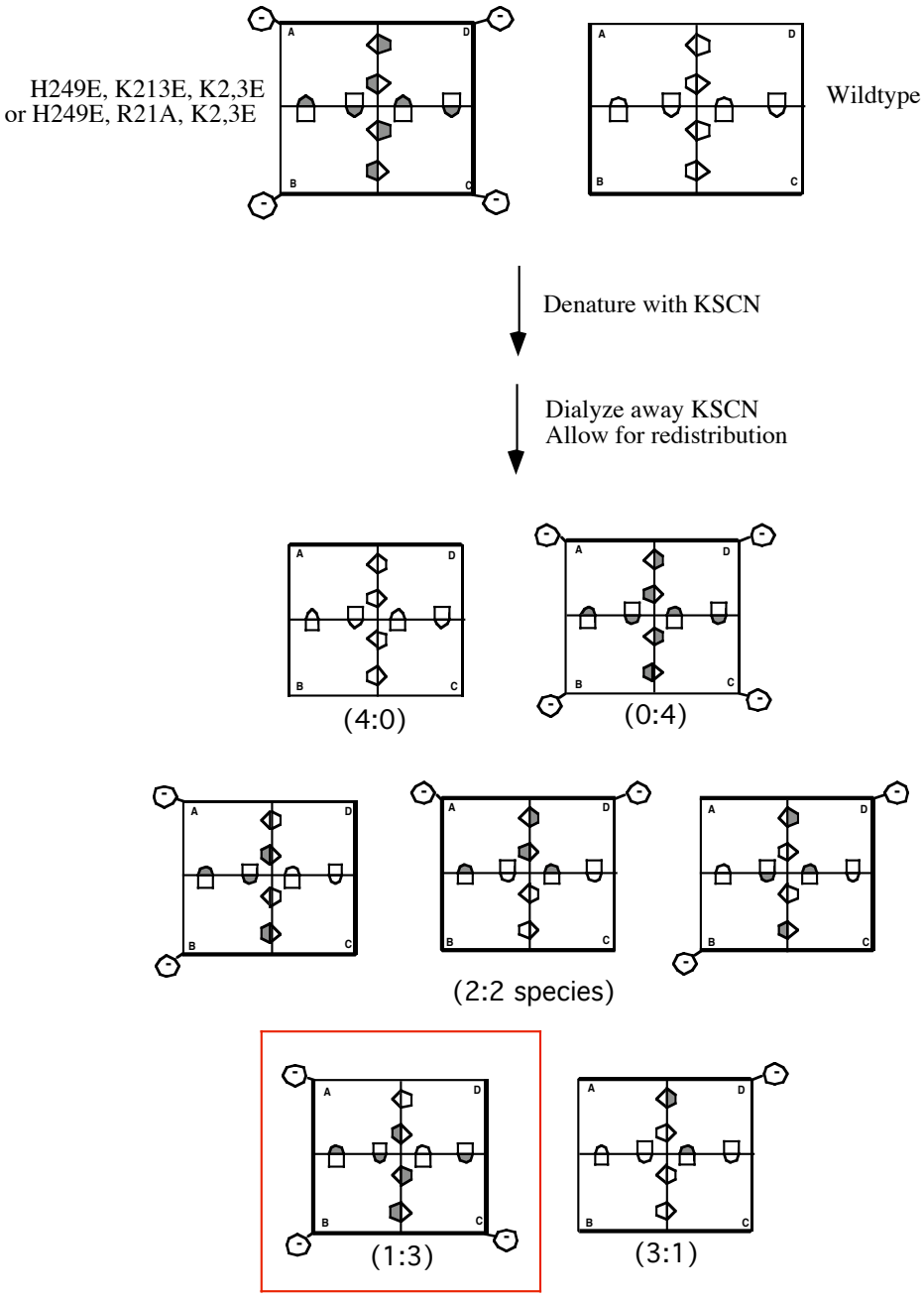

FIGURE 3-2: Strategy for creating hybrid tetramers. In the presence of KSCN, hybridization occurs between two parental proteins. The species containing one unique heterotropic interaction is boxed in red. The 30Å and the 33Å interactions were isolated using the 30Å mutant (K2,3E, R21A, H249E) and the 33Å mutant (K2,3E, K213E, H249E), respectively as one of the parent proteins.

dialyzed away at 4°C in Buffer A in the presence of 2 mM F6P for three hours to allow for redistribution and creation of each hybrid species. The protein mix was loaded onto a 10/10 MonoQ anion-exchange column on Pharmacia FPLC and the species separated by a shallow linear salt gradient from 0.23 to 0.3 M NaCl in Buffer A+2 mM F6P as seen in Figure 3-3A. This separation was facilitated by the presence of the mutations K2,3E which act as surface-charge tags. These mutations do not influence the kinetic properties of the enzyme (Data not shown). The identification and purity of each hybrid species were assessed using 7.5% native polyacrylamide gel electrophoresis (Figure 3-3B). The hybrid species of interest is the 1:3 hybrid i.e., a tetramer with one wildtype subunit and three mutated subunits. This hybrid contains one native active site and one native allosteric site capable of communicating with one another (a single heterotropic interaction). Subunit exchange of the 1:3 hybrid was prevented with the addition of F6P to a final concentration of 20 mM immediately after elution off the MonoQ column. The same strategy was followed to create control hybrids that contain one active site and no allosteric sites. These controls check for the influence of the mutated allosteric sites on the native active site. They are formed by incubating R21A or K213E with the 30Å or 33Å mutant, respectively.

Data Analysis. Data were fit to appropriate equations using the non-linear least squares analysis of Kaleidagraph 3.5 software (Synergy). Tetramers with sufficient affinity for F6P to achieve saturation were fit to the Hill equation (Equation 1-9, 2-1). For hybrids with a single active site, the linear region of the F6P titration curves were fit to a form of the Michaelis-Menten equation (Lehninger et al, 1993):

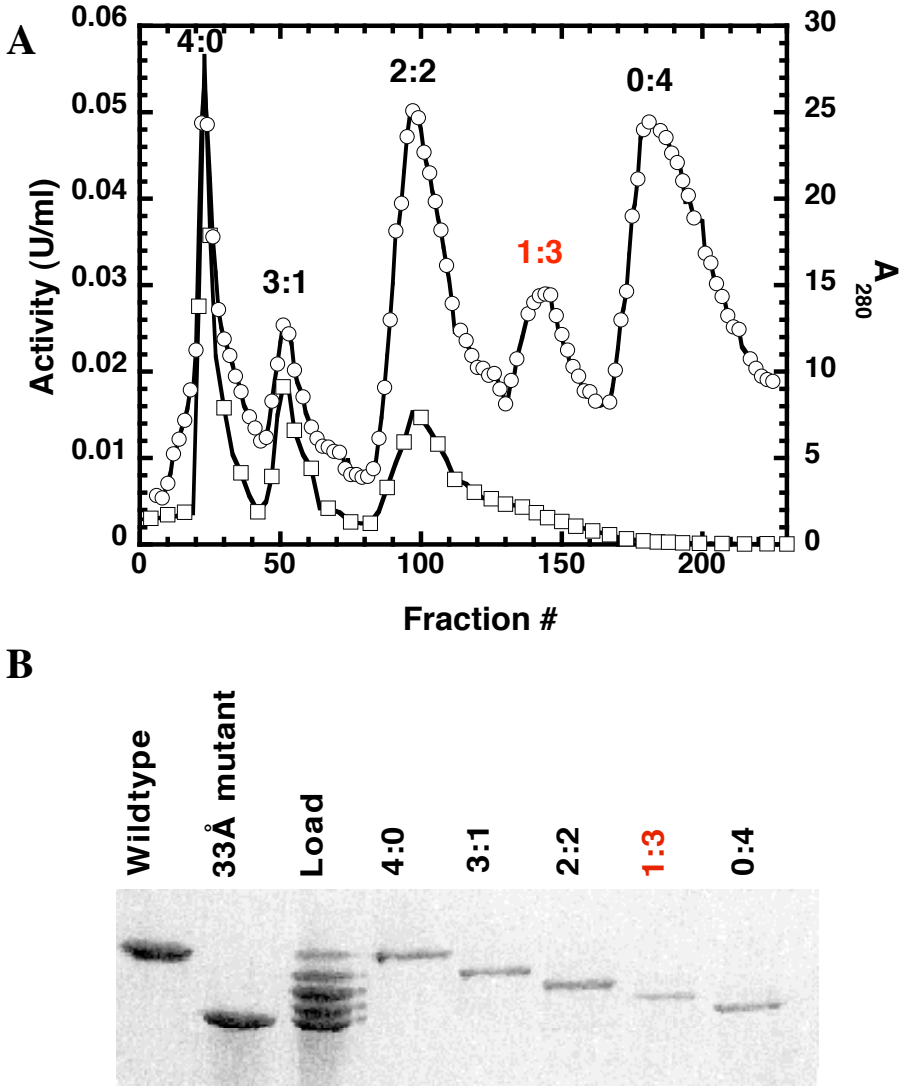

FIGURE 3-3: The purification of the hybrid tetramer containing the 33Å heterotropic interaction. A) Elution profile off the FPLC MonoQ column of the KSCN-treated proteins. The absorbance at 280 nm (○) and activity (□) of each fraction were assayed. Separation is facilitated by the presence of the surface mutations K2,3E. B) Identification and assessment of the purity of each hybrid species using 7.5% native PAGE. The 1:3 hybrid that contains one heterotropic interaction is shown in red. The purification of the 30Å interaction is similar.

$$\text{rate} = \left[\frac{V_{max}}{K_{0.5}}\right][F6P] \qquad [3\text{-}1]$$

that arises with the assumptions that the substrate (F6P) concentrations are much smaller than the concentration of F6P that would give one-half maximal activity ($K_{0.5}$) and the maximal activity (V_{max}) is constant. Parameters obtained from the fits to equation 2-1 ($K_{0.5}$) or equation 3-1 (1/(V/K)) were subsequently fit to equation 2-2 to obtain the values for the coupling constant Q_{ax} that measures the magnitude of MgADP activation of F6P binding. The larger the value of Q_{ax} is, the greater the activation. This coupling constant is related to the coupling free energy, ΔG_{ax}, by equation 1-8. Allosteric activation results in ΔG_{ax} values less than zero.

The coupling constants determined for the 30Å and the 33Å interactions were corrected for contributions from the mutated allosteric sites. This correction was accomplished by dividing the 1/(V/K) values obtained at each MgADP concentration for each interaction by its respective control. The corrected data were fit to equation 2-2.

Results and Discussion

The hybrid strategy allows for the creation and isolation of a hybrid tetramer containing one unique heterotropic interaction between F6P and MgADP in phosphofructokinase from *E. coli* (Fenton and Reinhart, 2002). This 1:3 hybrid (one wildtype subunit and three mutated subunits) contains a single native active site and a single native allosteric site capable of interacting with one another, which is the definition of a heterotropic interaction. There are four possible unique heterotropic

interactions in EcPFK, two of which are characterized in this study.

The secret behind this strategy lies in the ability to decrease the binding affinities of F6P and MgADP to the active and allosteric sites by modifying residues from one side of the binding site. Because of the interfacial nature of the F6P binding site and the allosteric site (Figure 3-4), mutating contact residues from each side of the binding site could greatly diminish binding. The binding affinities for F6P were significantly reduced in R162E and R243E, which lie on one side of the active site (Fenton and Reinhart, 2002). On the other side, R252E and H249E both exhibit decreased binding affinities for F6P by well over two orders of magnitude even without saturation, with H249E showing a greater effect (Figure 3-5). In the allosteric site, R21A has been shown to disrupt the binding of MgADP. Moreover, there was no apparent activation of F6P binding by MgADP (Fenton and Reinhart, 2002). On the other side of the allosteric site, we have studied R154E and K213E. Figure 3-6 shows that K213E does substantially decrease MgADP binding or activation, unlike R154E. Therefore, we find that H249E or R252E in the active site and K213E in the allosteric site are sufficient for decreasing the binding affinities of ligands to those sites.

Now that we have identified the contact residues that affect binding of F6P and MgADP, we can create hybrid tetramers containing each of the four unique heterotropic interactions as shown in Figure 3-7. Table 3-1 shows four constructs that would isolate their corresponding single heterotropic interactions when incubated with wildtype. Surface charge-tags, K2,3E, were also introduced to allow for the purification of the 1:3 hybrid. Incubating K2,3E, R21A, H249E with wildtype would create a 1:3 hybrid

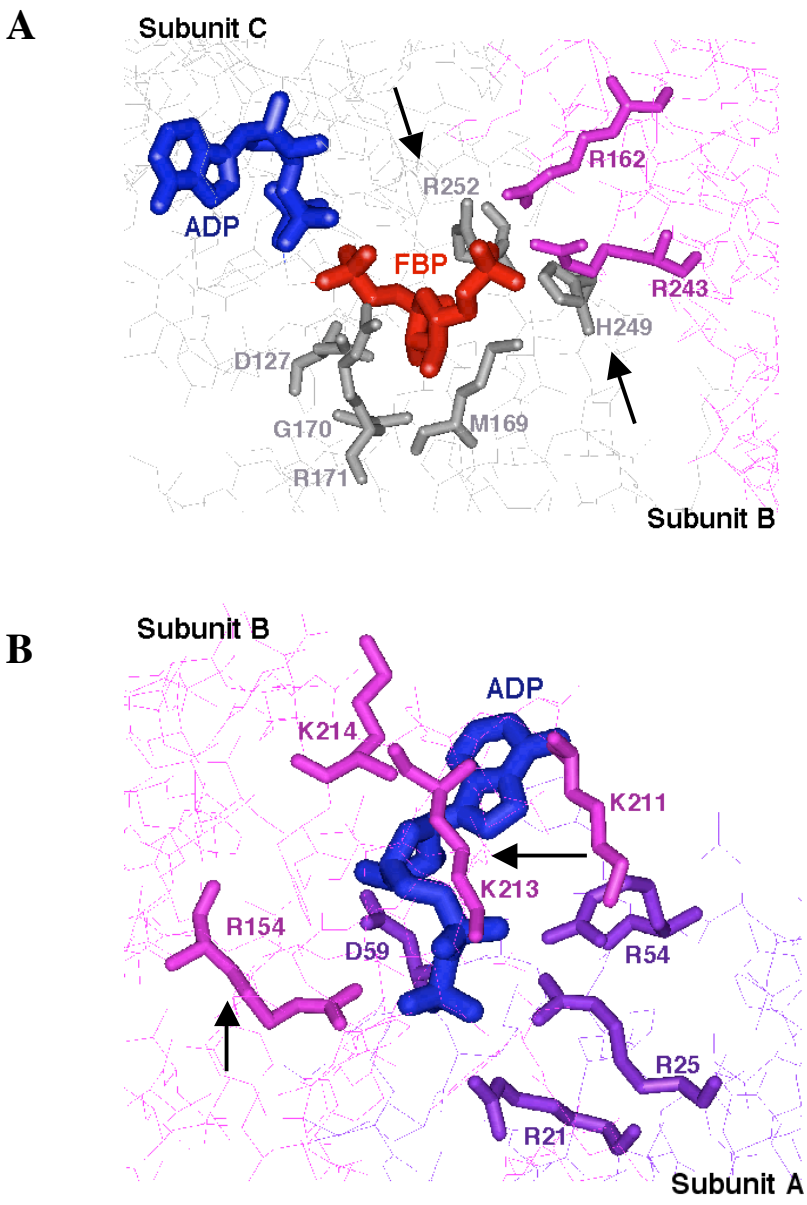

FIGURE 3-4: The interfacial nature of the binding sites in EcPFK as determined by Shirakihara and Evans, 1988. A) The active site. Residues that make up the binding pocket from two subunits are labeled in grey and purple. Fructose-1,6-bisphosphate and MgADP are labeled in red and blue, respectively. B) The allosteric site. Residues from two subunits are labeled in pink and purple. ADP is in blue. Arrows show the residues that have been mutated in this study.

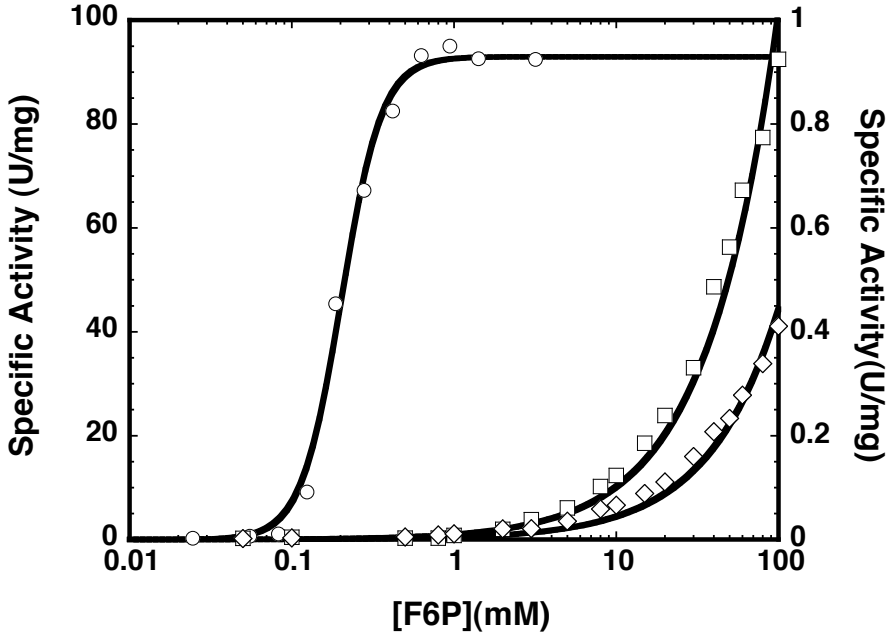

FIGURE 3-5: Specific activity measurements as a function of F6P for wildtype EcPFK (○, left vertical axis), R252E (□, right vertical axis) and H249E (◇, right vertical axis). Lines represent best fits to equation 2-1 (wildtype) and equation 3-1 (R252E and H249E).

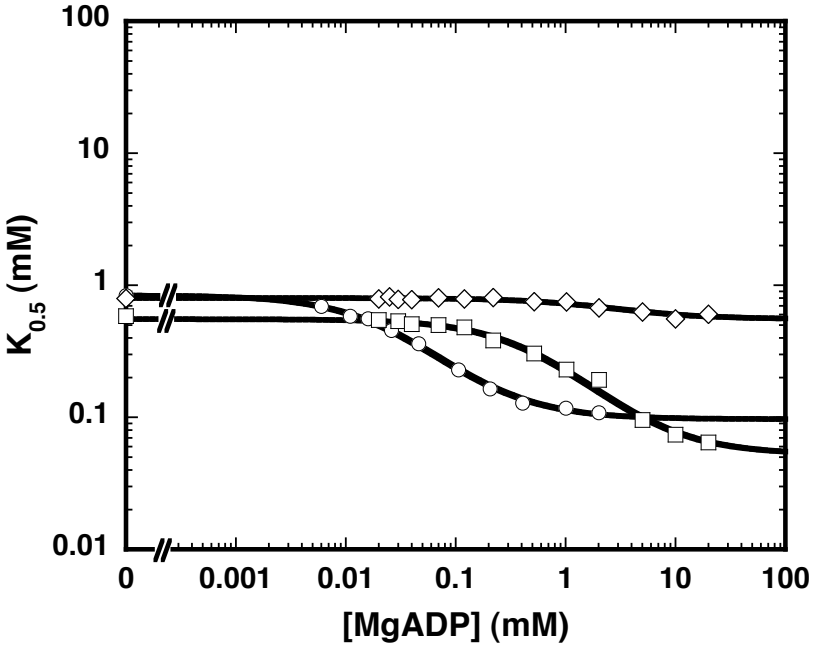

FIGURE 3-6: The influence of MgADP on wildtype (○), R154E (□) and K213E (◇). Lines represent fits to equation 2-2.

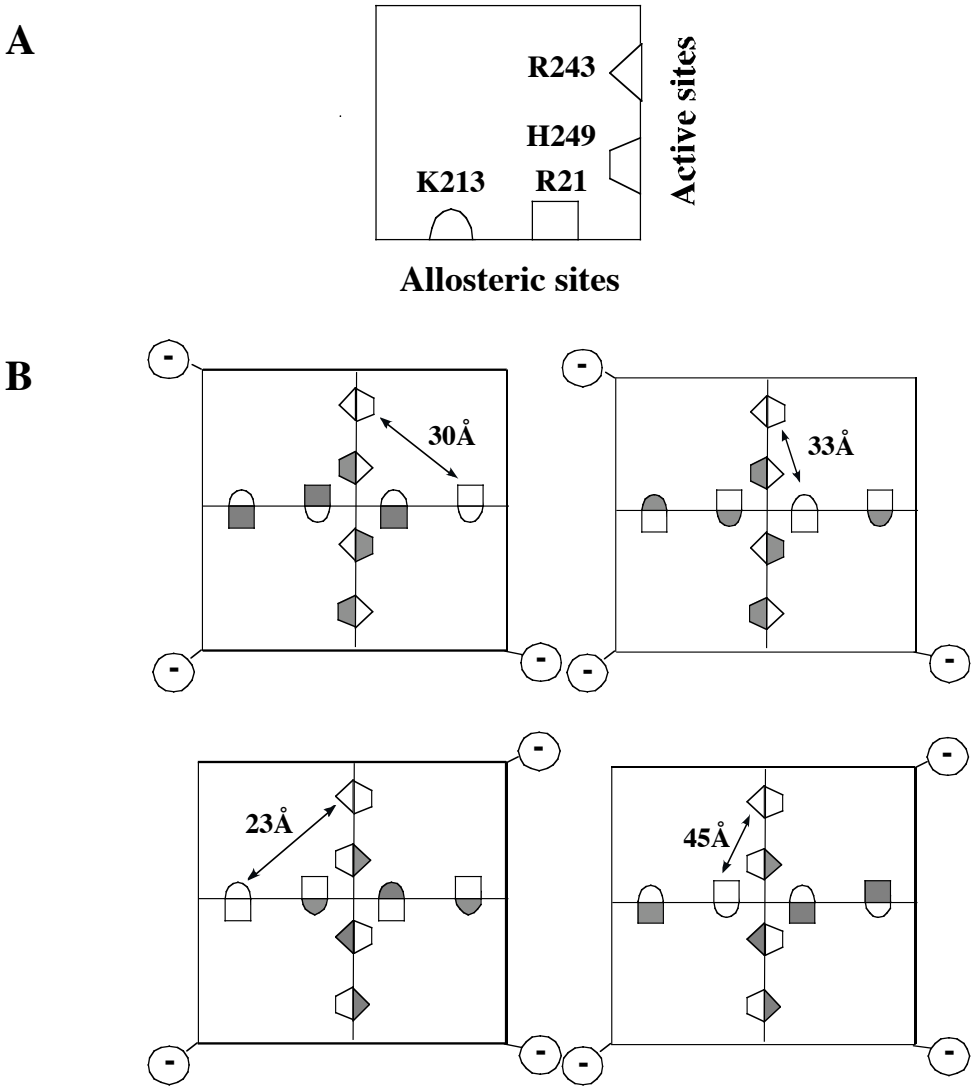

FIGURE 3-7: Schematic of the monomer (A) and the tetramer with each of the four unique heterotropic interactions (B) in EcPFK. The residues that were mutated to give reduced binding affinities for substrate and effectors are labeled. Depending on the mutations used (shaded), each of the four heterotropic interactions can be created. Surface-tags (K2,3E) were used to facilitate separation of hybrids. The 23Å and the 45Å interactions can be created using the active site mutation R243E (Fenton and Reinhart, 2002; Fenton et al., 2004).

TABLE 3-1: Constructs created containing mutations used to isolate the four heterotropic interactions in EcPFK.

Construct	Charge-tag	Active site	Allosteric site
33Å mutant	K2,3E	H249E	K213E
30Å mutant	K2,3E	H249E	R21A
23Å mutant*	K2,3E	R243E	K213E
45Å mutant*	K2,3E	R243E	R21A

* Created by Dr. Aron Fenton

containing the 30Å heterotropic interaction. The 33Å interaction can be formed by the the hybridization between wildtype and K2,3E, K213E, H249E. The 23Å and the 45Å interactions contain R243E in the mutated active sites and K213E and R21A in the mutated allosteric sites, respectively.

Control hybrids were also created for each heterotropic interaction to correct for any activation that could arise from the binding of MgADP to the mutated allosteric sites. These 1:3 hybrids contain one native active site and no native allosteric sites, and were created by mixing R21A or K213E instead of wildtype with their respective constructs. R252E instead of H249E as the active site mutation was used in two of the control hybrids. It does not matter which active site mutation is used as long as the binding of F6P is reduced and since we are only concerned with the effect of MgADP binding to the mutated allosteric sites. Figure 3-8 shows the effect of the 30Å and the 33Å control hybrids on MgADP activation. The Q_{ax} values for both controls were very close to one, indicating that there is little to no effect arising from either R21A or K213E mutated allosteric sites (Fenton et al., 2004).

Each of the four heterotropic interactions were isolated and characterized for the affect of MgADP activation (Fenton and Reinhart, 2002, Fenton and Reinhart, 2004). Activation by MgADP on the 30Å and the 33Å interactions is shown in Figure 3-9 with a two-fold enhanced activation in 33Å interaction as compared to that of the 30Å interaction after correcting for the effect of MgADP on the R21A and K213E mutated sites. The coupling constants and coupling free energies obtained for these heterotropic interactions, however, cannot be compared to that of wildtype since there is positive

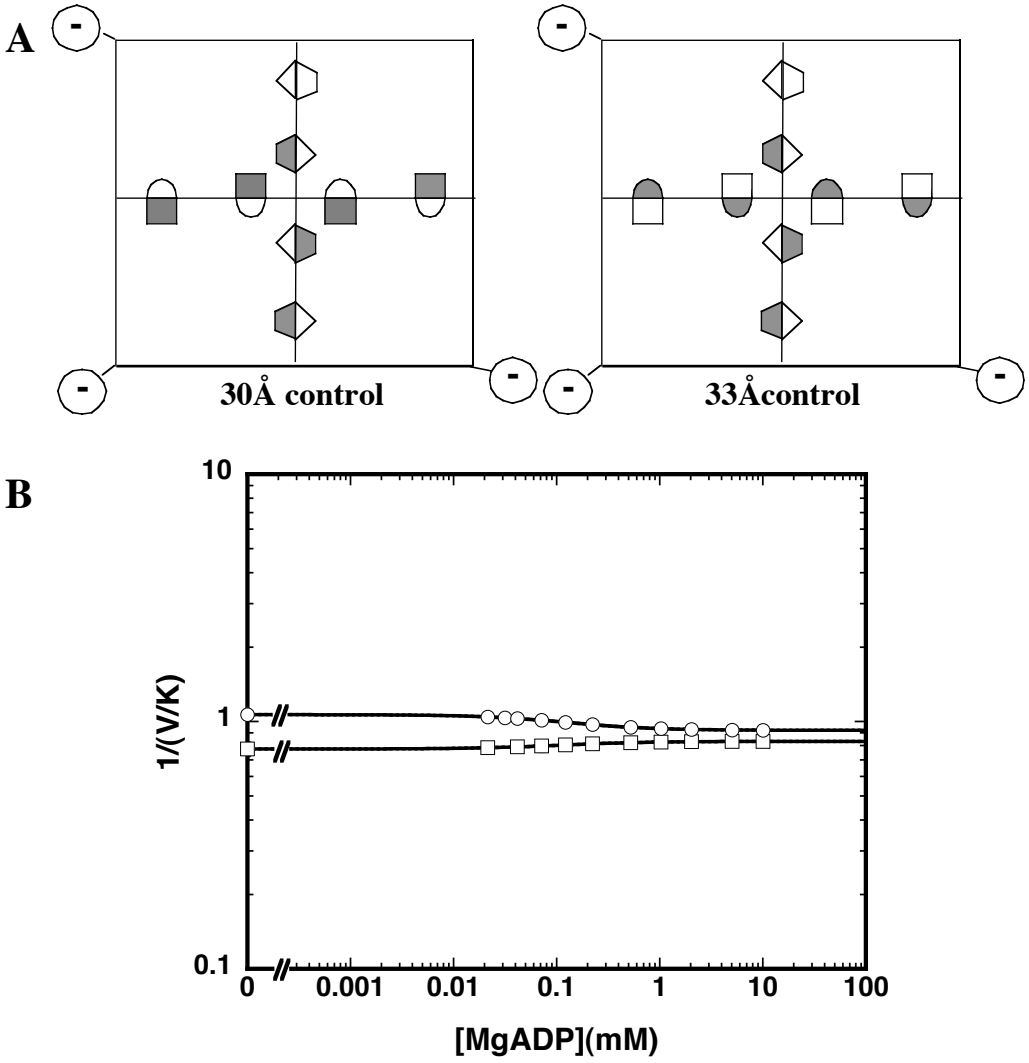

FIGURE 3-8: Controls used in this study. These controls contain one intact active site and no intact allosteric sites. A) Schematic of the two controls. B) The influence the mutated allosteric sites have on the one intact active site can be measured for the 30Å (○) and the 33Å(□) interactions. The Q_{ax} values for both controls are near one, indicating that there is little to no effect arising from either R21A or K213E mutated allosteric sites.

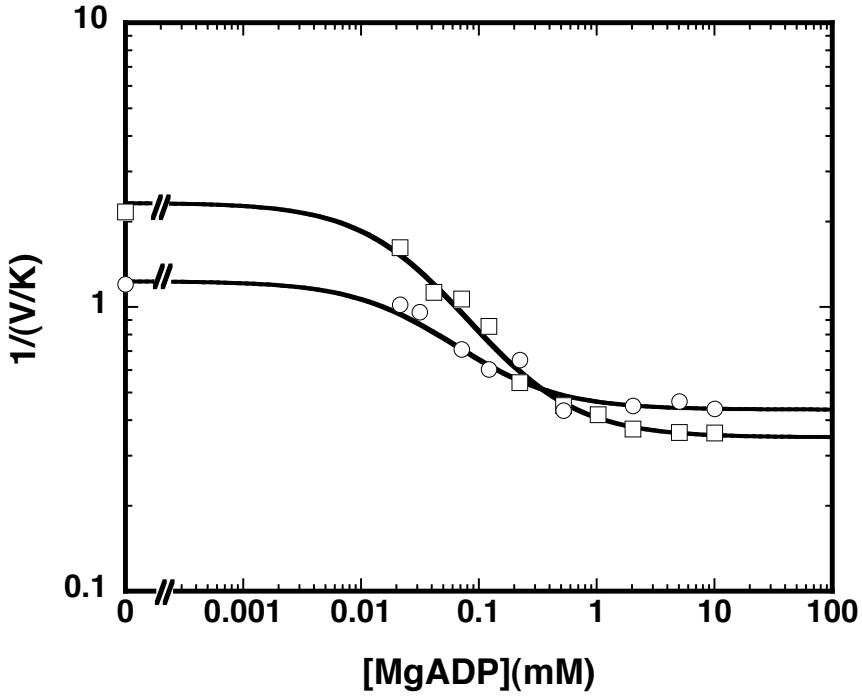

FIGURE 3-9: The influence of MgADP on the 30Å (○) and 33Å (□) interactions shown in Figure 3-7. These interactions have been corrected for the influence the mutated sites have on the native active site from Figure 3-8 by dividing the 1/(V/K) values obtained at each MgADP concentration for each interaction by its respective control. The lines represent best fits to equation 2-2. Errors are plotted on the points but are too small to be seen.the 1l4 control was created to eliminate this cooperativity (Fenton and Reinhart, 2002). This control contains one native active site and four native allosteric sites, thereby having all four heterotropic interactions without homotropic interactions.

cooperativity in F6P binding which was eliminated in the hybrids. Therefore, the 1|4 control, which contains one native active site capable of communicating with four native allosteric sites, was created to eliminate positive cooperativity in F6P binding in EcPFK (Fenton and Reinhart, 2002).

Table 3-2 and Figure 3-10 compare all the four unique heterotropic interactions with the 1|4 control, with the 33Å interaction contributing the largest percentage (36%) of total activation in the 1|4 control. The 30Å, the 23Å and the 45Å interaction contributes 23%, 25% and 20% of the total activation, respectively. Each individual interaction has a unique magnitude and the sum of all the four interactions is 104±4%, thereby accounting for all the couplings in the 1|4 control.

Conclusions

The dissection of the web of potential allosteric interactions has been successfully performed using the hybrid tetramer approach to study the effect of MgADP activation on the four unique heterotropic interactions within EcPFK. Contact residues that are important for the binding of F6P and MgADP have been determined for each side of the binding sites. R252E and more importantly H249E decreased the binding of F6P substantially on one side of the active site. K213E shows a decrease in MgADP binding and activation by MgADP on one side of the allsoteric site. The important residues from the other sides of the active and allosteric sites have already been determined (Fenton and Reinhart, 2002).

The 30Å and the 33Å heterotropic interactions were assessed for the effect of

TABLE 3-2: Thermodynamic parameters for the four unique heterotropic interactions at 8.5°C and pH 8.0.

Construct	Q_{ax}[a]	ΔG_{ax} (kcal/mol)[b]	% Contribution[c]
Wildtype EcPFK	14.4 ± 0.4	-1.49 ± 0.02	------
1|4 control[d]	155 ± 6	-2.87 ± 0.02	100
30Å interaction	3.0 ± 0.2	-0.62 ± 0.03	23 ± 1
33Å interaction	6.4 ± 0.2	-1.04 ± 0.02	36 ± 1
23Å interaction	3.6 ± 0.2	-0.73 ± 0.04	25 ± 1
45Å interaction	2.8 ± 0.1	-0.58 ± 0.01	20 ± 1

[a]Q_{ax} are obtained from the fits to equation 2-2 and are corrected for the effects from the mutated allosteric sites.
[b]ΔG_{ax}, the coupling free energy, was calculated using the equation: $\Delta G_{ax} = -RT\ln Q_{ax}$.
[c]%Contribution of each interaction with respect to ΔG_{ax} determined for the 1|4 control (Fenton and Reinhart, 2002; Fenton et al., 2004)
[d]1|4 control, containing one intact active site and four intact allosteric sites, eliminates homotropic cooperativity of F6P binding to EcPFK (Fenton and Reinhart, 2002).

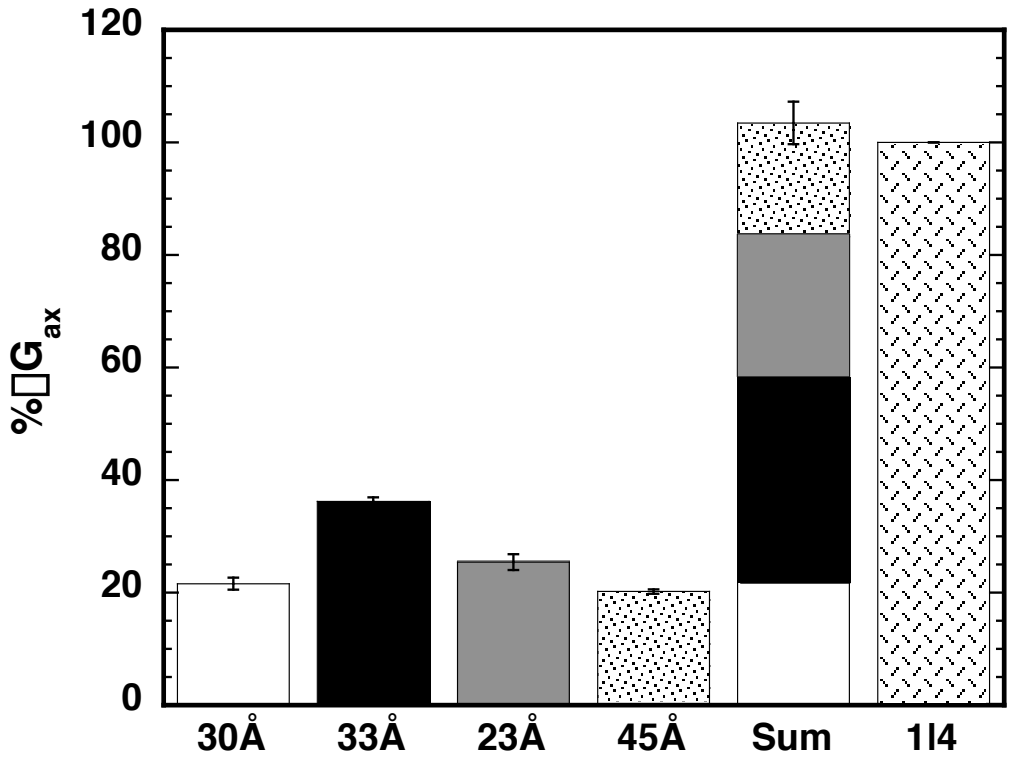

FIGURE 3-10: Percent coupling free energies for MgADP activation for the four unique heterotropic interactions in EcPFK. Data for the 23Å and the 45Å interaction were obtained by Dr. Aron Fenton (Fenton et al., 2004). Each interaction was compared to the heterotropic coupling exhibited by the 1|4 control (Fenton and Reinhart, 2002). The sum of all the four interactions are 104±4%, thereby accounting for all the couplings in the 1|4 control.

MgADP activation, with a two-fold greater activation observed in the 33Å compared to the 30Å interaction. The 23Å and the 45Å interactions were also studied (Fenton and Reinhart, 2002, Fenton et al., 2004). When each interaction was compared to the 1|4 control, which has homotropic cooperativity of F6P binding eliminated, we conclude that each heterotropic interaction is unique and adds up to 104±4% of the 1|4 control.

These results suggest that the allosteric activation of EcPFK cannot be adequately interpreted by the popular two-state models. The sequential model (Koshland et al, 1966) predicts that only one interaction would dominate substantially, whereas the concerted model (Monod et al., 1965) predicts that each interaction should produce 100% of the allosteric effect. Since each of the heterotopic interactions is unique and they are additive, our observations do not support these predictions.

A comparative study of the effects of MgADP and PEP on the four unique heterotropic interactions can be performed on EcPFK and BsPFK. The pattern of percent contributions of each of the heterotropic interactions found for MgADP activation in EcPFK is different from that for PEP inhibition in BsPFK. In BsPFK, the largest percentage was observed in the 23Å interaction with very little allosteric inhibition in the 45Å interaction (Ortigosa et al., 2004). These data suggest that PEP inhibition and MgADP activation use different communication pathways as previously suggested by Fenton et al., 2003. This could also mean that these differences are specific to the particular isozymes.

Finally, we can infer that the mutations used to create the hybrids themselves did not introduce any perturbations to the individual couplings since they are all accounted

for in the 1|4 control and that MgADP homotropic interactions are not present.

CHAPTER IV

INVESTIGATION INTO THE STRUCTURE-FUNCTION RELATIONSHIP OF PHOSPHOFRUCTOKINASE FROM *LACTOBACILLUS BULGARICUS*

Introduction

Interest in understanding the molecular basis of allostery brought us to study bacterial phosphofructokinases. Phosphofructokinase (PFK) catalyzes the first irreversible step in the glycolytic pathway. Bacterial PFKs respond to changing levels of MgADP and phospho(enol)pyruvate (PEP) (Blangy et al, 1968, Uyeda, 1979, Tlapak-Simmons and Reinhart, 1998, Johnson and Reinhart, 1994, 1997). These molecules compete for binding to the same allosteric site in the enzyme with different effects. MgADP activates PFK by increasing the binding affinity for F6P in the active site while PEP inhibits the binding of F6P. The means by which the enzyme can differentiate which molecule is bound and respond appropriately remains a compelling question.

Phosphofructokinases from *Escherichia coli* (EcPFK) and *Bacillus stearothermophilus* (BsPFK) are two of the most extensively characterized bacterial PFKs. Investigations into their allosteric properties and structures have been performed to understand the basis for allosteric regulation (Deville-Bonne et al, 1991, Tlapak-Simmons and Reinhart, 1998). The crystal structures of these enzymes have been solved and they show a high degree of similarity to one another (Evans et al, 1981; Shirakihara

and Evans, 1988).

Phosphofructokinase from *Lactobacillus delbrueckii* subspecies *bulgaricus* (LbPFK) contains 47% identity and 66% similarity to EcPFK, and 56% identity and 74% similarity to BsPFK. Interestingly, LbPFK has been reported to be unresponsive to allosteric ligands at pH 8.2 (Le Bras et al., 1991). According to that study, the maximal activity of the enzyme is influenced by pH. The activity of LbPFK was inhibited by the presence of 8mM and 20mM PEP at low pH values. MgGDP or MgADP binding to LbPFK was not observed and thereby no activation. From these data, Le Bras et al. concluded that LbPFK is a non-allosteric enzyme.

The study presented here describes a more thorough investigation into the kinetic properties of PFK from *L. bulgaricus* using a linked-function approach (Reinhart, 1983, 1988). In addition, we present the crystal structure of LbPFK, determined to 1.86Å resolution, to allow analysis of the three-dimensional structural features of this enzyme. A comparative analysis of the structure and function relationship between the non-allosteric LbPFK to the extensively studied PFKs from *E. coli* and *B. stearothermophilus* may facilitate our understanding of the allosteric response mechanisms of these enzymes.

Materials and Methods

Materials. PFK from *L. bulgaricus* B107, cloned into pKK223-3, was kindly provided by Danone Vitapole SA, France (Branny et al., 1993). All chemical reagents used in protein purification and enzymatic assays were obtained as mentioned in Chapter

II. Optimize solutions and crystallization materials were purchased from Hampton Research.

Methods. pKK223-3/PFK was transformed into DF1020 cells for overexpression of the PFK gene in a PFK minus strain (Daldal, 1983). Cells were grown up in 3 L LB broth in the presence of 0.1 mg/mL ampicillin, harvested after 24 hours, and stored at -20°C. Purification of PFK from *L. bulgaricus* was similar to that of *E. coli*, with a few modifications. DF1020 cells were resuspended in a lower ionic strength buffer (10 mM Tris-HCl pH 7.2, 0.1 mM EDTA) before lysis and centrifugation. After DNase treatment and centrifugation, the crude lysate with loaded onto a pre-equilibrated Mimetic Blue-1 resin. PFK was eluted with a gradient of 0 to 2 M NaCl in the same buffer. Fractions containing PFK were pooled, dialyzed against Buffer A and concentrated. Purity was assessed by SDS-PAGE. The purity of LbPFK at this point was sufficient for kinetic characterization, however, an additional purification step was required for crystallization trials. The concentrated protein was loaded onto a pre-equilibrated DE-52 anion exchange column. PFK was then eluted from the anion-exchange column with a 0 to 1 M NaCl gradient in Buffer A. Fractions containing PFK were pooled, dialyzed against Buffer A, concentrated and stored at 4°C. The Pierce BCA protein assay was used to determine protein concentrations.

Standard PFK activity assays were performed at pH 8.0 and 25°C, unless otherwise noted. Activity assays were performed as described in Chapter II. However, 15 mM MgATP was used instead of 3 mM for maximal activity. For pH studies, MES-KOH and MOPS-KOH buffers were used for pH 6 and pH 7, respectively.

Data Analysis. Data were fit to appropriate equations using the non-linear least squares fitting analysis of Kaleidagraph software (Synergy). The binding affinities for substrate F6P and MgATP were obtained by fitting to equation 2-1. In the presence of substrate inhibition, data were fit to the following equation (Cleland, 1986):

$$\frac{v}{E_T} = \frac{k_{cat}[A]}{K_{0.5} + [A] + [A]^2/K_i} \qquad [4\text{-}1]$$

where K_i is the inhibition constant. To quantify the allosteric responses of PFK to MgADP or PEP, parameters obtained from the fit to equation 2-1 were further fit to the equation 2-2. For LbPFK where effector binding is very weak and allosteric saturation could not be obtained, data were fit to the competitive inhibition equation (Cleland, 1986):

$$K_{0.5} = K^{o}_{0.5}\left(1 + \frac{[X]}{K_i}\right) \qquad [4\text{-}2]$$

where K_i is the inhibition constant or the dissociation constant of effector X.

Crystallization and Data Collection. PFK from *L. bulgaricus* was crystallized at 18°C using the hanging drop vapor diffusion method with 4 μL handing droplet consisting of a 1:1 mixture of the stock protein solution and the reservoir solution (0.1 M Tris-HCl pH 7.5, 1 mM DTT, at 0.1 M increments of 0.8 M to 1.4 M ammonium sulfate). Within 48 hours, PFK crystals were observed in all wells and were hexagonal in shape. Crystals, grown in 1.2 M ammonium sulfate, were flash frozen at 100K using 20% ethylene glycol as cryoprotectant and X-ray diffraction data was collected at the Advanced Photon Source (APS) beamline in Chicago. Diffraction data was processed and analyzed using HKL2000 programs (Otwinowski and Minor, 1997).

Structure Determination, Modeling Building and Refinement. Molecular replacement program AMoRe (Collaborative Computational Project, 1994) was used to solve the structure of LbPFK using PFK structure of *Bacillus stearothermophilus* (Schirmer and Evans, 1990) as a model. A clear solution with correlation coefficient of 42.9% was obtained from AMoRe. Iterative cycles of model building with XtalView (McRee, 1999) using the ARPwARP improved phases figure of merit weighted 2|Fo|-|Fc| maps (Perrakis et al., 2001) and refinement with REFMAC (Collaborative Computational Project, 1994) were performed for improving the quality of the model. Water molecules were added in the difference electron density maps at positions corresponding to peaks (>3.0□) and with appropriate hydrogen bonding geometry.

Results and Discussion

PFK from *L. bulgaricus* was purified to homogeneity as assessed by SDS-PAGE using affinity and anion-exchange chromatography (Figure 4-1 and 4-2). Saturating concentrations of MgATP and F6P were determined to obtain the maximal specific activity of this enzyme at pH 8.0 and 25°C. The dissociation constant for MgATP is 0.35±0.01 mM at high (5 mM) concentrations of F6P and the saturating concentration of MgATP is at least 15 mM (Figure 4-3). Substrate inhibition was observed for MgATP binding under low concentrations of F6P. This inhibition is also observed in PFK from *E. coli* that is attributed to an allosteric antagonism between substrates (Fenton and Reinhart, 2003). To alleviate this inhibition, a saturating concentration of MgATP (15 mM) was used in all assays for maximal activity. The binding of F6P to LbPFK is

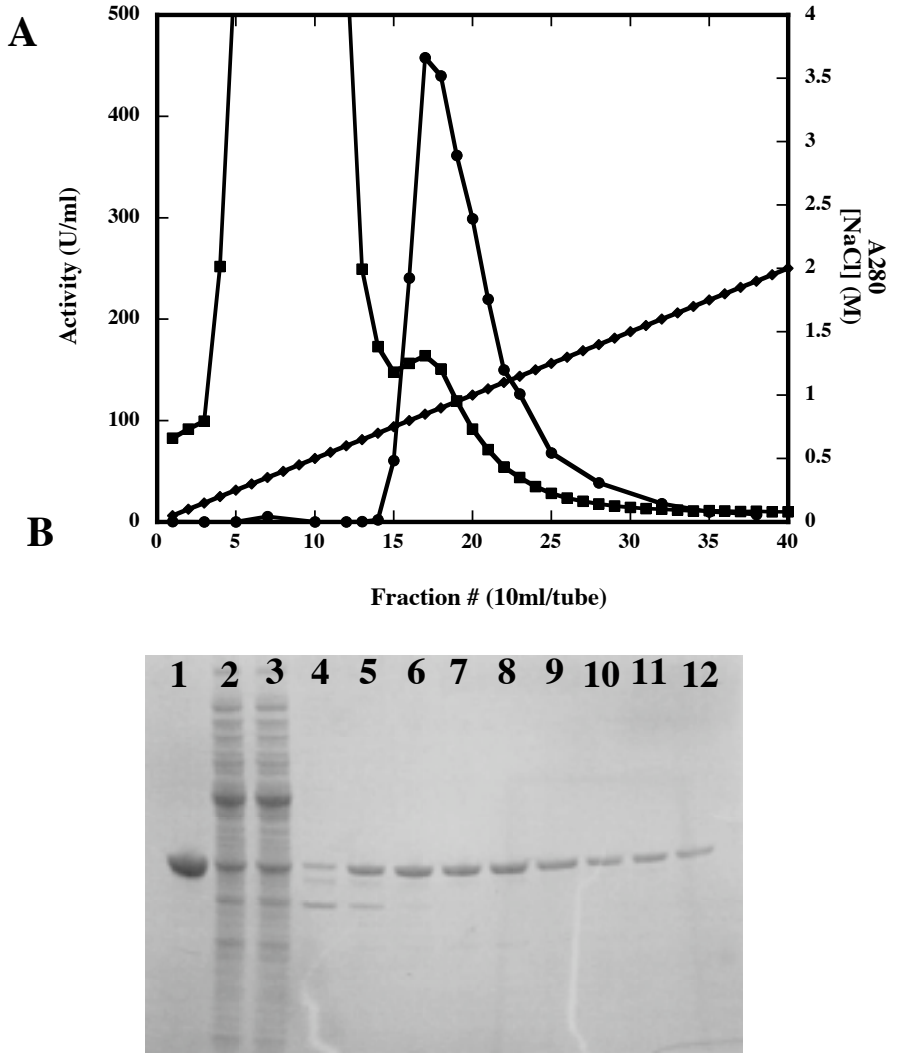

FIGURE 4-1: Purification of PFK from *L. bulgaricus* using affinity chromatography. A) Elution profile of PFK off the Mimetic Blue-1 column. The absorbance at 280 nm (■) and activity (●) were measured for fractions eluted with increasing salt concentrations (◆). B) Assessment of purity by SDS-PAGE. Lane 1 is a known PFK standard, lane 2 is crude lysate after sonication and centrifugation, lane 3 is supernatant after Dnase treatment, lane 4 to lane 10 corresponds to fractions 15 to 23. Fractions 17-26 were pooled and the salt dialyzed away.

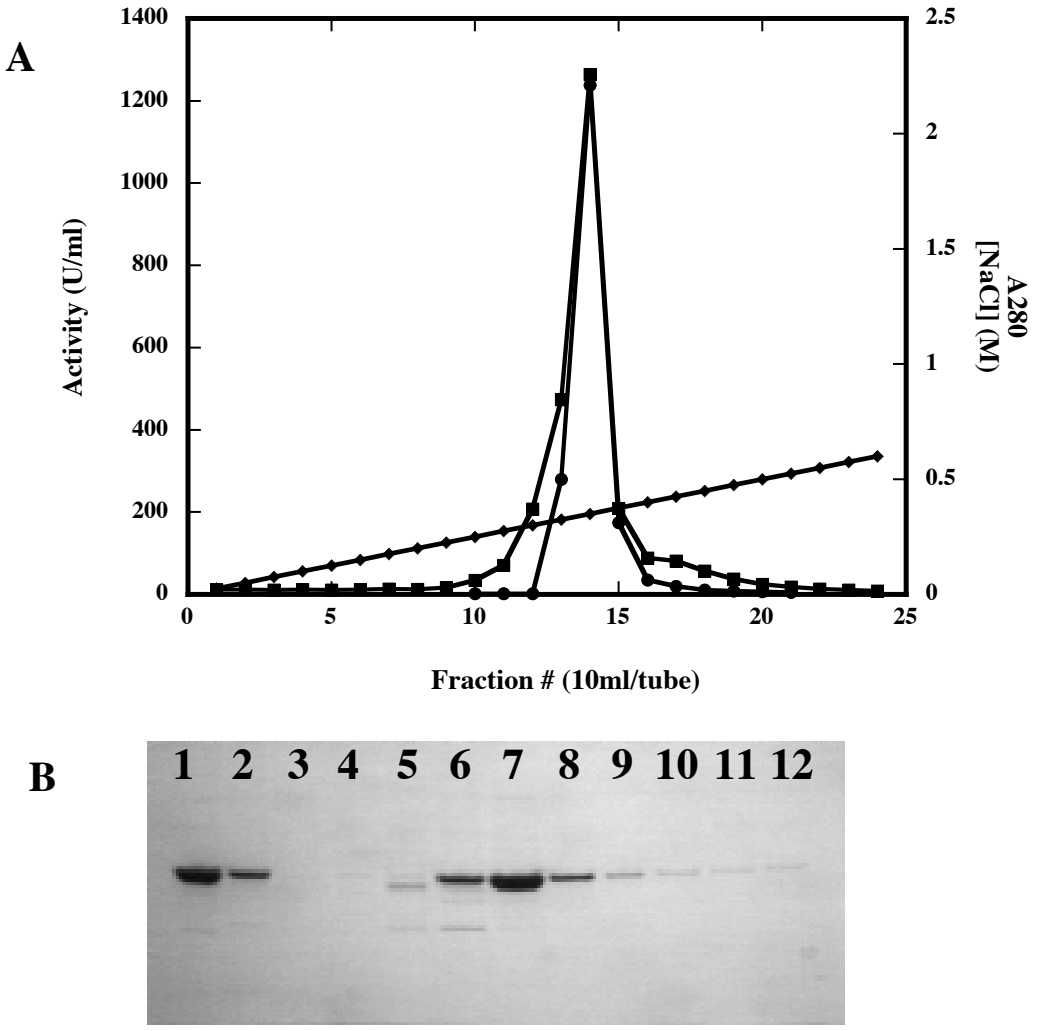

FIGURE 4-2: Purification of PFK from *L. bulgaricus* using anion-exchange chromatography. a) Elution profile off the DE-52 column. The absorbance at 280 nm (■) and activity (●) are measured for fractions eluted with increasing salt concentrations (◆). b) SDS-PAGE of protein fractions. Lane 1 is a known PFK standard, lane 2 is the pooled sample after Blue column, lanes 3 to 10 corresponds to fractions 10 to 19. Fractions 14-17 off the DE52 column were pooled and the salt dialyzed away.

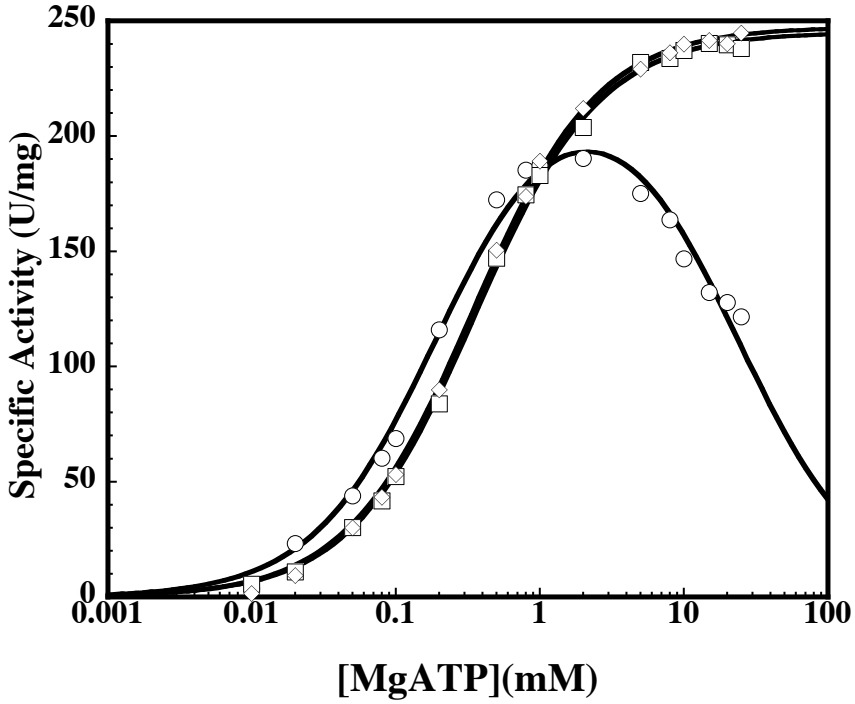

FIGURE 4-3: Kinetic characterization of LbPFK as a function of MgATP in the presence of 0.02 mM (○), 5 mM (□) and 10 mM (◇) F6P concentrations. Data for 0.02 mM F6P was fit to equation 4-1, while the others were fit to equation 2-1.

hyperbolic. At saturating MgATP concentrations, F6P binding is pH dependent (Figure 4-4). The dissociation constants for F6P are 0.060 ± 0.003mM, 0.030 ± 0.001mM and 0.020 ± 0.005 at pH 6, 7 and 8, respectively. The saturating concentration of F6P is 1 mM in the presence of 15 mM MgATP. The specific activity of LbPFK is 230±10 U/mg at saturating concentrations of both substrates and is pH independent at 25°C. This specific activity is more than two-fold higher than that obtained by Le Bras et al., which was probably due to the presence of monovalent cation, NH_4^+, that was included in our assaying buffer. Moreover, the concentration used by Le Bras et al. (2 mM) is not enough to saturate the enzyme with MgATP, thereby lowering the apparent maximal specific activity.

Allosteric Properties. We observe weak binding of PEP to the enzyme that is pH independent (Table 4-1). However, the extent of inhibition cannot be determined because of the inability to saturate the allosteric effect. Inhibition of F6P binding by PEP to LbPFK at pH 8 was only observed at high concentrations of PEP (Figure 4-5A). Decreasing the pH to 6 or 7 does not seem to change the extent of PEP inhibition (Data not shown). MgADP binding to the enzyme is weak and slightly inhibitory (Figure 4-5B). The extent of MgADP inhibition also cannot be determined due to experimental limitations and weak binding. To confirm that MgADP does bind to the enzyme, PEP inhibition was examined in the presence of two concentrations of MgADP. Competition between MgADP and PEP in the allosteric site was observed as the binding affinity for PEP weakens in the presence of MgADP (Figure 4-6). This suggests that MgADP does bind to the allosteric site though very weakly. Dissociation constants derived from data

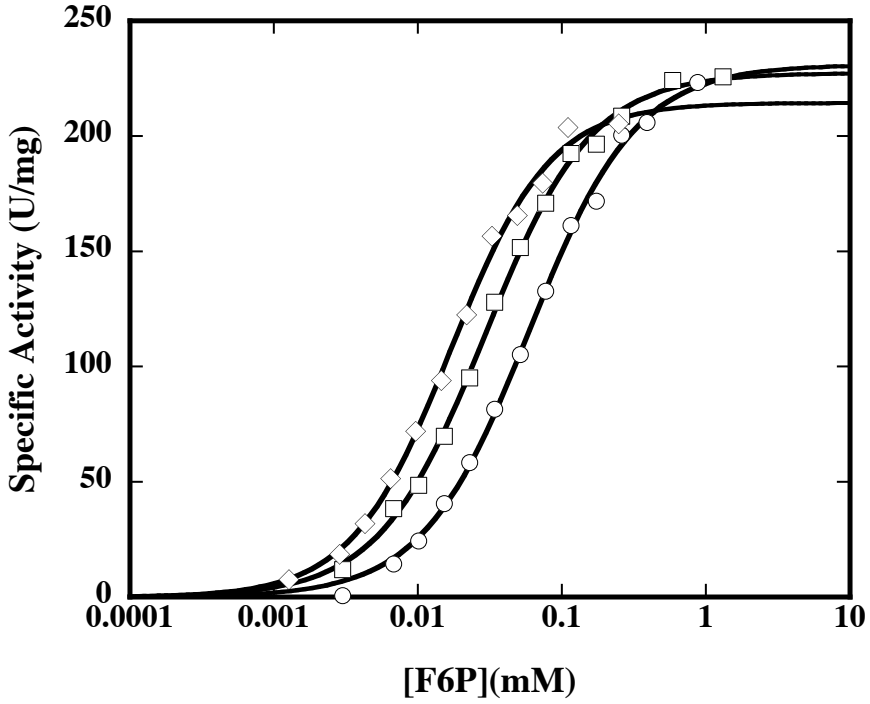

FIGURE 4-4: pH dependence of F6P binding in LbPFK at saturating MgATP. Activity was measured as a function of F6P concentration at pH 6 (○), pH 7 (□) and pH 8 (◇). Lines represent best fits to equation 2-1 and the resulting parameters are listed in Table 4-1.

TABLE 4-1: Summary of kinetic parameters for EcPFK, BsPFK and LbPFK at 25°C. X and Y are MgADP and PEP, respectively.

	K_{ia}^{o} (mM)	K_{ix}^{o} (mM)	K_{iy}^{o} (mM)	Q_{ax}	Q_{ay}
EcPFK[1]	0.30±0.01	0.048±0.002	0.30±0.01	11.1±0.2	0.0080±0.0003
BsPFK[2]					
pH 6	0.024±0.002	0.017±0.001	0.035±0.002	1.3±0.1	0.022±0.001
pH 7	0.027±0.001	0.019±0.002	0.051±0.008	1.7±0.1	0.0030±0.0001
pH 8	0.031±0.002	0.019±0.002	0.093±0.006	1.7±0.1	0.0021±0.0003
LbPFK[3]					
pH 6	0.060±0.003	15±3	30±3	N. D.	N. D.
pH 7	0.030±0.001	46±25	16±1	N. D.	N. D.
pH 8	0.020±0.005	28±8	24±2	N. D.	N. D.

[1] EcPFK is pH independent (Deville-Bonne et al, 1991)
[2] Data from Tlapak-Simmons and Reinhart, 1998
[3] Data fit to equation 4-2

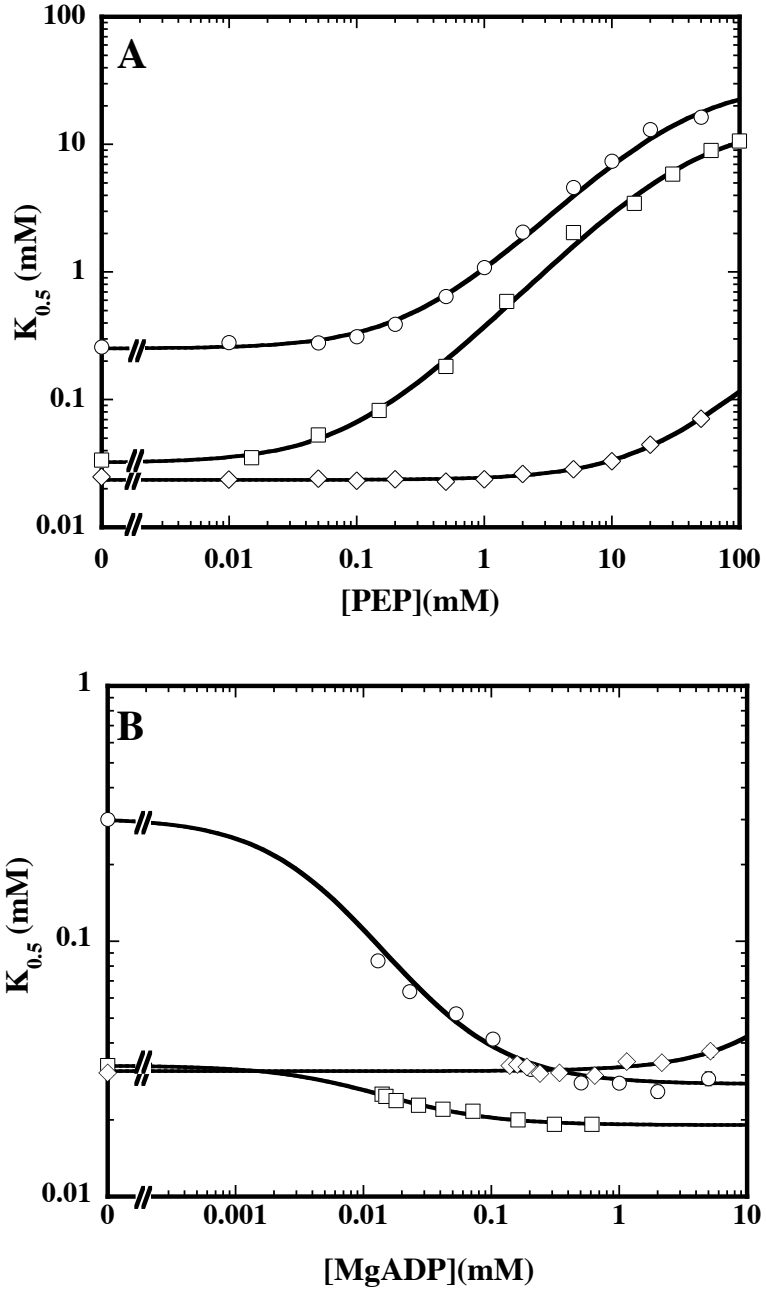

FIGURE 4-5: The effect of allosteric effectors on EcPFK (○), BsPFK (□) and LbPFK (◇) at pH 8 and 25°C. A) The influence of PEP on F6P binding. B) The influence of MgADP on F6P binding. Lines represent best fits to equation 2-2 for EcPFK and BsPFK, and to equation 4-2 for LbPFK.

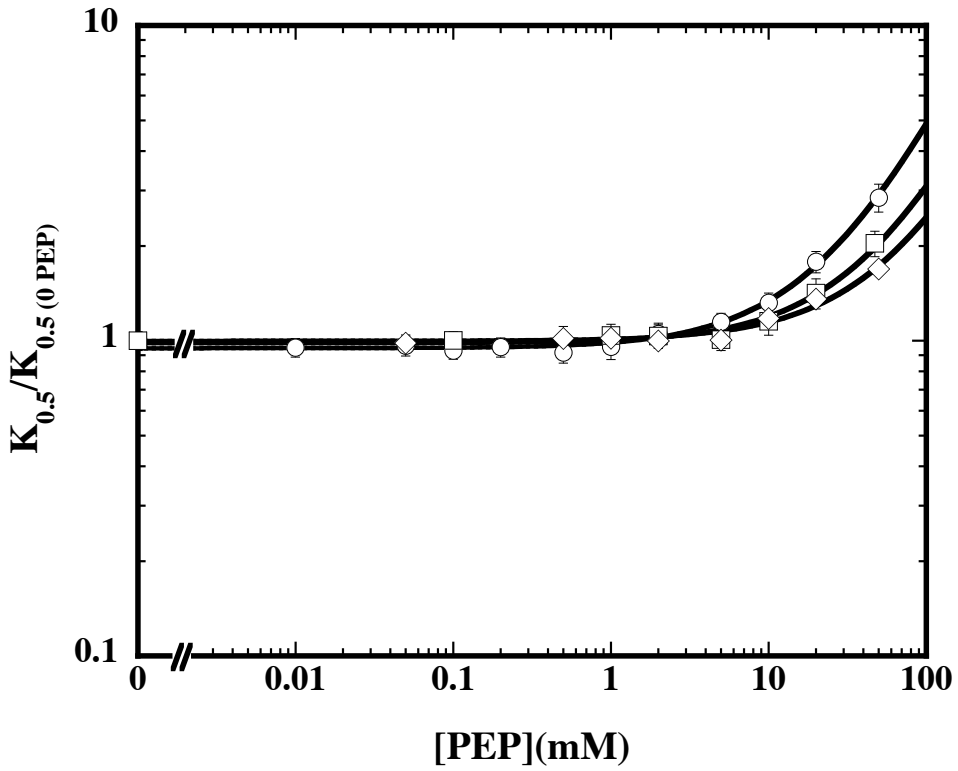

FIGURE 4-6: Competition between MgADP and PEP for the allosteric site in LbPFK. The effect of PEP inhibition in LbPFK was studied in the absence of MgADP (○), 10mM MgADP (□) and 20mM MgADP (◇). Data were fit to equation 4-2 to obtain the binding constants for PEP of 24±2 mM in the absence of MgADP, 47±9 mM in the presence of 10mM MgADP and 56±4 mM in the presence of 20mM MgADP.

for LbPFK can be compared to those obtained for EcPFK and BsPFK as shown in Table 4-1. LbPFK and BsPFK both bind F6P with similar affinities. The dissociation constants of LbPFK for PEP and MgADP (~20mM) are much weaker than that of either EcPFK or BsPFK. The errors for the dissociation constants for LbPFK are somewhat large because of the experimental limitations and thereby few data points at high effector concentrations to get a good fit to equation 4-2.

Structure Determination and Overall Structure. The crystals of PFK from *L. bulgaricus* belong to space group $P6_222$ with unit cell dimensions of a=135.0 Å and c=77.7 Å, one monomer per asymmetric unit, and a solvent content of 58.7 %. The structure was determined by molecular replacement with *B. stearothermophilus* phosphofructokinase model (PDB ID: 6PFK, Schirmer and Evans, 1990). The final structure, including all the 319 residues, two sulfate molecules and 252 water molecules, refined at 1.85Å resolution, has a crystallographic R-value of 22.2% and an R_{free} of 25.1%. The details of the final refinement parameter are presented in Table 4-2.

The 319 residues in the LbPFK molecule form two structural domains, both with 3-layered □□□ sandwich structures. The overall structure of the enzyme is very similar to that of EcPFK (Rypniewski and Evans, 1989; Shirakihara and Evans, 1988) and BsPFK (Evans et al., 1981; Evans and Hudson, 1979; Schirmer and Evans, 1990) as shown in Figure 4-7. Although there is only one molecule in the asymmetric unit, there exists a 222 symmetry in the space group $P6_222$, suggesting that the oligomeric state of LbPFK is still tetramer and with 222 symmetry, very much like that of EcPFK (Rypniewski and Evans, 1989; Shirakihara and Evans, 1988) and BsPFK (Evans et al,

TABLE 4-2: Statistics from the crystallographic analysis. Details of the crystallization and structure determination see text. $\mathbf{R_{sym}} = \Sigma_h \Sigma_i |I_{h,I} - I_h| / \Sigma_h \Sigma_i I_{h,I}$ for the intensity (I) of i observations of reflection h. $\mathbf{R\text{-factor}} = \Sigma |F_{obs} - F_{calc}| / \Sigma |F_{obs}|$, where F_{obs} and F_{calc} are the observed and calculated structure factors, respectively. R-free = R-factor calculated by using a subset (5%) of reflection data chosen ramdomly and omitted throughout refinement. rmsd, root-mean-square deviations from ideal geometry.

Data set	Native
Wavelength (Å)	1.0419
Resolution (Å)	1.86
Measured reflections	560384
Unique reflections	35567
Redundancy	15.8
Completeness (%, highest shell)	98.5 (92.8)
Mean I/I (highest shell)	50.6 (1.8)
R_{sym} (%, highest shell)	5.7 (69.8)
Refinement	
Resolution (Å)	20.0-1.85
No. of reflections |F|>0 F	33708
R-factor/R-free (%)	22.4 / 25.6
No. of non-H Atoms	2649
No. of Sulfate molecules	2
No. of Solvent Atoms	259
rmsd bond lengths (Å)	0.009
rmsd bond angles (°)	1.1
Ramachandran plot (%)	
Most favoured regions	92.6
Additional allowed regions	6.7
Generously allowed regions	0.0
Disallowed regions	0.7

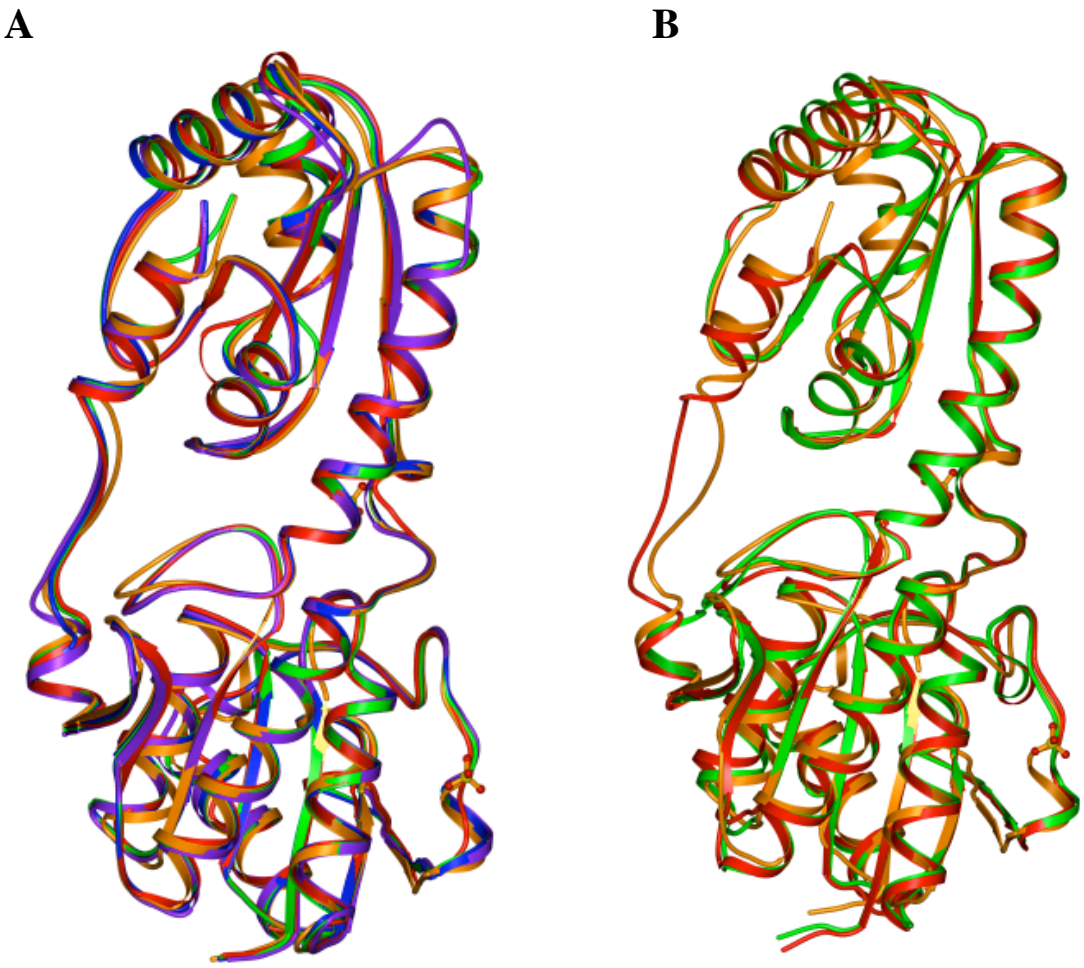

FIGURE 4-7: Comparison of the overall fold of LbPFK to the structures of EcPFK and BsPFK. A) Superimposition of LbPFK (gold) with four BsPFK structures: the structure of a mutant with F6P bound (1MTO.pdb) shown in red, with phosphate bound (3PFK.pdb) in green, with F6P and MgADP bound (4PFK.pdb) in blue and with inhibitor-analog phosphoglycolate bound (6PFK.pdb) in purple. B) Superimposition of LbPFK (gold) with two EcPFK structures: with products bound (1PFK.pdb) in red and unliganded (2PFK.pdb) in green.

1981; Evans and Hudson, 1979; Schirmer and Evans, 1990). The root-mean-square deviation (RMSD) between LbPFK and the active R-state BsPFK (PDB ID: 3PFK and 4PFK, (Evans et al., 1981; Evans and Hudson, 1979) is 0.81 ± 0.01 Å for 319 Cα atoms, whereas that between LbPFK and the inhibited T-state BsPFK (PDB ID: 6PFK, (Schirmer and Evans, 1990) is 1.23 ± 0.03 Å for 319 Cα atoms. Further superimposition analysis on the tetramer shows that the RMSD between LbPFK tetramer and the active R-state BsPFK (PDB ID: 3PFK and 4PFK, (Evans et al., 1981; Evans and Hudson, 1979) tetramer is 0.90 Å for 1276 Cα atoms, whereas that between LbPFK tetramer and the inhibited T-state BsPFK (PDB ID: 6PFK, (Schirmer and Evans, 1990) is 1.66 Å for 1276 Cα atoms, suggesting that the overall structure of LbPFK seems to correspond to the active R-state.

Binding Sites. Three binding sites have been reported in PFK structure, for substrate pair F6P and MgATP in the active site, for activator MgADP or inhibitor-analog phosphoglycolate (PGA) in the allosteric site (Evans and Hudson, 1979). In the LbPFK crystal structure, two inorganic sulfate ions from the crystallization condition were located, similar to the bound inorganic phosphate ions reported in BsPFK structure (Evans and Hudson, 1979). One sulfate is bound in the active site, in correspondence with the 6-phosphate group of F6P, the other one is bound in the allosteric site, in correspondence with the β-phosphate group of ADP or the phosphate group of PEP.

The Active Site. Based on the bound sulfates in LbPFK structure, and the available co-crystal structures of both BsPFK and EcPFK, we built the models of F6P and ADP in the active site, ADP or PGA in the allosteric site. The active site, lying

between the two domains of LbPFK subunit, is well conserved for both F6P and ATP. The F6P binding site is mainly formed in the small domain of LbPFK (Figure 4-8A). All residues involved in F6P binding are strictly conserved in LbPFK. These include Arg162, Arg243, His249 and Arg252 interacting with the 6-phosphate group of F6P, Asp127, Met169 and Glu222 interacting with the sugar group of F6P. The bound inorganic sulfate forms salt bridges with His249 and Arg252 from one subunit, Arg162 and Arg243 from the other subunit, presumably stabilizing the LbPFK conformation to the active R-state. The ATP binding site is well conserved in the large domain of LbPFK (Figure 4-8B). Two signature glycine residues (Gly104 and Gly108), which make space for the ATP, and Arg72, which interacts with the γ-phosphate of the ATP, are strictly conserved. The side chains of Ala77, His107, Phe41 and Phe76, also conserved, still form a non-specific hydrophobic slot for the adenine ring of ATP.

The Allosteric Site. The allosteric site is where there are most obvious differences (Figure 4-9). Studies in EcPFK (Shirakihara and Evans, 1988) showed that the main interactions between PFK and activator MgADP are with the phosphate groups and the magnesium ion. The magnesium ion forms octahedral co-ordination with the β and α phosphate groups of ADP, the carbonyl oxygen of Gly185, the carboxyl of Glu187 and two water molecules (Shirakihara and Evans, 1988). Glu187 is with special interest since it is the only residue that shows major differences with different ligands (activator or inhibitor) bound in the allosteric site. In the active R-state, the side chain of Glu187 adopts a folded conformation, ready to be coordinated to the magnesium ion of ADP. In the inhibited T-state, the side chain χ_1 torsion angle of Glu187 changes by

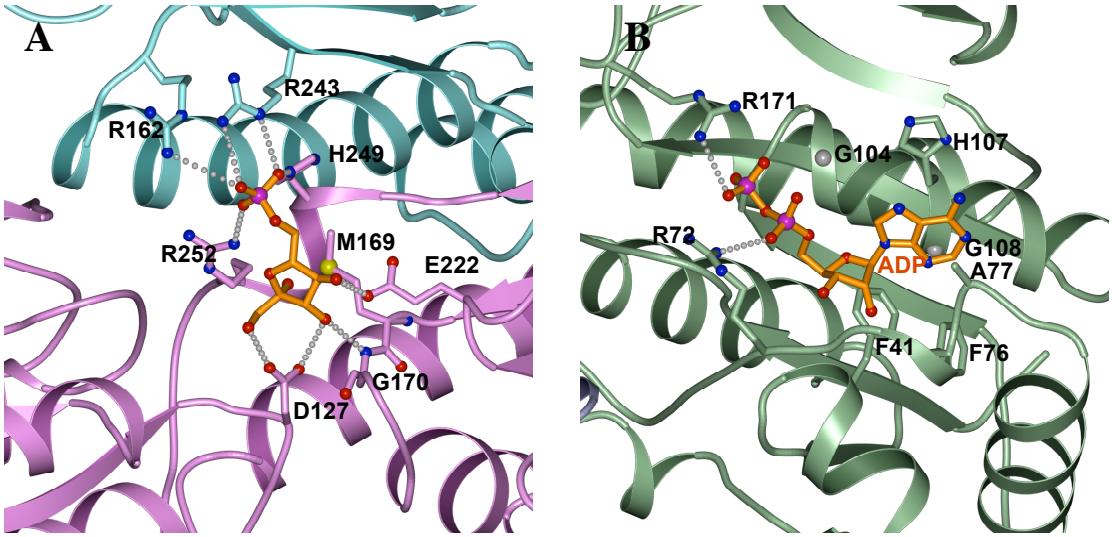

FIGURE 4-8: The active site of LbPFK. A) The F6P binding site of LbPFK with F6P modeled in the site. B) The ATP binding site of LbPFK with ADP modeled in the structure. Residues interacting with F6P and ADP are labeled.

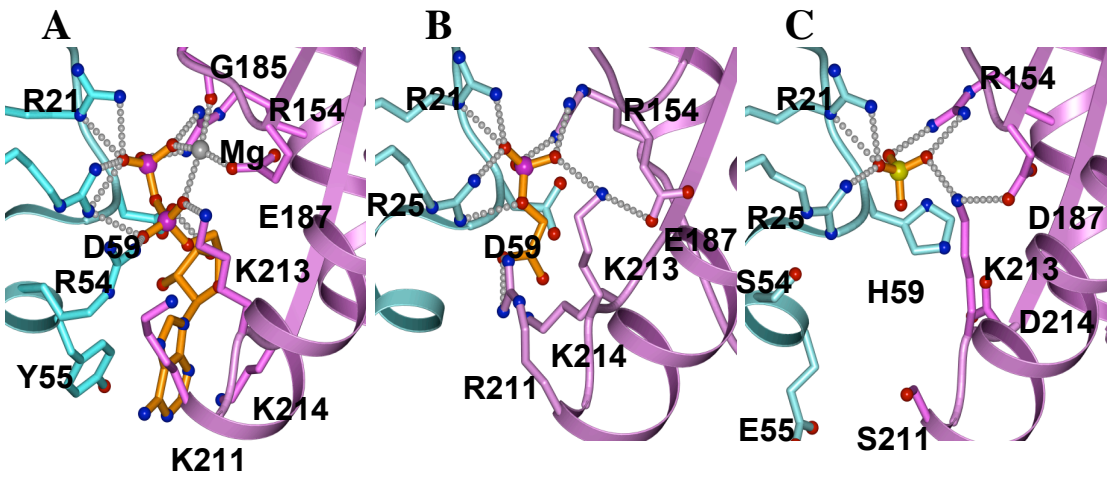

FIGURE 4-9: Comparison of the allosteric sites of PFK with different ligands present. A) MgADP-bound EcPFK. B) Phosphoglycolate-bound BsPFK. C) Sulfate-bound LbPFK.

140°, rotating away from the ligand. The new adopted position of the Glu187 side chain pushes the side chain of Leu205 to change its conformation. Glu187 was indicated to be important for allosteric responsiveness in EcPFK (Auzat et al., 1994; Lau and Fersht, 1987; Lau and Fersht, 1989). When substituted with an alanine at that position, PEP actually activates F6P binding, whereas MgADP has no effect on F6P binding (Pham et al. 2001). Aspartic residue is present at position 187 in LbPFK. The octahedral co-ordination between the carboxyl of Asp187 and the magnesium might be very weak or no longer exists. In addition, there are fewer residues involved in the interactions with the phosphate groups of ADP, which include Arg21, Arg25, Arg54, Arg154 and Lys213 in EcPFK (Shirakihara and Evans, 1988) or Arg21, Arg25, Arg154, Arg211 and Lys213 in BsPFK (Evans et al., 1981). Arg21, Arg25, Arg154 and Lys213 are conserved in LbPFK, whereas the corresponding residues for Arg54 and Arg211 are Ser54 and Ser211 in LbPFK. Furthermore, Asp59 in EcPFK and BsPFK forms hydrogen bond with the ribose O_3. A histidine residue is present at position 59 in LbPFK, which might break the interaction, further decreasing the affinity between LbPFK and ADP in allosteric site. There are still more differences that include Glu55 and Asp214. The effect is not clear.

Conclusions

Our kinetic characterization of phosphofructokinase from *L. bulgaricus* reveals an enzyme that binds substrates MgATP and F6P with dissociation constants of 0.35±0.01 mM and 0.020±0.001 mM, respectively and with a maximal specific activity

of 230±10 U/mg at pH 8.0 at 25°C. These numbers are different than those obtained by Le Bras et al., which is probably due to the presence of divalent cation NH_4 and a saturating MgATP concentration in our assays. When compared to EcPFK, F6P and MgATP binds to LbPFK with an order of magnitude tighter and weaker than to EcPFK, respectively (Johnson and Reinhart, 1994). On the other hand when compared to BsPFK, the dissociation constant for F6P is similar, with the dissociation constant for MgATP less than an order of magnitude weaker in LbPFK (Brynes et al., 1994; Riley-Lovingshimer and Reinhart, 2001). The specific activity of LbPFK is in between that of EcPFK and BsPFK (Valdez et al, 1989).

No pH dependence was observed for this enzyme, except for F6P binding, which also contradicts the observations made by Le Bras et al. There was no pH dependence on the maximal activity of LbPFK and no pH dependence on the effect PEP has on this enzyme. We observe weak binding (~20mM) of PEP and MgADP to LbPFK, which seems to also be pH independent. PEP inhibition is observed at pH 6, 7 and 8, unlike their conclusion that PEP inhibition is only observed at pH 6 and not at pH 8.2. Unfortunately, we cannot determine the extent of PEP inhibition. MgADP activation is not observed, however, MgADP inhibition seems to be present. These affinities are much lower than that for EcPFK and BsPFK (Table 4-1).

The crystal structure of LbPFK was solved to 1.86Å resolution. The overall fold is conserved between EcPFK, BsPFK and LbPFK. The active site of LbPFK remains intact, whereas the allosteric site is where the most differences lie within the structures of EcPFK, BsPFK and LbPFK. The tight binding of F6P to LbPFK is similar to that of

BsPFK, which supports the active sites of both enzymes being similar. The weak binding of MgADP and PEP observed for LbPFK likely can be explained by the differences in the allosteric site. However, the structure does not provide a clear answer to why the effects of MgADP and PEP on F6P binding are both inhibitory in LbPFK. More experiments need to be performed to address this issue.

Nature must have created an enzyme whose binding site is not amenable to the binding of allosteric effectors for a reason. The binding affinities for MgADP and PEP to LbPFK are very weak (~20 mM) and may be too weak to be physiologically significant. In contrast to Le Bras et al., we can conclude that at high concentrations of effectors, there is PEP inhibition of F6P binding at pH 8.0 in LbPFK though not to the same extent as that to EcPFK and BsPFK. MgADP, on the other hand, shows slight inhibition of F6P binding, unlike that to EcPFK and BsPFK.

Two other phosphofructokinases in the *Lactobacillus* family (*Lactobacillus casei* and *Lactobacillus plantarum*) are reported to be unresponsive to allosteric ligands (Doelle, 1972). Extensive characterization of these enzymes need to be conducted to study the binding and allosteric properties with regards to these effectors. If indeed the binding of allosteric effectors is also weak, we can hypothesize that PFK does not want to function as an allosteric enzyme in lactobacilli at physiological conditions.

CHAPTER V

IDENTIFICATION OF RESIDUES IMPORTANT FOR CONFERRING ALLOSTERY IN PHOSPHOFRUCTOKINASE FROM *ESCHERICHIA COLI*

Introduction

Due to the rapid and intensive move towards the genomics era, the partial or complete sequences of genomes of many organisms have been determined, published and annotated. Of the known sequences of phosphofructokinases (PFKs) from these organisms, extensive characterization of their respective proteins and their responses to allosteric ligands has yet to be performed for many. However, the amino acid sequences of several phosphofructokinases show significant similarity and thereby a highly probable conservation of function.

Since our interest lies in understanding allosteric regulation in bacterial phosphofructokinases, we study phosphofructokinases from *E. coli* (EcPFK), *Bacillus stearothermophilus* (BsPFK) and *Thermus thermophilus* (TtPFK). The sequence alignments show a 41% identity and 59% similarity between the three enzymes. These three proteins are homotetramers of similar size and function. Kinetic experiments performed with these enzymes (Johnson and Reinhart, 1994, 1997; Tlapak-Simmons and Reinhart, 1994; Xu et al., 1990) show that they respond to MgADP activation and PEP inhibition of F6P binding. High-resolution crystal structures of EcPFK and BsPFK show

the binding site residues to be almost identical (Shirakihara and Evans, 1988; Schirmer and Evans, 1990). Therefore, these three allosteric phosphofructokinases show significant similarities in sequence, structure and function.

In contrast, PFK from *Lactobacillus delbrueckii* subspecies *bulgaricus* (LbPFK), as characterized in the previous chapter, shows no MgADP activation and minimal PEP inhibition. The amino acid sequence of LbPFK is 47% identical and 66% similar to that of EcPFK, 56% identical and 74% similar to that of BsPFK, and 48% identical and 65% similar to that of TtPFK. Interestingly, there are twenty-two residues that are conserved in the three allosteric enzymes but not in LbPFK. We hypothesize that these differences in amino acid residues are crucial for the lack of allosteric response observed in LbPFK. In order to address this hypothesis, we have introduced these differences individually into EcPFK and studied the allosteric behavior of these mutant proteins as compared to wildtype EcPFK.

Materials and Methods

Materials. All chemical reagents used for protein purification and enzymatic assays were obtained as described in Chapter II. The following oligonucleotides were ordered from Integrated DNA Technologies (IDT) to be used for mutagenesis:

V24T: CAG-CGC-AGA-ACG-AGT-AAC-CCC-GCG-AAT-TGC-GGC-G

D59H: GCC-ACG-GTT-GAT-CAT-GTG-AGA-AAC-GCT-GTA-ACG-G

R63V: CCG-AGG-AAC-GTA-CCG-CCA-ACG-TTG-ATC-ATG-TCA-GAA-ACG-C

G64S: CCG-AGG-AAC-GTA-CCG-CTA-CGG-TTG-ATC-ATG-TCA-GAA-ACG-C

E114R: CGG-GAA-GCC-CAT-GCG-GGT-CAG-ACG-CAT-TGC-ACC-C

P118N: CGG-CAG-GCC-GAT-GCA-GTT-GAA-GCC-CAT-TTC-GG

G132Y: CCG-ATA-GTG-TAG-TCA-GTG-TAT-TTG-ATG-TCG-TTG-TCG

Y135A: CGC-AGT-GAA-GAA-ACC-GAT-AGT-CGC-GTC-AGT-GCC-TTT-GAT-GTC-G

L143C: CGC-TTC-TAC-AAC-GGT-GCT-GCA-CGC-AGT-GAA-GAA-ACC-G

V147M: CGG-TCG-ATC-GCT-TCC-ATA-ACG-GTG-CTC-AGC-G

E167N: CCA-CAA-TAA-CGG-CCC-ATC-ACG-TTC-ACC-ACG-GAA-ATA-CGC

L178M: CCG-GCA-ATG-GCC-GCA-GCC-ATC-GTC-AGA-TCG-CCA-C

G184A: CGA-ATT-CAC-AGC-CAG-CGG-CAA-TGG-CCG-C

G184C: CGA-ATT-CAC-AGC-CAC-AGG-CAA-TGG-CGC-C

G184S: CGA-ATT-CAC-AGC-CAC-TGG-CAA-TGG-CCG-C

K211S: CGC-GTG-TTT-TTT-ACC-GCT-CGC-GAT-ACC-GCG

K214D: CGC-CAC-GAT-CGC-GTG-GTC-TTT-ACC-TTT-CGC-G

A231M: CTC-GAT-GAA-ATG-CAT-CAG-TTC-GTC-AAC-ATC-ACA-C

T245N: GCG-CTG-GAT-GTG-GCC-CAG-CAC-ATT-TGC-GCG-GGT-TTC-ACG-ACC-GG

I250M: CCA-CCG-CGC-TGC-ATG-TGG-CCC-AGC-AC

A269S: GCA-GAT-CGA-TAG-CGT-AGC-TGC-CCA-TAC-GGG-AAG-CC

D273A: CCT-GCC-AGC-AGC-AGA-GCG-ATA-GCG-TAA-GCG-CC

D273H: GCC-AGC-AGC-AGA-TGG-ATA-GCG-TAA-GCG-CC

D273N: CCT-GCC-AGC-AGC-AGA-TTG-ATA-GCG-TAA-GCG-CC

C283A: CGT-TCT-GTA-TAC-CTA-CAG-CAC-GAC-CGC-CGT-AAC-CTG-CC

I300F: CGC-TTC-ATG-TTT-TCG-AAA-GCG-TCG-ATG-ATG-TCG

Methods. Altered Sites II in vitro Mutagenesis system from Promega was performed on pGDR16 (Johnson et al, 2001) using the above-mentioned oligonucleotides to introduce site-specific substitutions in EcPFK. Each mutation was confirmed by sequencing over the region of interest. The mutated plasmids were transformed into DF1020 cells (Daldal, 1983) and grown in 1.5 L LB broth in the presence of 0.1 mg/mL ampicillin. The cells were grown for 24 hours before harvested and stored at –20°C until ready to be purified. Purification of each mutant protein using Mimetic Blue-1 resin and its kinetic characterization was performed at pH 8.0 and 25°C as described in Chapter II.

Results and Discussion

The sequence alignment shown in Figure 5-1 between phosphofructokinases from *E. coli*, *B. stearothermophilus*, *T. thermophilus* and *L. bulgaricus* reveal twenty-two amino acid residues that are conserved between all but that from *L. bulgaricus*. These residues in EcPFK were substituted for their counterpart from LbPFK in order to study the role of these non-conserved residues in allosteric communication within EcPFK. The twenty-two constructs were created and their respective proteins were purified to homogeneity. The designation of each mutant protein was based on its amino acid sequence in EcPFK and the substitution at that position from EcPFK to LbPFK, e.g., V24T: the residue valine at position 24 has been substituted by threonine. All the

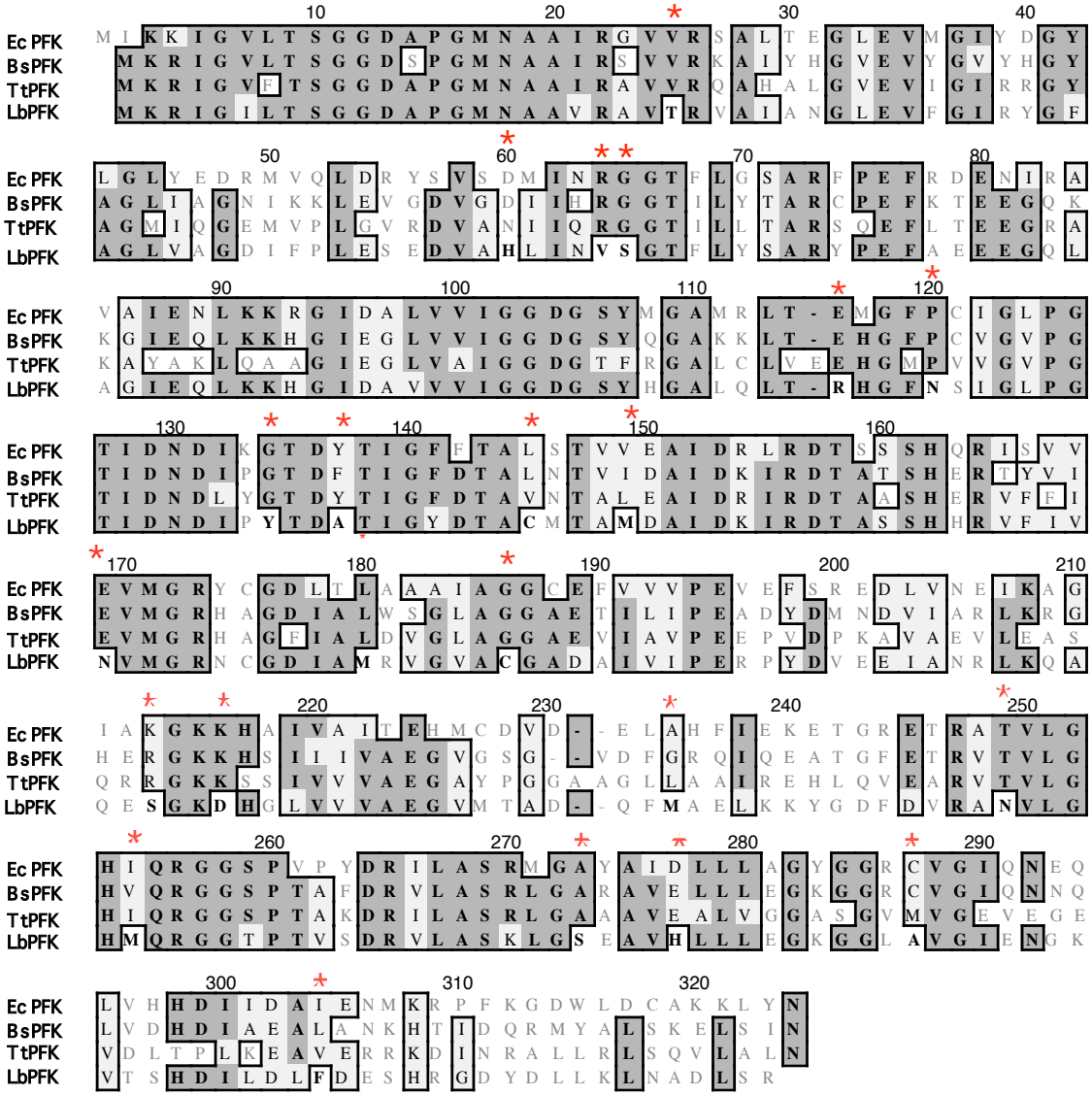

FIGURE 5-1: Amino acid sequence alignment for PFKs from *E. coli* (EcPFK), *B. stearothermophilus* (BsPFK), *T. thermophilus* (TtPFK) and *L. delbrueckii* subspecies *bulgaricus* (LbPFK). Residues highlighted by grey shading are identical, while residues highlighted by light gray shading are similar. The asterisks in red represent the positions where the single substitutions are located.

twenty-two mutant proteins (V24T, D59H, R63V, G64S, E114R, P118N, G132Y, Y135A, L143C, V147M, E167N, L178M, G184C, K211S, K214D, A231M, T245N, I250M, A269S, D273H, C283A and I300F) were characterized for binding affinities and allosteric responses to MgADP and PEP as compared to wildtype EcPFK at pH 8.0 and 25°C. All the data obtained for the twenty-two mutant proteins are summarized in Table 5-1.

As shown in Figure 5-2, many of the non-conserved residues, R63, G64, L143, V147, T245, I250, A269 and D273, lie at subunit interfaces. Two residues, E114 and P118, are at the surface with their side-chains facing outwards in the crystal structure. Three residues, D59, K211 and K214, lie in the allosteric site and are within hydrogen-bonding distance with MgADP (Figure 5-3). The remaining residues, V24, G132, Y135, E167, L178, G184, A231, C283 and I300, are in the interior of the protein.

Enzymatic Activity. Under the same conditions, all of the purified mutant proteins were active with specific activities comparable to that of wildtype, except for G64S, P118N and G132Y. These three mutant proteins are less active by an order of magnitude as compared with wildtype. G64 is located at the subunit interface, substituting that residue to a serine could weaken the subunit interface and cause dissociation of the tetramer and loss of activity. P118 is found in at the surface whereas G132 is in the interior of the protein. The introduction of a bulky side chain could disrupt proper folding, causing lower specific activities for the mutant proteins.

F6P Binding. The binding affinities of F6P to many of the mutant proteins are within two-fold to that of wildtype EcPFK. The greatest effects were observed for G64S

TABLE 5-1: Kinetic parameters for EcPFK mutants under standard assay conditions.

	V_{max} (U/mg)	$K_{0.5}^{o}$ (mM)	K_{ix}^{o} (mM)	K_{iy}^{o} (mM)	Q_{ax}	Q_{ay}
Wildtype	330±3	0.30±0.01	0.10±0.01	0.30±0.01	12.7±0.3	0.0083±0.0003
V24T	400±5	0.52±0.01	0.061±0.002	0.37±0.01	15.6±0.2	0.0069±0.0002
D59H	480±5	2.51±0.03	1.22±0.33	4.90±0.40	1.53±0.04	0.41±0.01
R63V	250±5	0.55±0.01	0.16±0.01	0.87±0.02	22.9±0.9	0.0088±0.0006
G64S	26±1	7.40±0.17	0.15±0.03	0.41±0.03	4.18±0.24	0.024±0.002
E114R	200±5	1.25±0.02	0.12±0.01	0.42±0.01	11.4±0.3	0.032±0.001
P118N	22±1	0.39±0.01	0.13±0.01	0.64±0.01	7.19±0.20	0.036±0.001
G132Y	35±1	0.51±0.01	0.19±0.01	0.26±0.01	20.6±0.5	0.020±0.001
Y135A	350±5	0.25±0.01	0.038±0.003	0.14±0.01	7.44±0.26	0.0096±0.0001
L143C	480±2	0.51±0.01	0.11±0.01	0.27±0.01	15.8±0.5	0.011±0.001
V147M	180±5	0.21±0.01	0.080±0.003	0.29±0.01	8.27±0.13	0.0083±0.0002
E167N	275±5	1.42±0.03	0.17±0.01	0.29±0.01	38.7±1.3	0.010±0.001
L178M	270±5	0.63±0.01	0.24±0.01	0.33±0.01	21.5±0.4	0.025±0.001
G184C	160±5	0.070±0.001	0.010±0.002	7.06±0.34	3.24±0.06	0.064±0.007
K211S	195±5	0.45±0.01	0.10±0.01	24.2±2.0	12.6±0.2	N. D.[a]
K214D	340±7	0.77±0.01	1.12±0.04	8.74±0.83	22.1±0.5	0.49±0.01
A231M	190±5	0.84±0.01	0.14±0.01	0.40±0.01	35.7±0.6	0.011±0.001
T245N	500±10	0.60±0.02	0.093±0.001	0.20±0.01	20.6±0.9	0.0087±0.0004
I250M	190±5	2.27±0.03	0.15±0.01	0.24±0.01	34.8±.8	0.0081±0.0005
A269S	190±5	0.47±0.01	0.10±0.01	0.25±0.01	20.3±0.6	0.011±0.001
D273H	250±10	0.32±0.01	0.094±0.004	0.55±0.02	6.59±0.16	0.075±0.003
C283A	120±3	0.58±0.01	0.18±0.01	0.37±0.01	21.2±0.4	0.013±0.001
I300F	260±10	0.21±0.01	0.28±0.01	0.40±0.01	7.82±0.17	0.014±0.001

[a] Cannot be determined

The residues in red show significant decreases in binding affinities and allosteric properties.

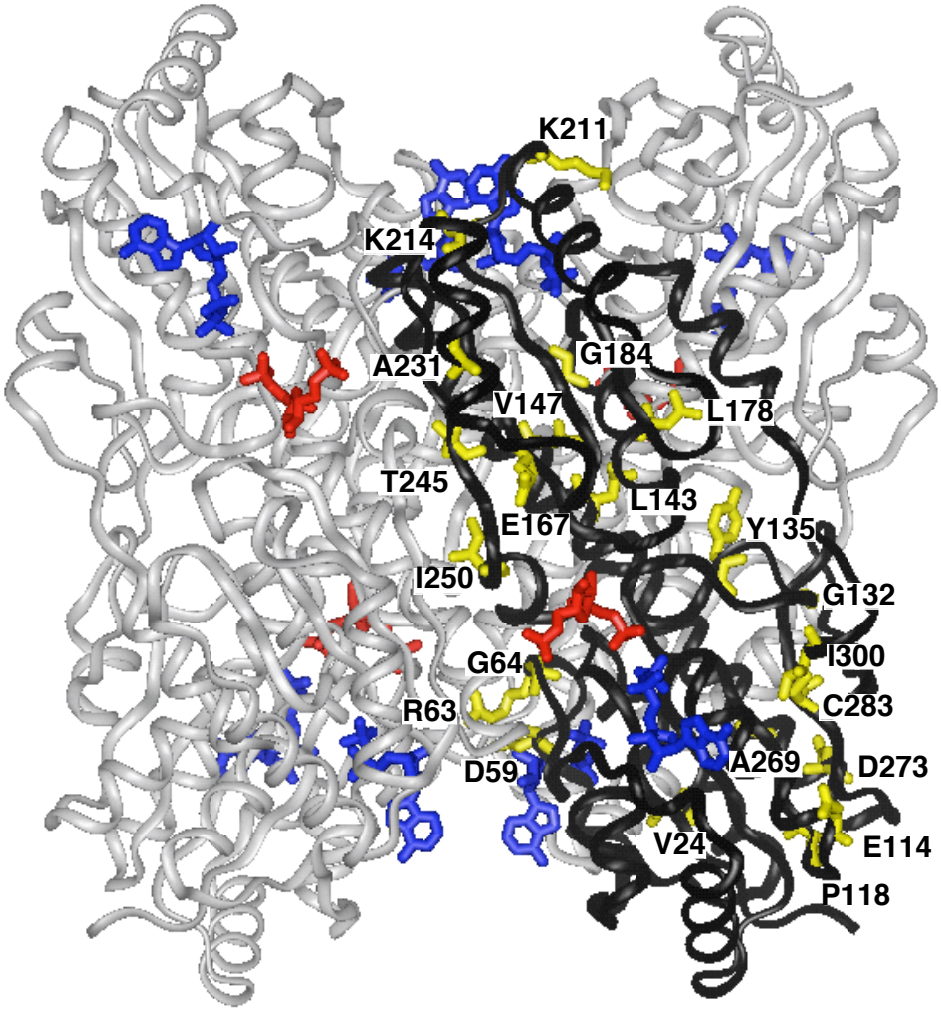

FIGURE 5-2: Location of the non-conserved residues in the crystal structure of EcPFK. The crystal structure of EcPFK, generated using the program InsightII, as determined by Shirakihara and Evans, 1988. The non-conserved residues are shown in yellow in the black subunit and are labeled in black. MgADP and fructose-1,6-bisphosphate, are shown in blue and red, respectively.

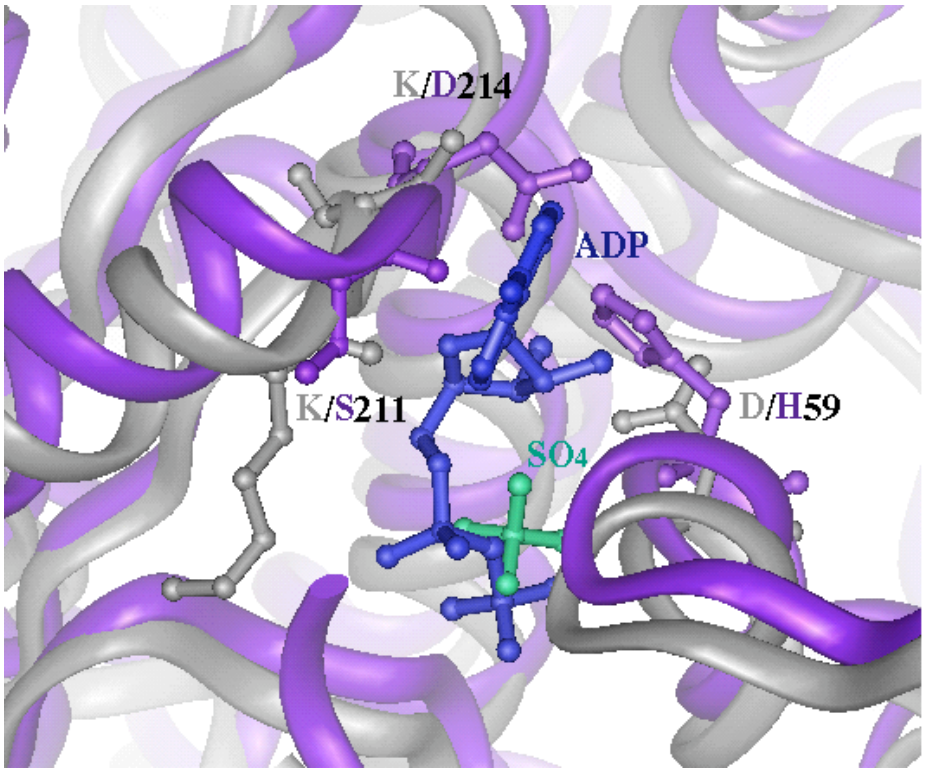

FIGURE 5-3: The allosteric sites of EcPFK and LbPFK. A superimposition of the crystal structures of EcPFK (grey) and LbPFK (purple) as determined by Shirakihara and Evans, 1988 and Paricharttanakul et al. (in prep). Residues at position 59, 211 and 214 in the allosteric site are labeled. The figures were generated on Insight II program.

with a twenty-five fold weaker binding affinity for F6P, and for D59H and I250M with eight-fold weaker binding affinities for F6P. F6P binding to E114R, E167N and A231M was four-fold weaker, however, a four-fold tighter binding was obtained for G184C. Interestingly of all the mutants that exhibited altered binding affinity of F6P, only the residue Glu167 lies within 9Å from the active site. Therefore, introducing mutations to the other residues must have caused long-range effects within the protein to affect binding to the active site.

Cooperativity in F6P Binding. In wildtype EcPFK, positive cooperativity is observed for F6P binding in the presence of saturating MgATP. This cooperativity, as measured by the Hill number, remains unchanged in the presence of PEP but diminishes in the presence of MgADP. This phenomenon is observed for all mutants characterized in this study except for D59H, in which the Hill number does not decrease as a function of MgADP as shown in Figure 5-4.

MgADP Binding. D59H and K214D bind MgADP with an order of magnitude weaker than wildtype EcPFK (Figure 5-5). It is not surprising that these two mutant proteins bind MgADP weaker since both residues lie within the allosteric site (Figure 5-3). However, we should expect an increase in the binding affinity D59H has for MgADP instead of a decrease because of the favorable attraction of the positively charged side-chain with the negatively charged ligand. On the other hand, there could be steric hindrance caused by the substitution of an imidazole ring in place of the carboxylic group, introduced by the mutation at position 59. The presence of this bulky side chain could inhibit the binding of MgADP to the allosteric site. At position 214,

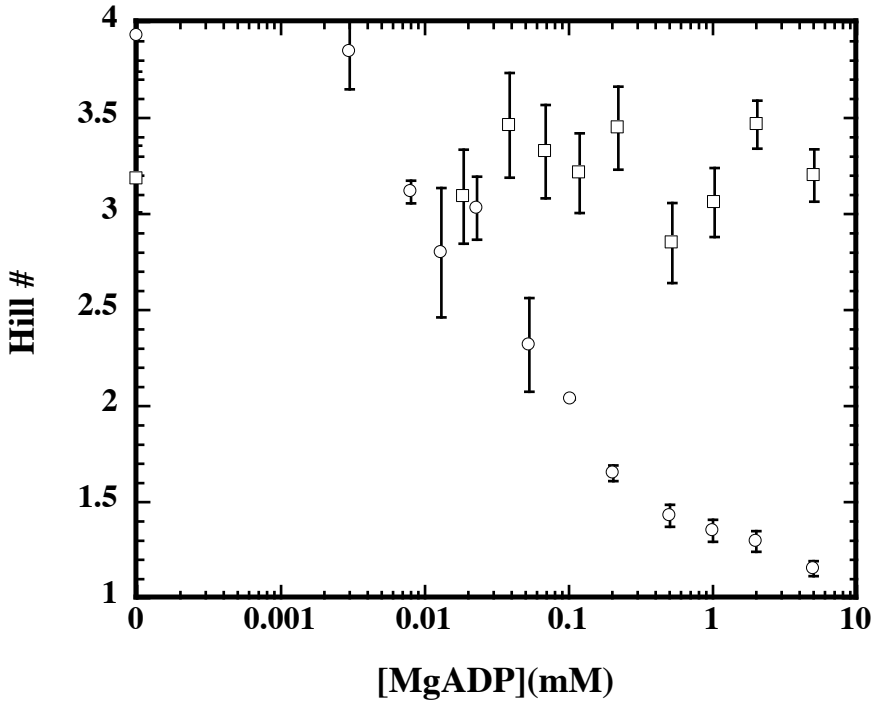

FIGURE 5-4: Homotropic cooperativity as a function of MgADP. ○ and □ represent wildtype EcPFK and D59H, respectively. In the presence of MgADP, the Hill number remains unchanged for D59H unlike wildtype.

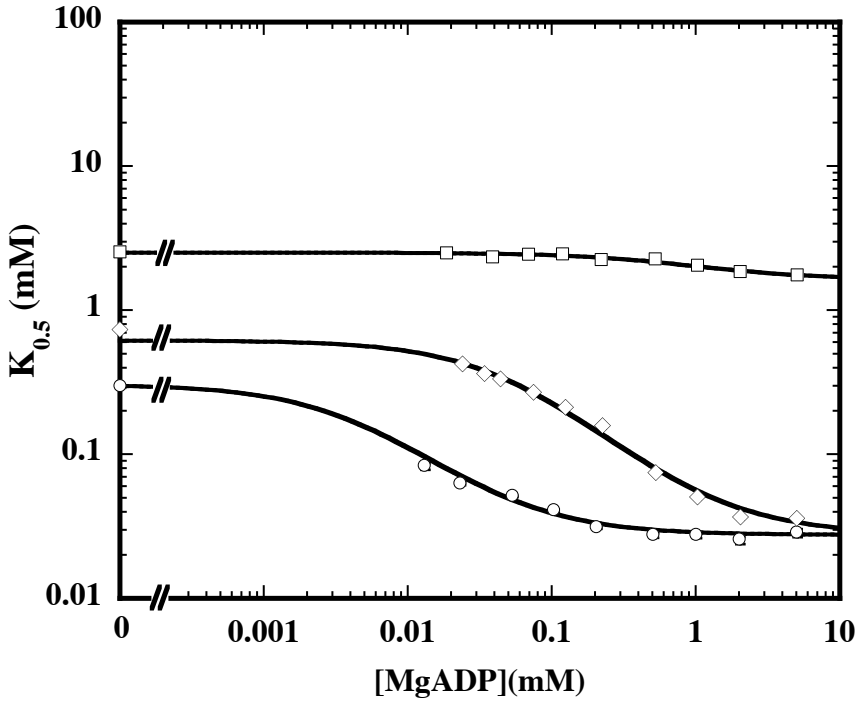

FIGURE 5-5: Comparison of mutant proteins to wildtype EcPFK in their responses to MgADP. The apparent dissociation constant for F6P was determined and plotted as a function of MgADP concentration. ○, □ and ◇ represent wildtype EcPFK, D59H and K214D, respectively.

there could be charge repulsion between the phosphate group of MgADP and the negative charge of the aspartate residue if MgADP were to bind as in wildtype. All the other mutants bind MgADP within two-fold of wildtype except for G184C and Y135A with more than a three-fold tighter binding affinities for MgADP. On the other hand, L178M and I300F both bind MgADP weaker by about three-fold than wildtype.

PEP Binding. The binding affinities for PEP are weaker by an order of magnitude for D59H, G184C, K211S and K214D (Figure 5-6). Lys211 lies in the allosteric site with Asp59 and Lys214 (Figure 5-3). The shortening of the side chain at position 211 and the removal of the positive charge would probably still allow proper contacts to be made with MgADP but not with PEP, since PEP is a smaller molecule than MgADP. Gly184 is in the interior of the protein and is within 9Å from the MgADP at the allosteric site. The addition of the cysteine side chain causes some conformational change within the protein that allows for the tighter binding of F6P, MgADP but not PEP.

MgADP Activation. D59H, G184C and G64S show reduced MgADP activation by eight-fold, four-fold and three-fold, respectively. There is a three-fold increase in activation for E167N and A231M, which probably mean that the extent of activation by MgADP to wildtype EcPFK is not the upper limit. The conformational changes that have occurred within the mutant proteins might have allowed for the enhanced activation observed. MgADP activation for all the other mutants was within two-fold to that of wildtype. One would think that K214D would show a decrease in activation, due to a weaker binding affinity for MgADP. Since this is not the case, there can be no parallel

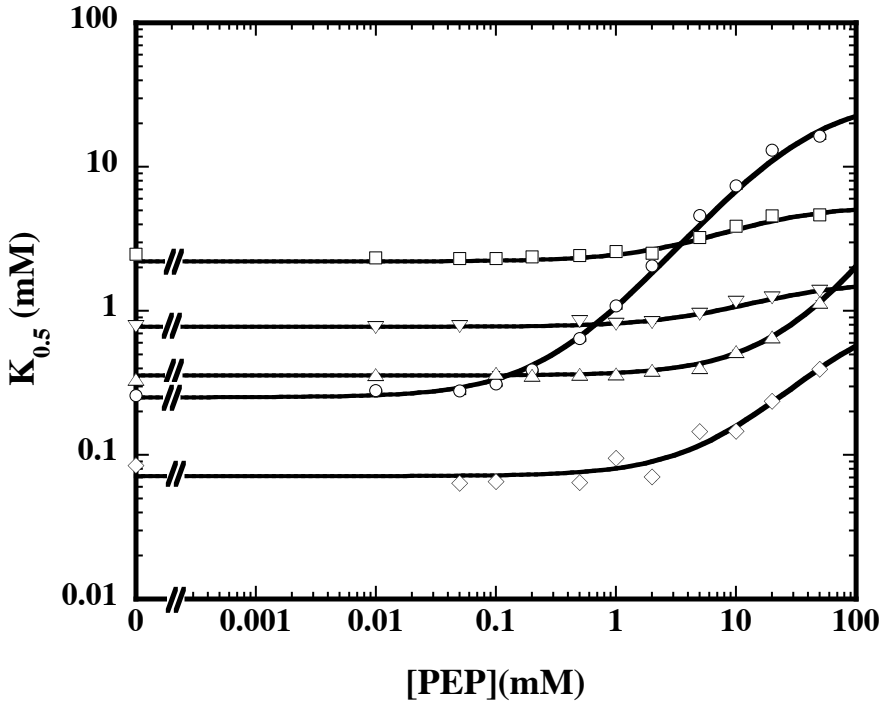

FIGURE 5-6: Comparison of mutant proteins to wildtype EcPFK in their responses to PEP. The apparent dissociation constant of F6P was plotted as a function of PEP concentration. ○, □, ◇, △ and ▽ represent wildtype EcPFK, D59H, G184C, K211S and K214D, respectively.

drawn between weaker binding and weaker activation or inhibition, and *vice versa* as seen before (Tlapak-Simmons and Reinhart, 1998; Fenton et al., 2003).

PEP Inhibition. The mutations in the allosteric site, D59H and K214D, decreased PEP inhibition by fifty-fold. Unfortunately, the extent of PEP inhibition forK211S cannot be determined due to the inability to saturate the allosteric effect. G184C and D273H have diminished inhibition by eight-fold and nine-fold, respectively. A four-fold weaker inhibition by PEP is observed for E114R, P118N and L178M as compared to wildtype.

These data show that the residues important for MgADP activation and PEP inhibition are different. D59H seems to be important for both types of allosteric effects. K214D, on the other hand, is only important for PEP inhibition but not MgADP activation. There could be a region close to the allosteric binding site that is involved in relaying information for inhibition and another for activation, with a region of overlapping influence. In other words, allosteric communication travels *via* different paths within the protein as previously suggested (Auzat et al, 1995, Fenton et al., 2003).

Stability. G184C is not stable under low concentrations and D273H has a specific activity that decreases over time. These single substitutions destabilize the proteins, probably causing dissociation of the tetramer thereby losing activity as a result. Gly184 lies in the interior of the protein and is close to the allosteric site, whereas Asp273 lies in the subunit interface (Figure 5-7). These two mutations are interesting because of their unique behavior in binding and allostery. G184C binds F6P tighter by almost four-fold, binds PEP weaker by more than 20-fold but binds MgADP tighter by

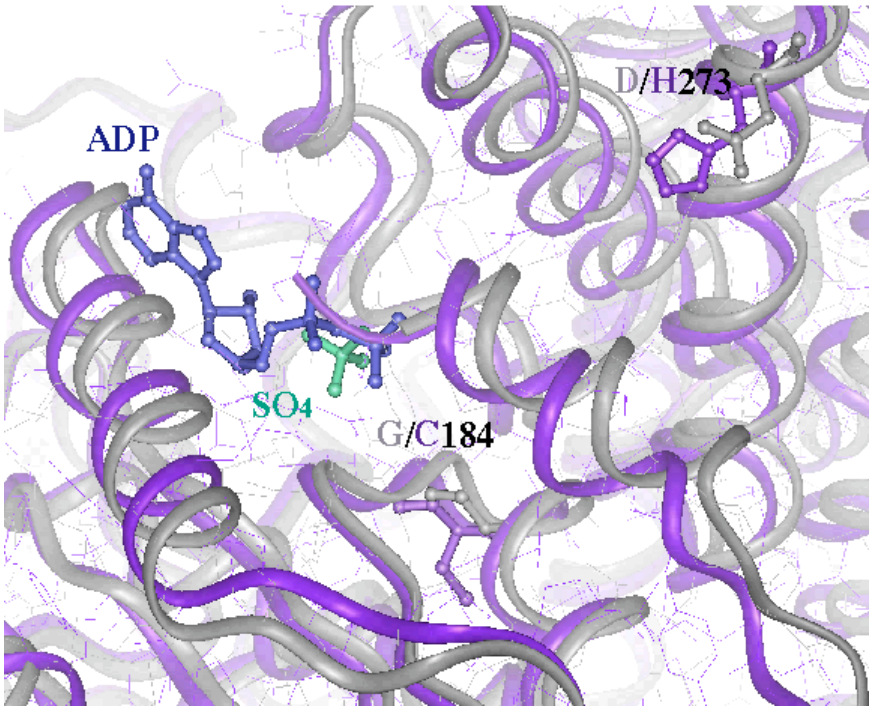

FIGURE 5-7: The location of residues at position 184 and 273 with respect to the allosteric site. A superimposition of the crystal structures of EcPFK (grey) and LbPFK (purple) as determined by Shirakihara and Evans, 1988 and Paricharttanakul et al (in prep). Residues at position 184 are within 9Å and residues at position 273 are 20Å away from ADP in the allosteric site. The figures were generated on Insight II program.

more than four-fold than to wildtype. Moreover, G184C has an eight-fold weaker PEP inhibition and a three-fold lower activation by MgADP than wildtype. D273H binds F6P with the same affinity, binds PEP and MgADP almost two-fold weaker than wildtype. D273H has a nine-fold weaker inhibition by PEP and a two-fold lower activation by MgADP than wildtype. These results further support that there is no correlation between binding and allostery; weaker binding does not necessitate a weaker allosteric effect.

More conservative mutations were created in order to increase the stability of the proteins. At position 273, aspartate was substituted with alanine and asparagine, instead of with histidine (Figure 5-8). These proteins behave very similarly to wildtype, including stability. F6P, PEP and MgADP binding to each of the mutant proteins were not affected to a great extent. PEP inhibition and MgADP activation of D273A and D273N are within two-fold of wildtype. At position 184, glycine was substituted with alanine and serine, instead of with cysteine (Figure 5-9). Instability was not a problem for these mutants. When compared to wildtype EcPFK, binding of F6P to G184A and G184S is very similar. MgADP binding is two-fold weaker for G184A, with not much difference for G184S and wildtype. Binding of PEP to G184A and G184S is two-fold and five-fold tighter than wildtype, respectively. Interestingly, there seems to be a trend with MgADP activation and PEP inhibition to varying extents with each substitution. Substituting the hydrogen atom with a methyl group at position 184 decreases both activation and inhibition. The addition of a hydroxyl group to the methyl group, then substituting a heavier atom from oxygen to sulfur further shows a decrease to the extent

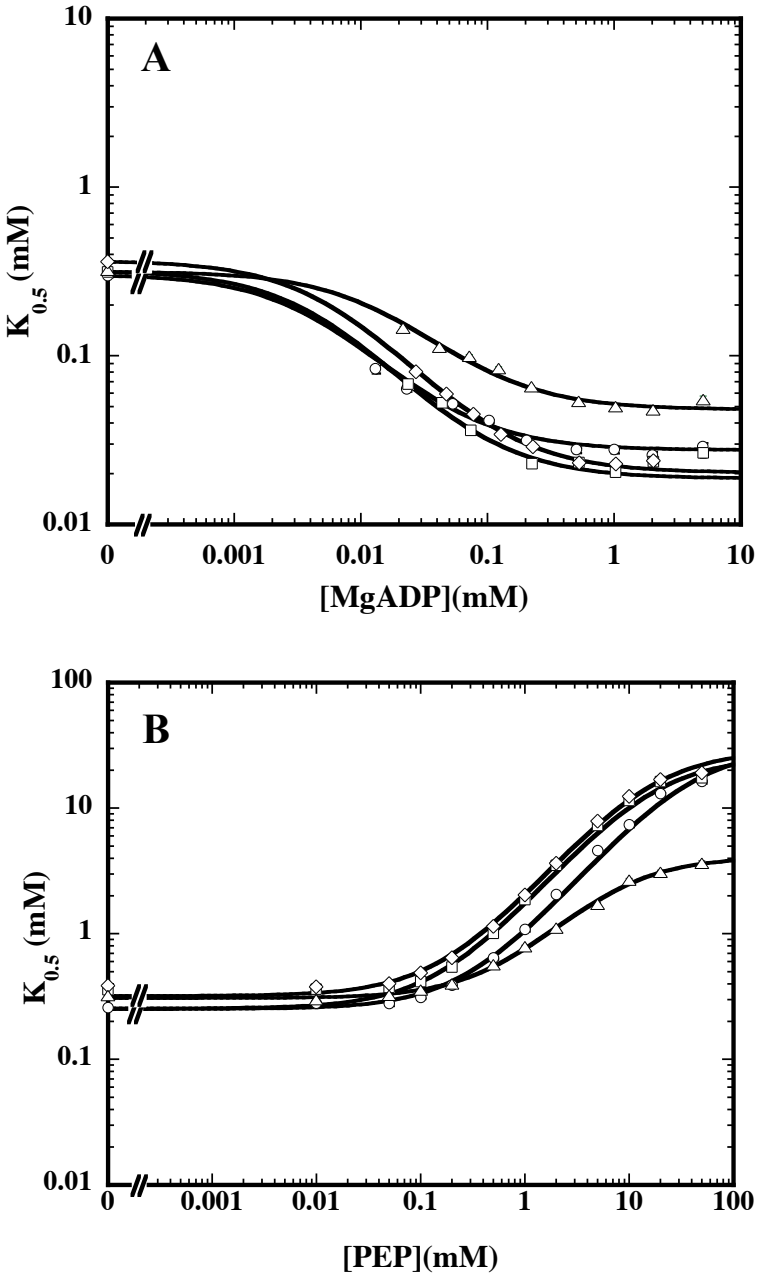

FIGURE 5-8: The importance of specific substitutions at position 273. The apparent dissociation constant for F6P was plotted as a function of MgADP (A) and PEP (B) for wildtype EcPFK (○), D273A (□), D273H (△) and D273N (◇).

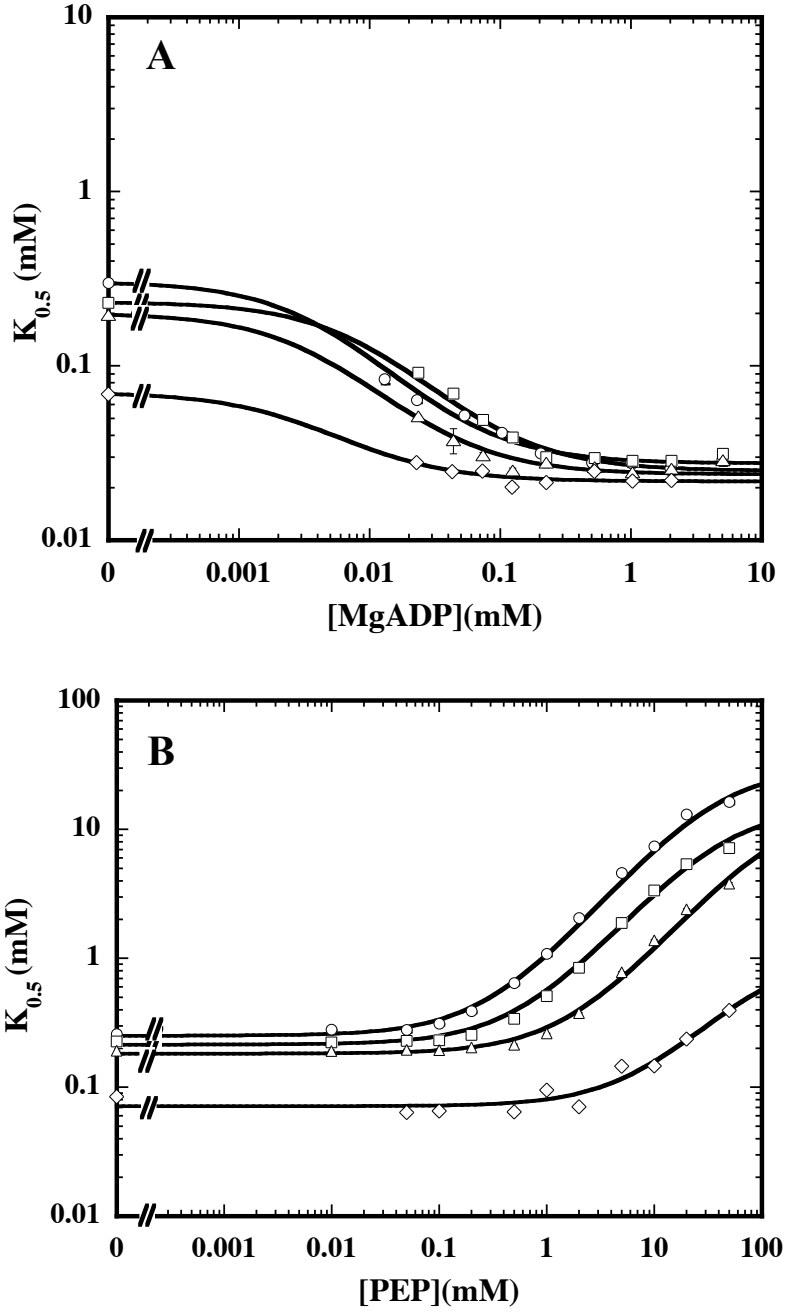

FIGURE 5-9: The importance of specific substitutions at position 184. The apparent dissociation constant for F6P was plotted as a function of MgADP (A) and PEP (B) for wildtype EcPFK (○), G184A (□), G184S (△) and G184C (◇).

of allostery. These results show that side chains are important for transmitting allosteric information through the protein.

Conclusions

Twenty-two mutant proteins were created to find residues crucial for binding of allosteric ligands and/or allosteric communication in phosphofructokinase from *E. coli* based on the sequence of phosphofructokinase from *L. bulgaricus*. Five mutant proteins show interesting characteristics. MgADP binding was diminished in D59H and K214D. The binding affinity for PEP was greatly reduced in D59H, G184C, K211S and K214D. All these residues lie within the allosteric site as shown in Figure 5-5, except for Gly184 that is close to that site. It is therefore not surprising that mutations in or near the allosteric site affect binding at the allosteric site. In addition, allosteric responses to MgADP and PEP are diminished in D59H, G184C and D273H. No significant reduction in the binding affinities for MgADP and PEP to D273H was observed. K211S did not exhibit any decrease in MgADP activation, however, the extent of PEP inhibition could not be determined. The most interesting result is that in K214D, no effect was observed on MgADP activation however, PEP inhibition was reduced as compared to wildtype. This suggests that PEP inhibition and MgADP activation is transmitted through the protein via different paths.

Out of the five, there were two mutant proteins not in the allosteric site that have decreased allosteric responses to MgADP and PEP. As shown in Figure 5-7, Gly184 lies in the interior of the protein but close to the allosteric site. Asp273 lies at the subunit

interface and is approximately 20Å away from the allosteric site. These two residues could be important for the transmission of allosteric information. However, G184C loses activity at low protein concentrations and the activity of D273H is lost within a week. To minimize instability, additional mutant proteins were created in order to get more stable mutant proteins of Gly184 and Asp273 by introducing more conservative mutations. Unfortunately, these mutant proteins do not differ significantly from wildtype unlike G184C or D273H. Therefore, specific substitutions are important for determining the loss of allosteric response. Further experiments need to be performed to definitively identify the role of these two mutations, G184C and D273H, in the relay of allosteric information.

CHAPTER VI

PINPOINTING THE ROLE OF GLY184 IN THE UNIQUE HETEROTROPIC INTERACTIONS IN PHOSPHOFRUCTOKINASE FROM *ESCHERICHIA COLI*

Introduction

EcPFK is a homotetramer with four active sites and four allosteric sites in which each site can interact with one another. This multiplicity of interactions can be simplified using the hybrid tetramer approach to isolate a single interaction between one active site and one allosteric site (heterotropic interaction). There are four unique heterotropic interactions possible in EcPFK, and each interaction has been quantified for its contribution to the allosteric responses of the enzyme to MgADP and PEP as described in Chapter III and Fenton et al., 2004. In this study, we want to ascertain whether we can differentially disrupt the heterotropic interactions with a mutation in the interior of the protein that has been shown to perturb the overall allosteric effect in the enzyme.

In the previous chapter, we have identified two residues in EcPFK that seem to be important in enabling PEP inhibition and MgADP activation. Gly184 and Asp273, when substituted with their counterparts from LbPFK show decreased allosteric effects by PEP and MgADP. At 25°C, G184C exhibits an eight-fold weaker PEP inhibition and a three-fold lower activation by MgADP than wildtype EcPFK. Similarly, D273H has a

nine-fold weaker inhibition by PEP and a two-fold lower activation by MgADP than wildtype. Asp273 is found at the subunit interface and is 20Å from the allosteric site. Gly184 is 9Å away from the allosteric site and is in the interior of the protein. Due to its location in the protein and the greater stability G184C exhibits compared to D273H, we introduced G184C into each of the four heterotropic interactions to investigate more thoroughly how allosteric information is transmitted in phosphofructokinase from *E. coli*. These experiments would reveal the importance of Gly184 in the four heterotropic interactions and whether allosteric information is transmitted in a subset of interactions or via the whole protein.

Materials and Methods

Materials. All chemical reagents used for protein purification and enzymatic assays were obtained as described in Chapter II. G184C and the constructs in Table 3-1 were created using Promega Altered Sites Mutagenesis and Stratagene QuikChange protocols.

Methods. The purifications of G184C, the 30Å and 33Å mutant proteins follow that described in Chapter II. Additional considerations were given to the 23Å and 45Å mutant proteins. The 45Å mutant protein is sensitive to temperature and must be kept at 4°C throughout purification and further manipulation. Expression of the 23Å mutant protein was very poor, purification from a total of 24 L cell culture was needed.

Hybrid tetramers of EcPFK containing G184C were created using a modified protocol from Chapter III (Figure 6-1). 3 mg G184C was incubated with 10 mg of 23Å,

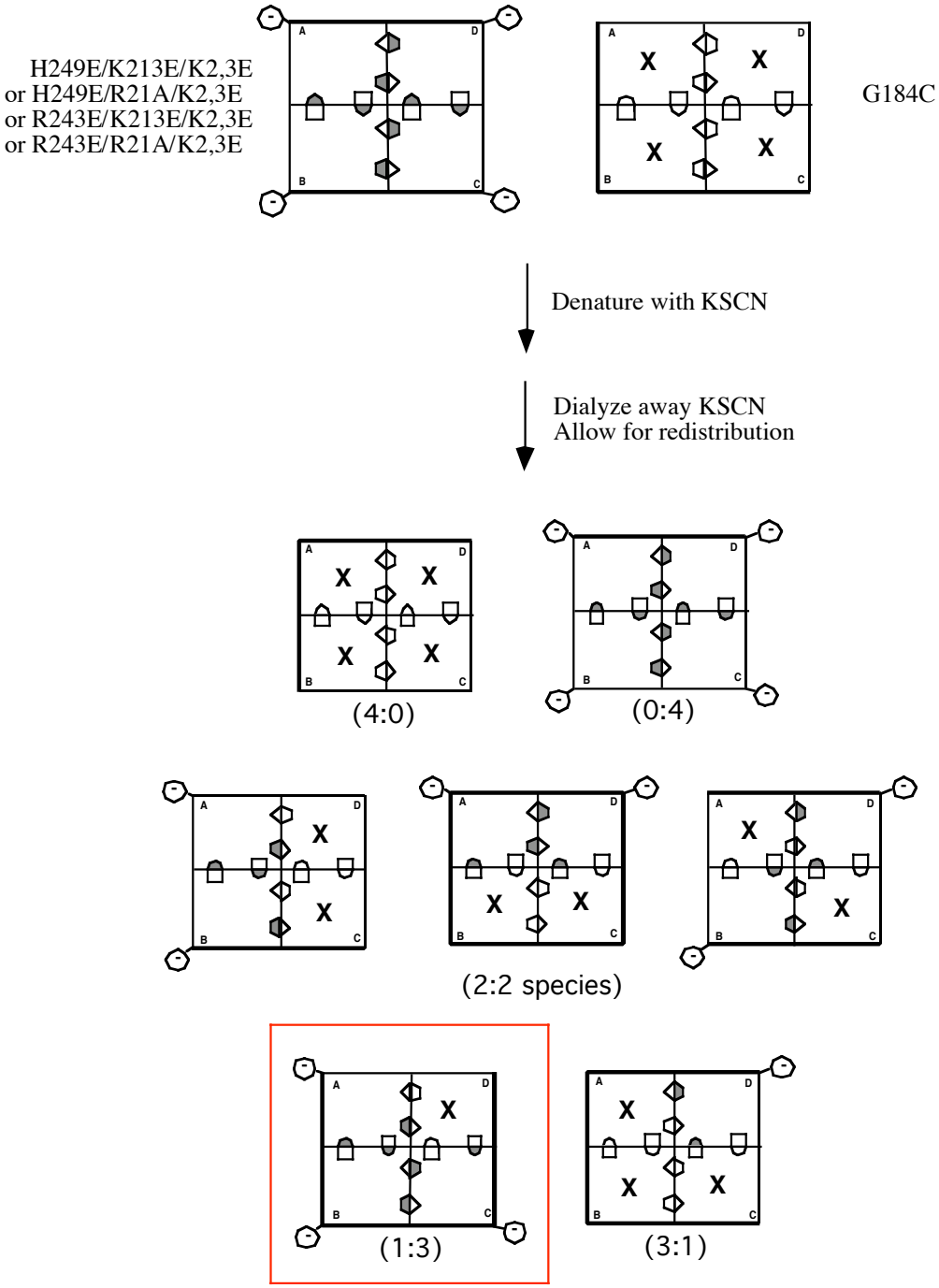

FIGURE 6-1: Strategy used to create hybrid tetramers of EcPFK containing G184C. The 1:3 hybrid tetramer (boxed in red) contains only one unique heterotropic interaction that contains G184C.

30Å, 33Å or 45Å mutant proteins in the presence of 0.35M to 0.5M KSCN for 1.5 hours. The proteins were dialyzed into Buffer A + 2 mM F6P with an hour between each buffer change for a total of three hours at 4°C. The dialyzed proteins were loaded onto the MonoQ column on Pharmacia FPLC and each hybrid tetramer species was separated with a salt gradient as shown in Figure 6-2A. Additional F6P (up to 20mM) was added to the 1:3 hybrid to prevent rehybridization. The identity and purity of each hybrid species were confirmed on a 7.5% native PAGE as shown in Figure 6-2B.

G184C and the isolated 1:3 hybrid proteins that contained G184C were characterized for their allosteric behavior with regards to MgADP and PEP at 8.5°C and were subject to the same kinetic analyses performed in Chapter II and III.

Results and Discussion

G184C shows a three-fold decrease in MgADP activation and a two-fold decrease in PEP inhibition as compared to wildtype EcPFK at 8.5°C (Figure 6-3). Introduction of this mutation into each of the four unique heterotropic interactions via the hybrid tetramer approach shown in Figure 6-1 has been successfully utilized in three of the four interactions. For the three successful hybrid tetramer formations, isolation of each of the 1:3 hybrids yields a protein that contains a single heterotropic interaction with the mutation G184C as seen in Figure 6-2.

Each of the three heterotropic interactions was characterized for the effects of MgADP and PEP as shown in Figure 6-4. The 30Å and 45Å interactions show substantial MgADP activation, with minimal activation in the 33Å interaction. There is

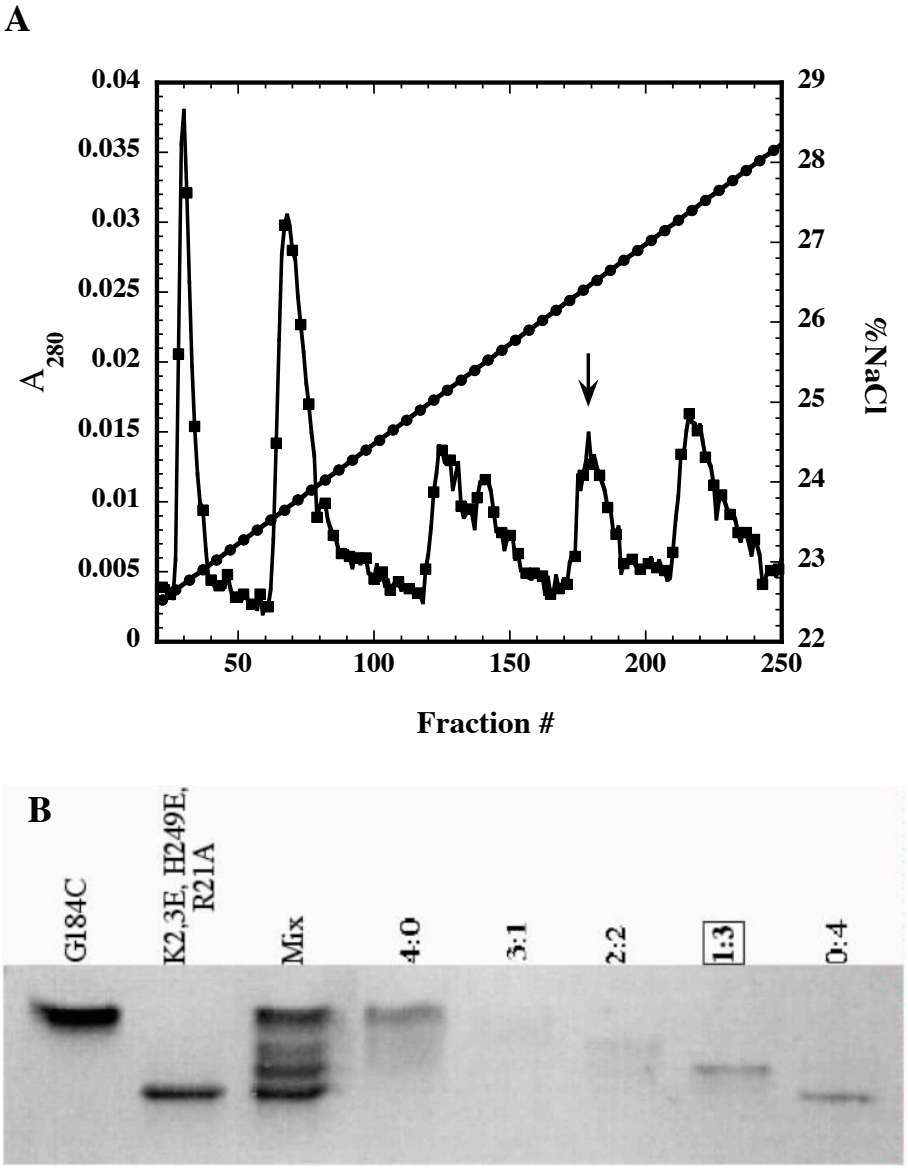

FIGURE 6-2: Separation and isolation of the 30Å heterotropic interaction containing G184C. A) Elution profile off MonoQ FPLC. Each hybrid tetramer was separated based on its charge composition with a salt gradient. The arrow shows the peak containing the 1:3 hybrid tetramer. B) 7.5% native gel of each peak fraction. These are representative of the 33Å and the 45Å heterotropic interactions.

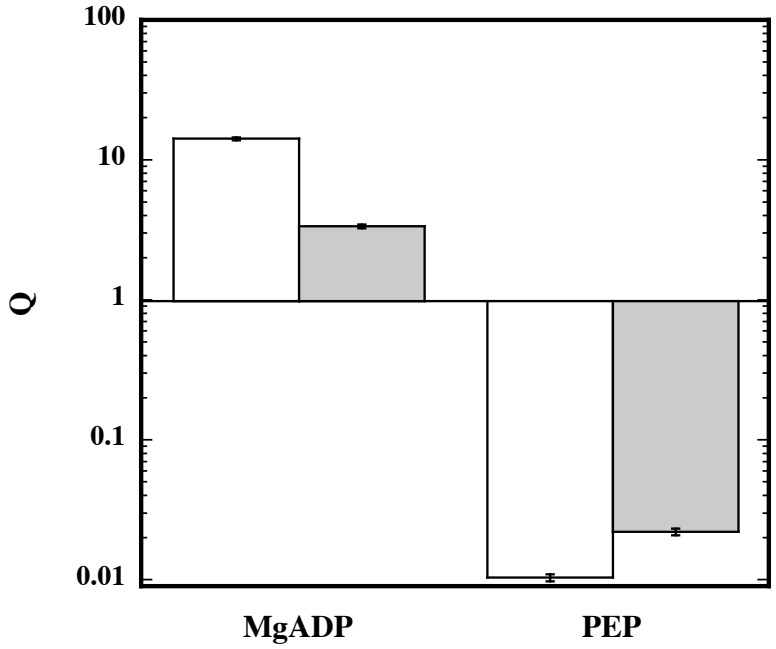

FIGURE 6-3: The allosteric effect of MgADP and PEP on G184C as compared to wildtype EcPFK at 8.5°C. The empty and shaded bars represent data of wildtype and G184C, respectively.

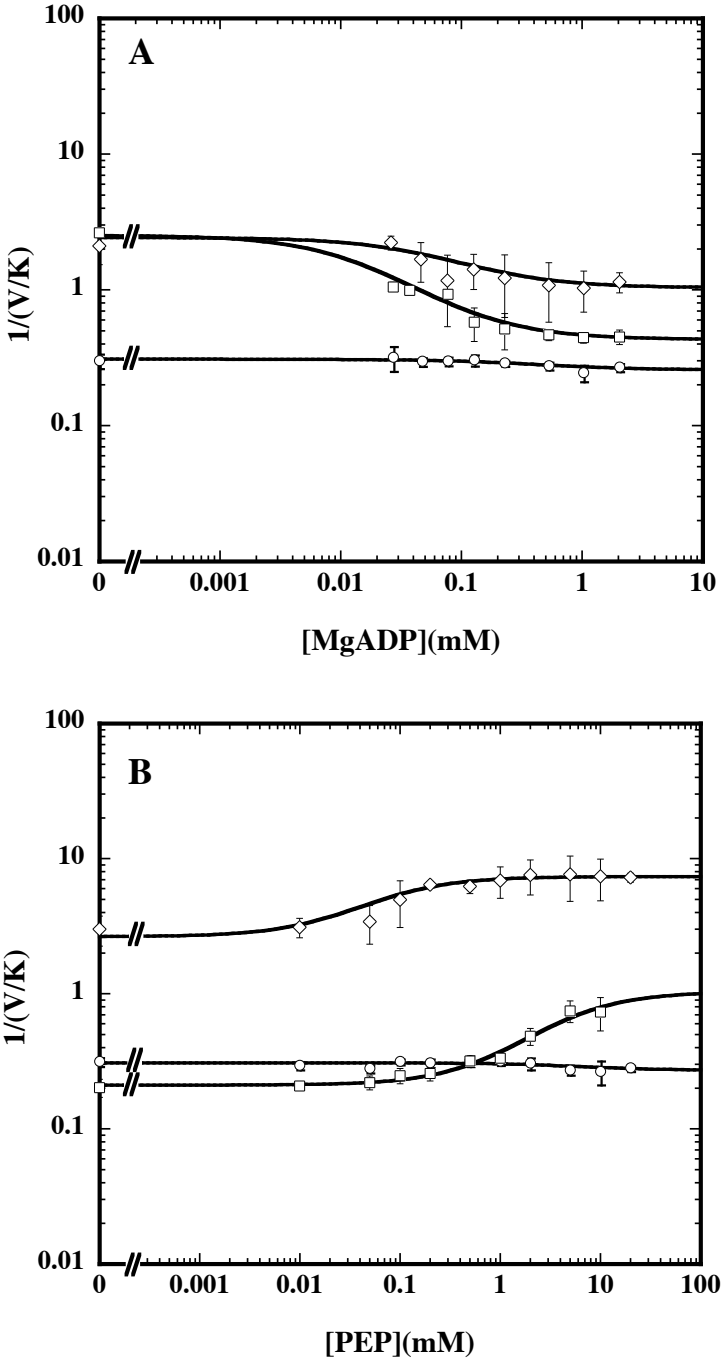

FIGURE 6-4: The influence of MgADP (A) and PEP (B) on three of the four heterotropic interactions. ○, □ and ◇ represent data for the 33Å, 30Å and 45Å interaction, respectively. The lines represent fits to equation 2-2 from Chapter II.

a slight activating effect of PEP on the 33Å interaction, and some inhibitory effect on the 30Å and the 45Å interactions. These data show that each interaction is unique and that MgADP and PEP affect each interaction differently. Figure 6-5 and Table 6-1 show the comparison of the allosteric effects in the heterotropic interactions in wildtype EcPFK with that containing G184C. G184C increases activation by MgADP by two-fold in the 30Å interaction, but substantially decreases activation in the 33Å interaction by five-fold as compared to wildtype. G184C does not appreciably affect PEP inhibition on the three interactions investigated.

No hybrids were observed for G184C and the 23Å mutant even when denaturant concentration and/or incubation time was increased (Figure 6-6). Hybrid tetramers have been successfully created between wildtype and the 23Å mutant (Fenton et al., 2004) and between G184C and each of the other three mutants in our study. Since there is evidence that KSCN can dissociate G184C and the 23Å mutant, it is therefore reasonable to conclude that either hybrids cannot be created between these two proteins or are too unstable to be detected under our experimental conditions.

We can hypothesize that the two-fold decrease in PEP inhibition observed in the G184C tetramer as compared to wildtype could be found in the 23Å interaction since it was not present in the other three interactions, assuming all four interactions are additive. Moreover, since there is a three-fold decrease in MgADP activation observed in the G184C tetramer, it is all accounted for in the 33Å and 30Å interactions. We would therefore not expect to see a change in the extent of MgADP activation in the 23Å interaction in the presence of G184C. It is really unfortunate that we cannot form the

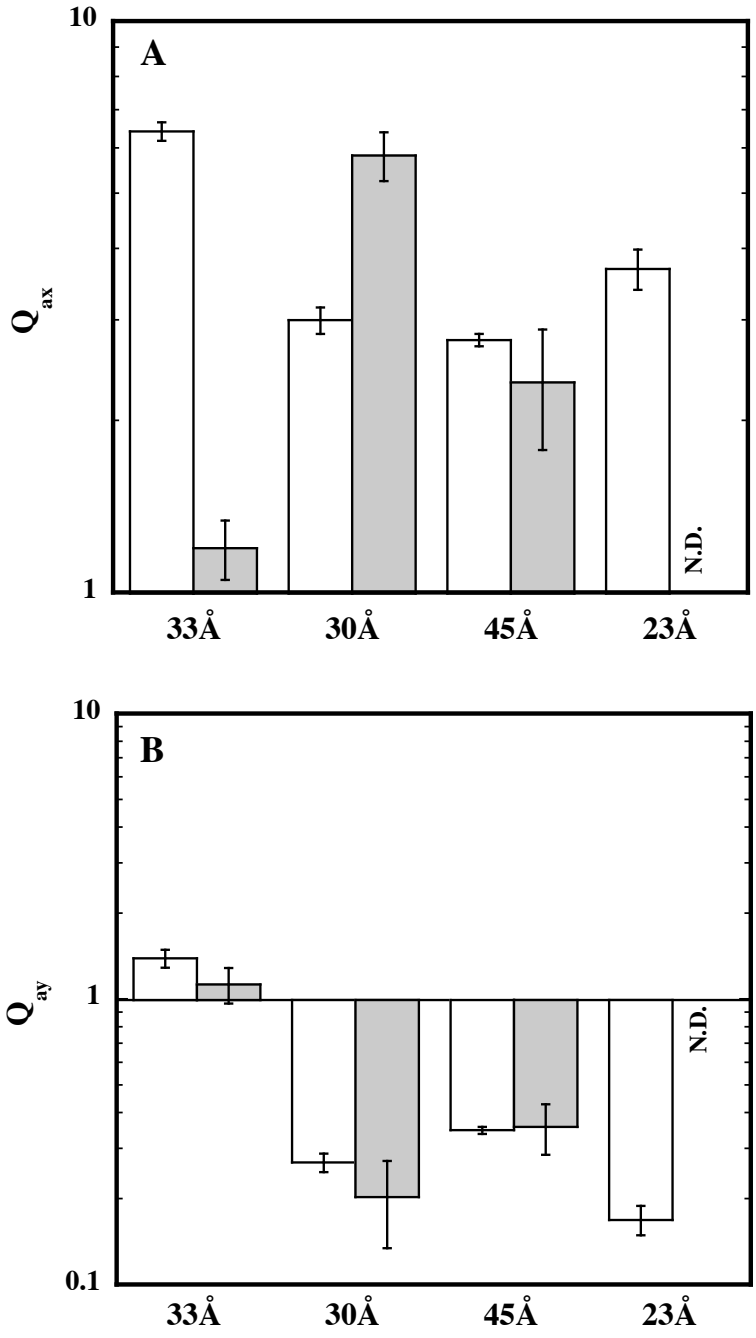

FIGURE 6-5: Distribution of the allosteric effect in the four heterotropic interactions in EcPFK at 8.5°C. The empty and shaded bars represent data of the four heterotropic interactions contained in wildtype and G184C, respectively for the effect of MgADP (A) and PEP (B).

TABLE 6-1: Coupling constants for each of the four heterotropic interactions at 8.5°C.

	Q_{ax} Wildtype	Q_{ax} G184C	Q_{ay} ‡ Wildtype	Q_{ay} G184C
33Å	6.4 ± 0.2	1.2 ± 0.1	1.4 ± 0.1	1.1 ± 0.2
30Å	3.0 ± 0.2	5.9 ± 0.6	0.27 ± 0.02	0.20 ± 0.07
45Å	2.9 ± 0.2*	2.3 ± 0.6	0.35 ± 0.01	0.36 ± 0.07
23Å	3.6 ± 0.2*	N.D.	0.17 ± 0.02	N.D.

* Data obtained from Fenton et al., 2004

‡ Data obtained from Fenton and Reinhart (unpublished)

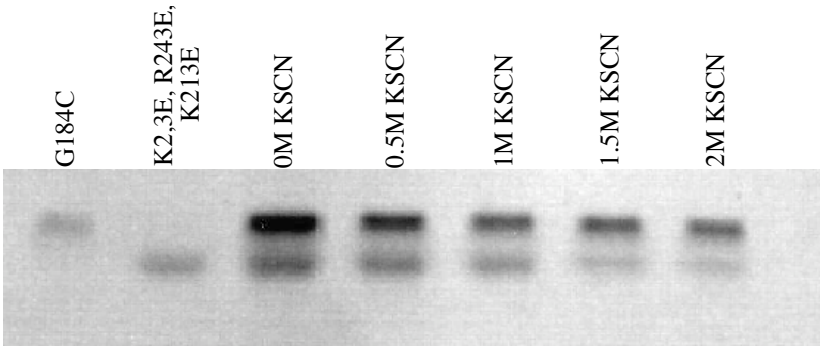

FIGURE 6-6: No formation of the 23Å interaction. A 7.5% native gel was run on samples of G184C and the 23Å mutant protein at various concentrations of KSCN.

23Å interaction to validate our hypothesis. However, we have sufficient information to support our conclusion yet again that PEP inhibition and MgADP activation follow different paths within the protein, with the 33Å interaction being very important for MgADP activation. Finally, we have successfully disrupted activation but not inhibition in the 33Å interaction with the introduction of the mutation at position 184. The crystal structure of EcPFK could reveal a possible explanation into why Gly184 is important in the 33Å interaction. Figure 6-7 shows the location of Gly184 with respect to the four heterotropic interactions. This residue lies directly in between the sites in the 33Å interaction. This could explain why mutating this residue to cysteine interrupted the 33Å interaction. Moreover, the effect of this mutation is differentially manifested in the different MgADP interactions. However, there was no effect of this mutation on the three PEP interactions studied.

Conclusions

Introduction of G184C into three of the four heterotropic interactions in phosphofructokinase in *E. coli* was successful and kinetic characterization have provided insight into the mode of transmission of allosteric information within the enzyme. There is certainly a different path of communication for activation by MgADP and inhibition by PEP. Moreover, we have determined the Gly184 is important in MgADP activation in the 33Å interaction, possibly because this residue lies directly between the sites in the 33Å interaction. Interestingly, this residue does not seem to be important for PEP inhibition.

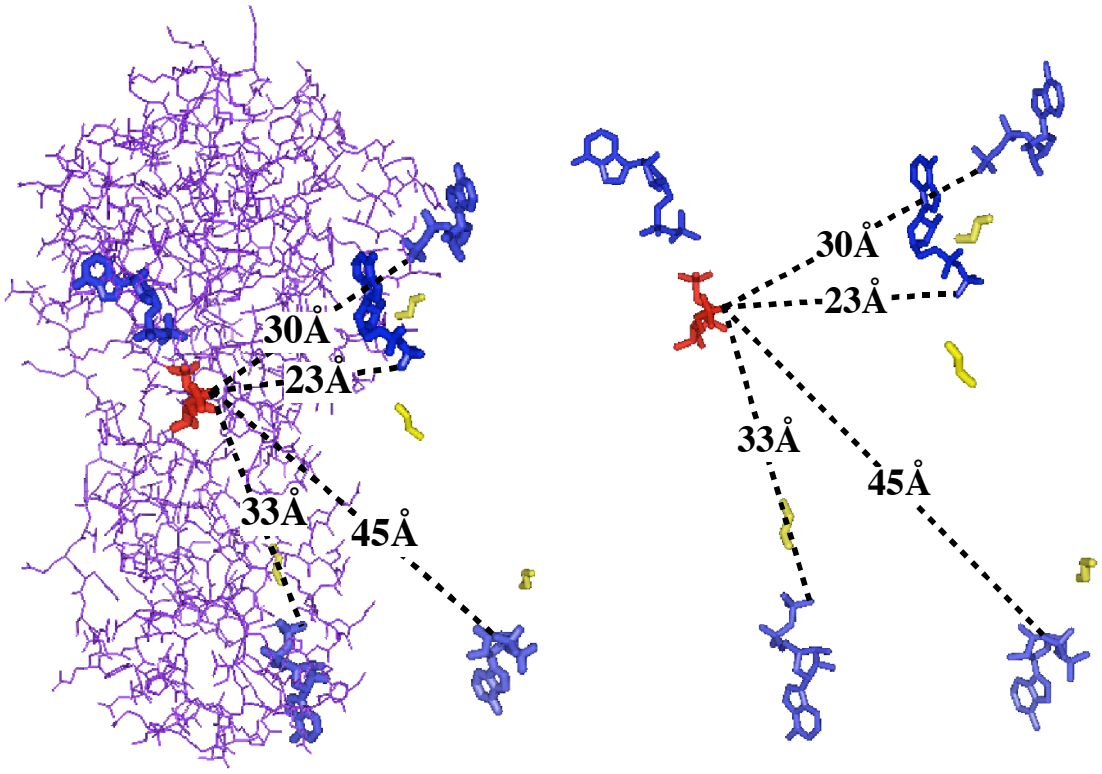

FIGURE 6-7: Location of G184C in the four heterotropic interactions of EcPFK. Subunit A is shown on the left and the heterotropic interactions denoted by their distances in the crystal structure. Fructose-1, 6-bisphosphate, MgADP and G184C are in red, blue and yellow, respectively.

We cannot really compare our heterotropic results to that of the tetrameric G184C. There is homotropic cooperativity in F6P binding in G184C like wildtype, but not in the unique heterotropic interactions (Fenton and Reinhart, 2002). Additional experiments need to be performed to eliminate homotropic cooperativity in G184C. Moreover, we cannot check additivity in the extent of allosteric responses to MgADP and PEP in the interactions containing G184C since we could only create and characterize three of the four unique interactions. Additivity in the coupling free energies of the four heterotropic interactions have been observed in wildtype EcPFK (Fenton et al., 2004) and wildtype PFK from *Bacillus stearothermophilus* (Ortigosa et al, 2003) after homotropic cooperativity is accounted for.

We have assumed that allosteric communication in the 1:3 hybrid proceeds through the subunit containing G184C, and not communicated through the other three subunits. This may or may not be the case; the perturbations caused by G184C on the tetramer can be localized within that subunit or throughout the whole tetramer. Another set of experiments could be performed to put G184C in all four subunits. This would eliminate the need for any assumptions. These experiments however, would be harder to perform due to the decrease in stability with the addition of G184C on all subunits.

CHAPTER VII

CONCLUSIONS

Extensive kinetic, mutagenic and structural studies have been performed to study allosteric regulation in phosphofructokinase from *Escherichia coli* (Blangy et al., 1968; Shirakihara and Evans, 1988; Johnson and Reinhart, 1994, 1997; Wang and Kemp, 1999; Pham and Reinhart, 2001; Fenton et al., 2003). However, a more thorough investigation into the path and/or residue(s) important for allosteric communication in this enzyme has yet to be conducted.

In Chapter III, we created hybrid tetramers to simplify the allosteric web of potential interactions present in EcPFK. In collaboration with Dr. Aron Fenton, we have successfully characterized all four unique heterotropic interactions with respect to MgADP activation in the homotetramer (Fenton et al., 2004). Each interaction is unique in magnitude and they combine additively to the total heterotropic effect observed in the tetramer that has homotropic cooperativity of F6P removed. A similar result was obtained for the effect of PEP on the four unique heterotropic interactions in PFK from *B. stearothermophilus* (Ortigosa et al., 2003).

Chapter IV describes the kinetic and structural characterization of PFK from *L. bulgaricus*. The 1.86Å resolution crystal structure of LbPFK reveals a fold similar to that of EcPFK and BsPFK. The residues that contact both substrates are conserved however, the residues in the allosteric site are not. This could explain why the binding of either MgADP or PEP to LbPFK is very weak as compared to EcPFK and BsPFK.

Moreover, allosteric effects by PEP and MgADP are observed, both slightly inhibitory to F6P binding. This is in contrast to the study performed by Le Bras et al., 1991. We conclude that the enzyme has some allosteric control at very high concentrations of MgADP and PEP but not to the same extent of EcPFK and BsPFK.

To address the question on which residue in EcPFK is important for enabling allosteric communication (Chapter V), we took advantage of published amino acid sequences of EcPFK, BsPFK, TtPFK and LbPFK All but PFK from *L. bulgaricus* respond to MgADP activation and PEP inhibition of F6P binding at pH 8.0 (Xu et al., 1990; Le Bras et al., 1991; Johnson and Reinhart, 1994, 1997; Tlapak-Simmons and Reinhart, 1998). Our experiments from Chapter IV have shown no MgADP activation and slight PEP inhibition in LbPFK. Sequence alignment of these four enzymes reveal twenty-two residues that are conserved in the three allosteric PFKs but not LbPFK. Each of the twenty-two residues in EcPFK was substituted for its counterpart from LbPFK and characterized for its responses to MgADP and PEP. Three residues when mutated (D59H, G184C and D273H) show significant reductions in the magnitude of PEP inhibition and MgADP activation. K214D, however, reduced the extent of PEP inhibition and not MgADP activation. This lysine residue at position 214 seems to be important for only PEP inhibition. Therefore, we can conclude that paths of allosteric communication for inhibition and activation are different, which was also observed in Fenton et al., 2003.

The question now arises to be whether these reductions in allosteric response are differentially manifested in the heterotropic interactions in EcPFK (Chapter VI). To

study the effect of these mutations on the heterotropic interactions, we introduced only G184C into the hybrid tetramers since Gly184 is in the interior of the protein and 9Å from the allosteric site. The other three did not fit our criteria of being in the interior of the protein. Asp59 and Lys214 lie in the allosteric site and Asp273 is solvent exposed. Unfortunately, we can only create and characterize three of the four unique heterotropic interactions containing G184C. However with the three isolated, we have determined that Gly184 is important for MgADP activation via the 33Å interaction, but not inhibition. Once again, we have established that PEP inhibition and MgADP activation of F6P binding are communicated in different paths in the enzyme.

Additional experiments need to be performed to identify residues that make up the paths of allosteric communication by MgADP and PEP. We have identified four residues, Asp59, Gly184, Lys214 and Asp273, which are important for allostery. So far Gly184 has been shown to be important for MgADP activation in only the 33Å interaction. The role of the other three residues in the unique heterotropic interactions is still unknown. This type of dissection into the transmission of allosteric information can be performed to reveal more residues that play significant roles in the allosteric communication pathway in EcPFK.

In summary, we have successfully simplified the allosteric web by characterizing the four unique heterotropic interactions between MgADP and F6P binding sites, and have identified some residues in EcPFK that are important in transmitting allosteric information by PEP and MgADP. One of these residues has differentially disrupted the responses to MgADP in the heterotropic interactions but not to PEP. Therefore, we have

established that allosteric communication follows different pathways in EcPFK between one active site and one allosteric site. Moreover, the path is also different for MgADP activation and PEP inhibition.

REFERENCES

Auzat, I., G. G. Le Bras, P. Branny, F. De La Torre, B. Theunissen, and J. R. Garel. 1994. The role of Glu187 in the regulation of phosphofructokinase by phosphoenolpyruvate. *J. Mol. Biol.* 235:68-72.

Auzat, I., W. M. Byrnes, J. R. Garel, and S. H. Chang. 1995. Role of residue 161 in the allosteric transitions of two bacterial phosphofructokinases. *Biochemistry.* 34:7062-7068.

Auzat, I., G. Le Bras, and J. R. Garel. 1997. Allosteric activation increases the maximum velocity of E. coli *phosphofructokinase. J. Mol. Biol.* 267:476-480.

Babul, J. 1978. Phosphofructokinases from *Escherichia coli.* Purification and characterization of the nonallosteric isozyme. *J. Biol. Chem.* 253:4350-4355.

Baumann, P., and B. E. Wright. 1968. The phosphofructokinase from *Dictyostelium discoideum. Biochemistry.* 7:3653-3661.

Berger, S. A., and P. R. Evans. 1990. Active site mutants altering the cooperativity of *E. coli* phosphofructokinase. *Nature.* 343:575-576.

Berger, S. A., and P. R. Evans. 1992. Site-directed mutagenesis identifies catalytic residues in the active site of *Escherichia coli* phosphofructokinase. *Biochemistry.* 31:9237-9242.

Blangy, D., H. Buc, and J. Monod. 1968. Kinetics of the allosteric interactions of phosphofructokinase from *Escherichia coli. J. Mol. Biol.* 31:13-35.

Branny, P., F. De La Torre, and J. R. Garel. 1993. Cloning, sequencing, and expression in *Escherichia coli* of the gene coding for phosphofructokinase from *Lactobacillus bulgaricus. J. Bacteriol.* 175:5344-5349.

Braxton, B. L., V. L. Tlapak-Simmons, and G. D. Reinhart. 1994. Temperature-induced inversion of allosteric phenomena. *J. Biol Chem.* 269:47-50.

Burgos-Rubio, C., M. R. Okos, and P. C. Wankat. 2000. Kinetic study of the conversion of different substrates to lactic acid using *Lactobacillus bulgaricus. Biotechnol. Prog.* 16:305-314.

Byrnes, M. X. Xhu., E. S. Younathan, and S. H. Chang. 1994. Kinetic characteristics of phosphofructokinase from *Bacillus stearothermophilus*: MgATP nonallosterically inhibits the enzyme. *Biochemistry*. 33:3424-3431.

Cleland, W. W. 1986. Enzyme kinetics as a tool for determination of enzyme mechanisms, in *Investigations of Rates and Mechanisms of Reactions*. C. F. Bernasconi, editor. John Wiley & Sons, New York. pp 791-870.

Collaborative Computational Project, N. 1994. The CCP4 suite: programs for protein crystallography. *Acta Crystallogr. D. Biol. Crystallogr*. 50:760-763.

Daldal, F. 1983. Molecular cloning of the gene for phosphofructokinase-2 of *Escherichia coli* and the nature of a mutation, pfkB1, causing a high level of the enzyme. *J. Mol. Biol*. 168:285-305.

Daubner, S. C., J. Melendez, P. F. Fitzpatrick. 2000. Reversing the substrate specificities of phenylalanine and tyrosine hydroxylase: aspartate 425 of tyrosine hydroxylase is essential for L-DOPA formation. *Biochemistry*. 39:9652-9661.

Delley, M. and J. E. Germond. 2002. Differentiation of *Lactobacillus helveticus, Lactobacillus delbrueckii* subsp *bulgaricus*, subsp *lactis* and subsp *delbrueckii* using physiological and genetic tools and reclassification of some strains from the ATCC collection. *Syst. Appl. Microbiol*. 25:228-231.

Deville-Bonne, D., G. Le Bras, W. Teschner, and J. R. Garel. 1989. Ordered disruption of subunit interfaces during stepwise reversible dissociation of *Escherichia coli* phosphofructokinase with KSCN. *Biochemistry*. 28:1917-1922.

Deville-Bonne, D., R. Laine, and J. R. Garel. 1991. Substrate antagonism in the kinetic mechanism of *E. coli* phosphofructokinase-1. *FEBS Letters*. 290:173-176.

Doelle, H. W. 1972. Kinetic characteristics of phosphofructokinase from *Lactobacillus casei* var. *Rhamnosus* ATCC 7469 and *Lactobacillus plantarum* ATCC 14917. *Biochim. Biophys. Acta*. 258:404-410.

Evans, P. R., and P. J. Hudson. 1979. Structure and control of phosphofructokinase from *Bacillus stearothermophilus*. *Nature*. 279:500-504.

Evans, P. R., G. W. Farrants, and P. J. Hudson. 1981. Phosphofructokinase: structure and control. *Phil. Trans. R. Soc. Lond. B*. 293:53-62.

Fenton, A. W., and G. D. Reinhart. 2002. Isolation of a single activating allosteric interaction in phosphofructokinase from *Escherichia coli*. *Biochemistry*. 41:13410-13416.

Fenton, A. W., and G. D. Reinhart. 2003. Mechanism of substrate inhibition in *Escherichia coli* phosphofructokinase. *Biochemistry*. 42:12676-12681.

Fenton, A. W., N. M. Paricharttanakul, and G. D. Reinhart. 2003. Identification of substrate contact residues important for the allosteric regulation of phosphofructokinase from *Escherichia coli*. *Biochemistry*. 42:6453-6459.

Fenton, A. W., N. M. Paricharttanakul, and G. D. Reinhart. 2004. Disentangling the web of allosteric communication in a homotetramer: Heterotropic activation in phosphofructokinase from *Escherichia coli*. *Biochemistry*. 43:14104-14110.

Ferdinandus, J., and J. B. Clark. 1969. The phosphofructokinase of *Arthrobacter crystallopoietes*. *Biochem. J.* 113:735-736.

Hansen, T., and P. Schonheit. 2000. Purification and properties of the first-identified, archael, ATP-dependent 6-phosphofructokinase, an extremely thermophilic non-allosteric enzyme, from the hyperthermophile *Desulfurococcus amylolyticus*. *Arch. Microbiol*. 173:103-109.

Hansen, T., and P. Schonheit. 2001. Sequence, expression, and characterization of the first archael ATP-dependent 6-phosphofructokinase, a non-allosteric enzyme related to the phosphofructokinase-B sugar kinase family, from the hyperthermophilic crenarchaeote *Aeropyrum pernix*. *Arch. Microbiol*. 177:62-69.

Hellinga, H, W., and P. R. Evans. 1987. Mutations in the active site of *Escherichia coli* phosphofructokinase. *Nature*. 327:437-439.

Hill, A. V. 1910. The possible effects of the aggregation of the molecules of hemoglobin on its dissociation curves. *J. Physiol*. 40:iv-vii.

Jaworek, D., W. Gruber, and H. U. Bergmeyer. 1974. Adenosine-5'-diphosphate and adenosine-5'-monophosphate, in *Methods of Enzymatic Analysis*. Volume 4. H. U. Bergmeyer, editor. Academic Press, Inc., New York. pp 2127-2131.

Johnson, J. L., and G. D. Reinhart. 1992. MgATP and fructose-6-phosphate interactions with phosphofructokinase from *Escherichia coli*. *Biochemistry*. 31:11510-11518.

Johnson, J. L., and G. D. Reinhart. 1994. Influence of MgADP on phosphofructokinase from *Escherichia coli*. Elucidation of coupling interactions with both substrates. *Biochemistry*. 33:2635-2643.

Johnson, J. L., and G. D. Reinhart. 1997. Failure of a two-state model to describe the influence of phospho(enol)pyruvate on phosphofructokinase from *Escherichia coli*. *Biochemistry*. 36:12814-12822.

Johnson, J. L., M. D. Lasagna, and G. D. Reinhart. 2001. Influence of a sulfhydryl cross-link across the allosteric-site interface of *E. coli* phosphofructokinase. *Protein Science*. 10:2186–2194.

Kimmel, J. L., and G. D. Reinhart. 2000. Reevaluation of the accepted allosteric mechanism of phosphofructokinase from Bacillus stearothermophilus. *Proc. Natl. Acad. Sci. USA*. 97:3844-3849.

Kimmel, J. L., and G. D. Reinhart. 2001. Isolation of an individual allosteric interaction in tetrameric phosphofructokinase from *Bacillus stearothermophilus*. *Biochemistry*. 40:11623-11629.

Koshland, D. E., G. Nemethy, and D. Filmer. 1966. Comparison of experimental binding data and theoretical models in proteins containing subunits. *Biochemistry*. 5:365-385.

Kotlarz, D., and H. Buc. 1977. Two *Escherichia coli* fructose-6-phosphate kinases: Preparative purification, oligomeric structure, and immunological studies. *Biochem. Biophys. Acta*. 484: 35–48.

Kundrot, C. E., and P. R. Evans. 1991. Designing an allosterically locked phosphofructokinase. *Biochemistry*. 30:1478-1484.

Laemmli, U. K. 1970. Cleavage of structural proteins during the assembly of the head of bacteriophage T4. *Nature*. 227:680-685.

Laine, R., D. Deville-Bonne, I. Auzat, and J. R. Garel. 1992. Interactions between the carboxyl groups of Asp 127 and Asp 129 in the active site of *Escherichia coli* phosphofructokinase. *Eur. J. Biochem.* 207:1109-1114.

Lau, F. T., and A. R. Fersht. 1987. Conversion of allosteric inhibition to activation in phosphofructokinase by protein engineering. *Nature*. 326:811-812.

Lau, F. T., A. R. Fersht, H. W. Hellinga, and P. R. Evans. 1987. Site-directed mutagenesis in the effector site of *Escherichia coli* phosphofructokinase. *Biochemistry*. 26:4143-4148.

Lau, F. T., and A. R. Fersht. 1989. Dissection of the effector-binding site and complementation studies of *Escherichia coli* phosphofructokinase using site-directed mutagenesis. *Biochemistry*. 28:6841-6847.

Le Bras, G., and J. R. Garel. 1982. A proteolyses derivative of *Escherichia coli* phosphofructokinase is no longer sensitive to allosteric effectors and still shows cooperativity in substrate binding. *Biochemistry*. 21:6656-6660.

Le Bras, G., and J. R. Garel. 1985. Fructose-6-phosphate prevents the proteolyzed derivative of *Escherichia coli* phosphofructokinase from dissociation and inactivation. *J. Biol. Chem.* 260:13450-13453.

Le Bras, G., W. Teschner, D. Deville-Bonne, and J. R Garel. 1989. Urea-induced inactivation, dissociation and unfolding of the allosteric phosphofructokinase from *Escherichia coli*. *Biochemistry*. 28:6836-6841,

Le Bras, G., D. Deville-Bonne, and J. R. Garel. 1991. Purification and properties of the phosphofructokinase from *Lactobacillus bulgaricus*. A non-allosteric analog of the enzyme from *Escherichia coli*. *Eur. J. Biochem.* 198:683-687.

Lehninger, A. L., D. L. Nelson, and M. M. Cox. 1993. Principles of Biochemistry. 2nd ed. Worth Publishers, Inc., New York.

McRee, D. E. 1999. XtalView/Xfit: A versatile program for manipulating atomic coordinates and electron density. *J. Struct. Biol.* 125:156-165.

Monod, J., J. Wyman, and J. P. Changeux. 1965. On the nature of allosteric transitions: a plausible model. *J. Mol. Biol.* 12:88-118.

Murray, R. K., D. K. Granner, P. A. Mayes, and V. W. Rodwell. 1996. Harper's Biochemistry. 24th ed. Appleton & Lange, Stamford, Connecticut.

Ortigosa, A. D., J. L. Kimmel, and G. D. Reinhart. 2004. Disentangling the web of allosteric communication in a homotetramer: Heterotropic inhibition of phosphofructokinase from *Bacillus stearothermophilus*. *Biochemistry*. 43:577-586.

Otwinowski, Z., and W. Minor. 1997. Processing of x-ray diffraction data collected in oscillation mode. *Methods Enzymol.* 276:307-326.

Paricharttanakul, N. M., S. Ye, A. L. Menefee, F. Javid-Majd, J. C. Sacchettini and G. D. Reinhart. Investigation into the Structure-function Relationship of Phosphofructokinase from *Lactobacillus bulgaricus*. (manuscript in prep).

Perrakis, A., M. Harkiolaki, K. S. Wilson, and V. S. Lamzin. 2001. ARP/wARP and molecular replacement. *Acta Crystallogr. D. Biol. Crystallogr.* 57:1445-1450.

Pham, A. S., F. Tlapak-Simmons, and G. D. Reinhart. 2001. Persistent binding of MgADP to the E187A mutant of *Escherichia coli* phosphofructokinase in the absence of allosteric effects. *Biochemistry*. 40:4140-4149.

Poorman, R. A., A. Randolph, R. G. Kemp, and R. L. Heinrikson. 1984. Evolution of phosphofructokinase: gene duplication and reaction of new effector sites. *Nature*. 309:467-469.

Reinhart, G. D. 1983. The determination of thermodynamic allosteric parameters of an enzyme undergoing steady-state turnover. *Arch. Biochem. Biophys*. 224:389-401.

Reinhart, G. D. 1985. Influence of pH on the regulatory kinetics of rat liver phosphofructokinase: a thermodynamic linked-function analysis. *Biochemistry*. 24:7166-7172.

Reinhart, G. D. 1988. Linked-function origins or cooperativity in a symmetrical dimer. *Biophys. Chem*. 30:159-172.

Reinhart, G. D., S. B. Hartleip, and M. M. Symcox. 1989. Role of coupling entropy in establishing the nature and magnitude of allosteric response. *Proc. Natl, Acad. Sci. USA*. 86:4032-4036.

Reinhart, G. D. 2004. Quantitative analysis and interpretation of allosteric behavior. *Methods Enzymol*. 380:187-203.

Riley-Lovingshimer, M. R., and G. D. Reinhart. 2001. Equilibrium binding studies of a tryptophan-shifted mutant of phosphofructokinase from *Bacillus stearothermophilus*. *Biochemistry*. 40:3002-3008.

Rypniewski, W. R., and P. R. Evans. 1989. Crystal structure of unliganded phosphofructokinase from *Escherichia coli*. *J Mol. Biol*. 207:805-821.

Schirmer, T., and P. R. Evans. 1990. Structural basis of the allosteric behavior of phosphofructokinase. *Nature*. 343:140-145.

Serre, M. C. and J. R. Garel. 1990. Role of the C-terminal region in the allosteric properties of *Escherichia coli* phosphofructokinase-1. *Eur. J. Biochem*. 189:487-492.

Serre, M. C., W. Teschner, and J. R. Garel. 1990. Specific suppression of heterotropic interactions in phosphofructokinase by the mutation of leucine 178 into tryptophan. *J. Biol. Chem*. 265:12146-12148.

Shirakihara, Y. and P. R. Evans. 1988. Crystal structure of the complex of phosphofructokinase from *Escherichia coli* with its reaction products. *J. Mol. Biol.* 204:973-994.

Smith, D. K., R. I. Krohn, G.T. Hermanson, A. K. Mallia, F. H. Gartner, M. D. Provenzano, N. M. Goeke, B. J. Olson, and D. C. Klenk. 1985. Measurement of protein using bicinchoninic acid. *Anal. Biochem.* 150:76-85

Teschner, W., D. Deville-Bonne, and J. R. Garel. 1990. Fructose-6-phosphate modifies the pathway of the urea-induced dissociation of the allosteric phosphofructokinase from *Escherichia coli*. *FEBS Letters*. 267:96-98.

Tlapak-Simmons, V. L., and G. D. Reinhart. 1994. Comparison of the inhibition of phospho(enol)pyruvate and phosphoglycolate of phosphofructokinase from *B. stearothermophilus*. *Arch. Biochem. Biophys.* 308:226-230.

Tlapak-Simmons, V. L., and G. D. Reinhart. 1998. Obfuscation of allosteric structure-function relationships by enthalpy-entropy compensation. *Biophys. J.* 75:1010-1015.

Uyeda, K. 1979. Phosphofructokinase. *Adv. Enzymol.* 48:193-224.

Valdez, B. C., S. H. Chang, and E. S. Younathan. 1988. Site-directed mutagenesis at the regulatory site of fructose-6-phosphate-1-kinase from *Bacillus stearothermophilus*. Mutations at the substrate binding site affects allosteric behavior. *Biochem. Biophys. Res. Comm.* 156:537-542.

Valdez, B. C., B. A. French, E. S. Younathan, and S. H. Chang. 1989. Site-directed mutagenesis in *Bacillus stearothermophilus* fructose-6-phosphate 1-kinase. *J. Mol. Biol.* 264:131-135.

Voet , D., and J. G. Voet. 1995. Biochemistry. 2nd ed. John Wiley and Sons, New York.

Wang, X., and R. G. Kemp. 1999. Identification of residues of *Escherichia coli* phosphofructokinase that contribute to nucleotide binding and specificity. *Biochemistry.* 38:4313-4318.

Weber, G. 1972. Ligand binding and internal equilibrium in proteins. *Biochemistry.* 11:864-878.

Weber, G. 1975. Energetics of ligand binding to proteins. *Adv. Prot. Chem.* 29:1-83.

Wyman, J. 1964. Linked functions and reciprocal effects in hemoglobin: a second look. *Adv. Prot. Chem.* 19:223-286.

Xu, J., T. Oshima, and M. Yoshida. 1990. Tetramer-dimer conversion of phosphofructokinase from *Thermus thermophilus* induced by its allosteric effectors. *J. Mol. Biol.* 215:597-606.

Xu, J., M. Seki, K. Denda, and M. Yoshida. 1991. Molecular cloning of the phosphofructokinase 1 gene from a thermophilic bacterium, *Thermus thermophilus. Biochem. Biophys. Res. Commun.* 176:1313-1318.

Zheng, R. L., and R. G. Kemp. 1992. The mechanism of ATP inhibition of wild type and mutant phosphofructo-1-kinase from *Escherichia coli*. *J. Biol. Chem.* 267:23640-23645.

Zheng, R. L., and R. G. Kemp. 1994a. Site-directed mutagenesis of two highly conserved residues near the active site of phosphofructo-1-kinase. *Biochem. Biophys. Res. Comm.* 199:577-581.

Zheng, R. L., and R. G. Kemp. 1994b. Identification of interactions that stabilize the transition state in *Escherichia coli* phosphofructo-1-kinase. *J. Biol. Chem.* 269:18475-184479.

Zheng, R. L. and R. G. Kemp. 1995. Phosphofructo-1-kinase: role of charge neutralization in the active site. *Biochem. Biophys. Res. Comm.* 213:765-770.

VITA

Nilubol Monique Paricharttanakul
125/7 Moo 9 Soi Phipornphong 1, Viphavadee Rangsit Rd,
Don Muang, Bangkok 10210, Thailand

Education:

Texas A&M University	Biochemistry and Genetics	B.S.	1997
Texas A&M University	Biochemistry	Ph.D.	2004

Publications:

N. M. Paricharttanakul, S. Ye, A. L. Menefee, F. Javid-Majd, J. C. Sacchettini, and G. D. Reinhart. Investigation into the structure-function relationship of phosphofructokinase from *Lactobacillus bulgaricus*. (manuscript in preparation)

N. M. Paricharttanakul and G. D. Reinhart. Identification of residues important for conferring allostery in phosphofructokinase from *Escherichia coli* (manuscript in preparation)

N. M. Paricharttanakul and G. D. Reinhart. Pinpointing the role of a particular residue in the unique heterotropic interactions in phosphofructokinase from *Escherichia coli* (manuscript in preparation)

A. W. Fenton, N. M. Paricharttanakul, and G. D. Reinhart. 2004. Disentangling the web of allosteric communication in a homotetramer: heterotropic activation in phosphofructokinase from *Escherichia coli*. *Biochemistry*. 43:14104-14110.

A. W. Fenton, N. M. Paricharttanakul, and G. D. Reinhart. 2003. Identification of substrate contact residues important for the allosteric regulation of phosphofructokinase from *Escherichia coli*. *Biochemistry*. 42:6453-6459.

Presentations:

Differential paths of allosteric communication in phosphofructokinase from *Escherichia coli*. Biophysical Night Out, Texas A&M University. October 5, 2004.

Identification of residues important for conferring allostery. Center for Advanced Biomolecular Research (CABR) Annual Retreat, Texas A&M University, Camp Allen, Texas. October 25-26, 2003

Professional Societies:

Biophysical Society